1987

The effect of closed classical orbits on quantum spectra: Ionization of atoms in a magnetic field

Meng Li Du
College of William & Mary - Arts & Sciences

INFORMATION TO USERS

The most advanced technology has been used to photograph and reproduce this manuscript from the microfilm master. UMI films the original text directly from the copy submitted. Thus, some dissertation copies are in typewriter face, while others may be from a computer printer.

In the unlikely event that the author did not send UMI a complete manuscript and there are missing pages, these will be noted. Also, if unauthorized copyrighted material had to be removed, a note will indicate the deletion.

Oversize materials (e.g., maps, drawings, charts) are reproduced by sectioning the original, beginning at the upper left-hand corner and continuing from left to right in equal sections with small overlaps. Each oversize page is available as one exposure on a standard 35 mm slide or as a 17" × 23" black and white photographic print for an additional charge.

Photographs included in the original manuscript have been reproduced xerographically in this copy. 35 mm slides or 6" × 9" black and white photographic prints are available for any photographs or illustrations appearing in this copy for an additional charge. Contact UMI directly to order.

Order Number 8803967

The effect of closed classical orbits on quantum spectra: Ionization of atoms in a magnetic field

Du, Meng Li, Ph.D.

The College of William and Mary, 1987

U·M·I
300 N. Zeeb Rd.
Ann Arbor, MI 48106

PLEASE NOTE:

In all cases this material has been filmed in the best possible way from the available copy. Problems encountered with this document have been identified here with a check mark __✓__.

1. Glossy photographs or pages _____
2. Colored illustrations, paper or print _____
3. Photographs with dark background _____
4. Illustrations are poor copy _____
5. Pages with black marks, not original copy _____
6. Print shows through as there is text on both sides of page _____
7. Indistinct, broken or small print on several pages ✓
8. Print exceeds margin requirements _____
9. Tightly bound copy with print lost in spine _____
10. Computer printout pages with indistinct print _____
11. Page(s) _____ lacking when material received, and not available from school or author.
12. Page(s) _____ seem to be missing in numbering only as text follows.
13. Two pages numbered _____. Text follows.
14. Curling and wrinkled pages _____
15. Dissertation contains pages with print at a slant, filmed as received _____
16. Other _____

U·M·I

THE EFFECT OF CLOSED CLASSICAL ORBITS ON QUANTUM SPECTRA

Ionization of atoms in a magnetic field

A Dissertation

Presented to

The Faculty of the Department of Physics

The College of William and Mary in Virginia

In Partial Fulfillment

of the Requirements for the Degree of

Doctor of Philosophy

by

Meng Li Du

1987

APPROVAL SHEET

This dissertation is submitted in partial fulfillment of

the requirements for the degree of

Doctor of Philosophy

Author

Approved, November 1987

John B. Delos

Roy L. Champion

Edward A. Remler

George M. Vahala

Stephen K. Knudson
Department of Chemistry

for my parents

TABLE OF CONTENTS

FOREWORD

Last summer about this time I asked myself to do a serious study which would lead to a degree. But was there an interesting enough project around? At that time I was absorbing many new ideas. I started to learn about the complexity within classical mechanics that is born out of regular and irregular motions; I also began to learn the beauty, simplicity and power of semiclassical mechanics. A recurring question based on the correspondence principle is: How will quantum motion be affected by the variety of classical motions? To try to answer this, should I just do another calculation on a model system which can not be directly measured? Apparently this would not be a very good thing to do. Near the end of the summer I was impressed by a few papers in which the near threshold spectrum of Hydrogen atoms in a strong magnetic field was measured. I knew that classical motion near the threshold is chaotic. But the authors claimed that somehow, unstable, isolated periodic orbits were related to the quantum spectrum; however they were unable to explain why! I soon found out that the history of this subject went back to 1969, but over the years the theory on the subject has been in a very unsatisfactory state. Now it seemed that developing a

theory for the near threshold spectrum of a Hydrogen atom in a strong magnetic field would make a good Ph.D thesis. On one hand it has connection with fundamental questions of "quantum chaos", and on the other hand it is a system that can be tested experimentally.

In the fall before leaving Williamsburg for Boulder for a one year visit I vaguely agreed to take this project after talking with Dr. J. B. Delos. I was not sure then that anything could come out soon. After arriving in Boulder I began to read some papers on periodic orbit theory which were believed to have something to do with the subject. It took me many weeks before I understood most of the materials in the papers. Once they were understood, a clear picture of this theory emerged.

The theory presented in this thesis is a result of many discussions, many hours sitting in front of computers and many days of quiet thinking.

M.L.D

June 1987

ACKNOWLEDGEMENTS

The author wishes to express his deep appreciation to Professor John B. Delos for his guidance and encouragement, and to his family for their hospitality throughout the last four years. In particular, the new theory on the oscillatory spectra would not have been born by now, and this thesis would not be in its current form without his insight and suggestions.

The author is also indebted to Professors Steve K. Knudson, Roy L. Champion, Edward A. Remler, and George M. Vahala for their careful reading and criticisms of the manuscript.

The author thanks many people who have helped him in the last few years.

Finally the author acknowledges the Department of Physics, College of William and Mary for providing the opportunity to continue his study and research and the Joint Institute for Laboratory Astrophysics where most of the work in this thesis was completed.

LIST OF TABLES

LIST OF FIGURES

ABSTRACT

The purpose of this study is to understand the absorption spectrum of an atom in a magnetic field; the specific transitions involved are from the low levels to states with energies close to the ionization threshold. This is an example of a system that is classically chaotic, so this work advances our understanding of the quantum behaviour of classically chaotic systems.

A quantitative quantum mechanical theory of the process is developed. A simple physical picture associated with the theory enables us to establish the connection between closed orbits existing in the system and oscillations in the spectrum.

A sample theoretical computation for transition $2P_z \rightarrow m=0$ agrees very well with the measurement. Thus this theory provides us a complete understanding of the oscillatory spectrum which has remained a mystery ever since its first discovery in 1969.

THE EFFECT OF CLOSED CLASSICAL ORBITS ON QUANTUM SPECTRA:

ionization of atoms in a magnetic field

CHAPTER 0

AN INTRODUCTION

In this very first chapter, I present a simplified overview of this thesis. The purpose of doing this is clear: for those who want to know the problem and the result in just a few words, reading the following few pages is enough; for those who ask the why and how types of questions, this chapter will serve as a map of the logical thinking, so the danger of getting lost in the mathematical details of later chapters will be minimized.

A. A Mini Version of the Thesis[1]

The relationship between classical mechanics and quantum mechanics is rather well understood for integrable systems. Such systems admit a set of *conserved classical action* variables, and the energy eigenvalues correspond closely to trajectories having appropriately quantized values of these action variables. For systems in which the classical motion is irregular or chaotic, on the other hand, the quantum behaviour is poorly understood, and the whole field of "quantum chaos" is marked by confusion and controversy.[2] It is easier to identify properties which chaotic

systems lack (e. g. conservation laws) than the properties they possess.

There is evidence that in such systems, when the density of states gets very high, eigenfunctions and eigenvalues become very unstable under small changes in the Hamiltonian, and also unstable under small changes in the calculational method.[3] This would mean that these most fundamental quantities may be exceedingly difficult to calculate and to measure. If this is correct, then the major problem is to identify properties which can be calculated and measured, and which in this sense constitute stable attributes of the system.

Important insight comes from experimental measurements of the absorption spectrum of atoms near the ionization threshold. If the atom is in field-free space, then the observed oscillator strength is a smooth and slowly varying function of photon energy, going continuously from a finite value above threshold to the same average value below threshold. Almost twenty years ago, Garton and Tomkins[4] showed that if the atom is placed in a magnetic field, then the absorption spectrum shows an oscillation superimposed on this smooth background. Edmonds[5] pointed out that this oscillation is correlated with a periodic orbit in the system.[6]

Recently the near-threshold spectrum of Hydrogen atoms in magnetic fields has been measured with much

improved resolution.[7] It was found that the observed oscillator strength is in fact a superposition of many sinusoidal oscillations. Furthermore, the "wavelength" (or peak to peak energy spacing ΔE_n) of each oscillation corresponds to the period T_n of a classical periodic orbit of the system through the relationship $\Delta E_n \approx 2\pi\hbar / T_n$.

Computational evidence indicates that these systems are classically chaotic, with only isolated, unstable periodic orbits. Why do these orbits produce such phenomena?[8]

Many years ago Gutzwiller[9] proved that periodic classical orbits produce oscillations in the density of states of a quantum system. However, spectral measurements do not directly observe the state density, but rather the average oscillator strength density: the transition dipole moment averaged over the small range of energy corresponging to the experimental resolution.[10]

$$\overline{Df}(E) = \left(\frac{2m_e}{\hbar^2}\right) \int \langle \psi_f | D | \psi_i \rangle^2 (E_f - E_i) f(E_f) g(E_f, E) dE_f \quad (0.1)$$

This thesis describes the development of a quantitative theory which shows the relationship between closed orbits and the observed oscillations in the spectrum.

The theory and calculations are based upon two approximations. (1) Close to the nucleus ($r < 50 a_0$), the effect of the magnetic field is neglected, and the

electron wave function corresponds to zero-energy scattering in a Coulomb field. (2) Far from the nucleus ($r>50a_0$) a semiclassical approximation is used. These approximations lead to a simple physical picture.

When the atom absorbs a photon, the electron goes into a near-zero energy Coulomb outgoing wave. This wave propagates away from the nucleus to large distances. For $r>50$ a_0 the outgoing wave-fronts propagate according to semiclassical mechanics, and they are correlated with outgoing classical trajectories. Eventually the trajectories and wave fronts are turned back by the magnetic field; some of the orbits return to the nucleus, and the associated waves (now incoming) interfere with the outgoing waves to produce the observed oscillations.

From these ideas, and with these approximations, we show that the observed oscillator strength can be written as a smooth, slowly varying background term plus a sum of sinusodial oscillations:

$$\overline{Df}(E) = Df_0(E) + \sum_n A_n(E)\sin\left(\int_0^E T_n(E')dE' + x_n\right) \qquad (0\cdot 2)$$

The background term $Df_0(E)$ is precisely the oscillator strength density that would be obtained in the absence of an external field.

Each oscillatory term corresponds to a closed orbit of the electron in the combined Coulomb and magnetic fields. Each closed orbit begins and ends at

the atomic nucleus." $T_n(E)$ is the transit time for the electron on this orbit; it is a slowly varying function of E (in most cases essentially constant over the relevant range of E). If the spectrum is measured at low resolution, then only the orbits of shortest duration contribute to this sum; orbits of longer duration produce rapidly oscillating terms that average to zero. With increasing resolution, more and more terms become significant, and the spectrum is found to oscillate wildly.

The amplitudes of the oscillations, $A_n(E)$, depend upon: (1) the initial state of the system; (2) the polarization of the absorbed light; (3) the initial and final directions of the orbit, as it leaves and returns to the nucleus; and (4) the relative stability of the closed orbit, i.e. the divergence of adjacent trajectories from the central closed orbit.

The phase constant γ_n for each oscillatory term is also related to the initial state, light polarization and initial and final directions; in addition it is related to the classical action integral $\int \vec{p} \cdot d\vec{q}$ on the orbit at zero energy, and it contains Maslov phase corrections associated with caustics or focal points through which the orbit passes.

A complete set of formulas for these quantities and the derivation of these formulas is presented in Chapter III through Chapter VII. Here we show some of

our results that can be compared with experiment. Because the spectrum itself is wildly oscillatory, a direct comparison between theoretical and experimental oscillator strength is unhelpful. More appropriate for comparison is the Fourier transform of the spectrum, which was obtained in Ref. 7*b*. We show their result compared to our calculated amplitudes in Fig. 0.1. Very pleasing agreement is obtained for the short-period orbits ($T/T_c < 4.6$).

To conclude, we show in this thesis that stable and orderly properties of a quantum system are associated with closed classical orbits of the system. In the present case, the spectrum shows orderly patterns correlated with the orderly behaviour of the classical trajectories for restricted periods of time.

B. What Is in Other Chapters?

Chapter I is devoted to a brief review of regular and irregular classical motions and their effect on quantum properties.

Chapter II describes the spectrum of atoms in a magnetic field, specifically the diamagnetic effect. Problems which are the research subject of this thesis is also identified.

In Chapter III, the experimentally measurable spectrum will be related to the theoretical defined oscillator strength density, which will be calculated

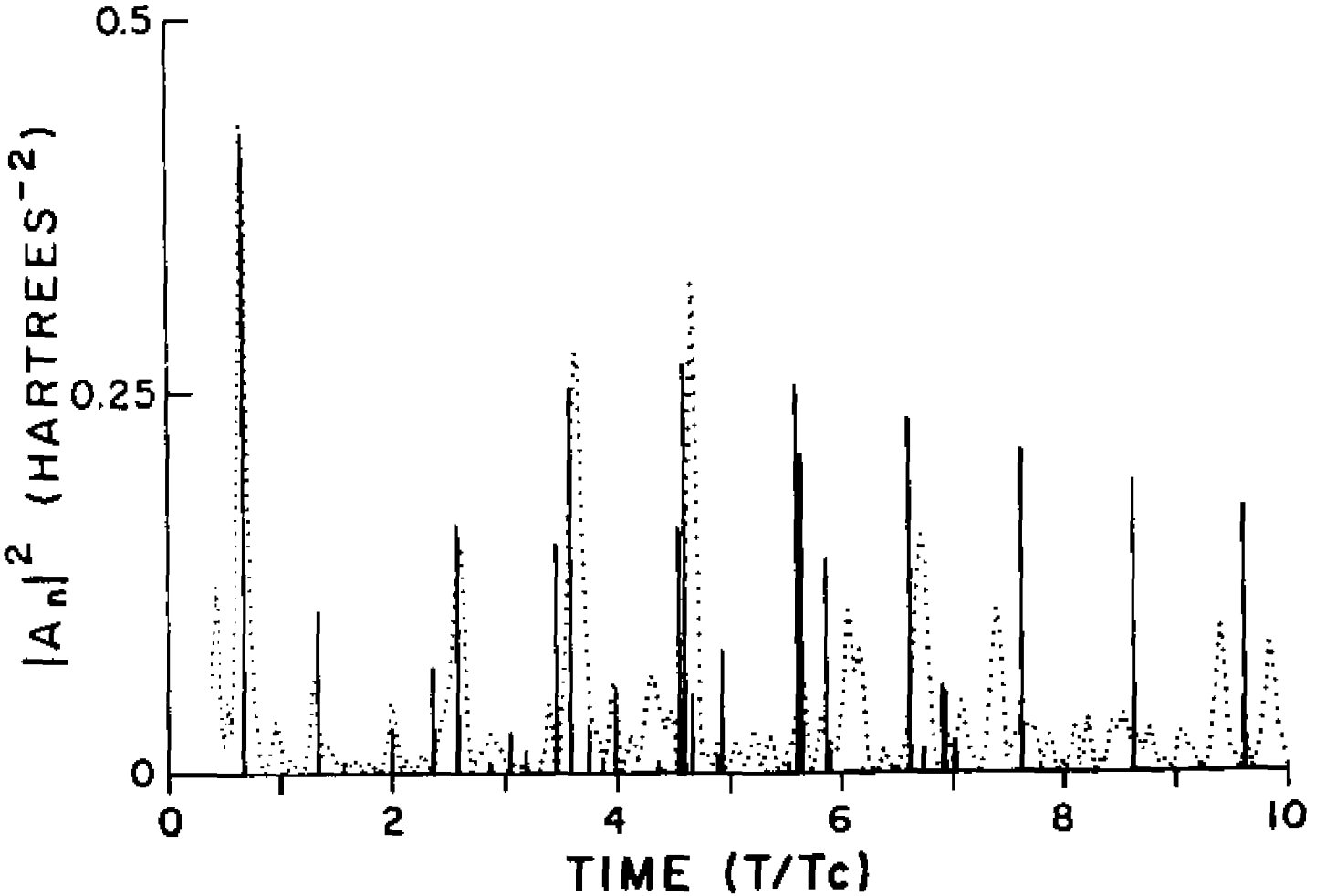

Fig. 0.1 Fourier-transformed spectrum. Vertical lines show calculated amplitudes $|A_n|^2$ vs orbit durations T_n . Light dotted line is experimental result from ref.7b. The experimental result was normalized to match the height of the largest peak (T/T_c =0.67).

in later chapters. The oscillator-strength density is shown to be related to matrix elements of the Green's function.

In Chapter IV, I study the behavior of the Hydrogen atom wave functions close to the nucleus. There the diamagnetic field can be neglected. In Chapter V , I examine semiclassical propagation of waves. This semiclassical approximation describes the waves when they are far from the nucleus.

In Chapter VI different approximations in different regions are put together, and the final formula for the spectrum is derived. A procedure for computing the spectrum is also presented.

Finally in Chapter VII, a computation is presented. The result is compared with the best available experimental measurements. Implications and predictions of the theory are also discussed.

CHAPTER I

REGULAR AND IRREGULAR CLASSICAL MOTIONS AND THEIR CONSEQUENCES IN QUANTUM MECHANICS

In the early days of quantum mechanics, Bohr's correspondence principle was used to find the quantum properties of a system from knowledge of the corresponding classical system.[12-14] Once the correct quantum mechanics formalism was established and shown to be successful in interpreting and predicting new phenomena, it might seem that the connection between quantum mechanics and classical mechanics can be forgotten, and one should pursue a pure quantum view of the world. It is a fact that many times only the quantum theory can satisfactorily explain a phenomenon; it is also a fact that many times a parallel classical theory exists beside the quantum one. In such cases our understanding is always deepened by comparing the two theories.

Quantum equations(i.e. the Schroedinger equation) are obtained from classical mechanics by well-defined prescriptions("write the Hamiltonian in Cartesian coordinates and substitute $p_i \to (\hbar/i)\partial/\partial q_i$").[15] However, it is not always so clear how the solutions of the Schroedinger equation are related to the solutions of classical equations of motion. Nevertheless the

correspondence principle tells us that the classical properties should be reflected, under proper conditions, in the quantum properties.

Modern studies of classical systems have changed our picture of classical motion.[16-17] We now know that simple classical systems can exhibit regular, orderly motion (like that of a two-dimensional harmonic oscillator) and irregular, chaotic motion(like that of a molecule in a gas). If we believe the correspondence principle, it would mean that quantum motions corresponding to these two different types of classical motions must be very different.[18]

Exactly how they differ is still an active research area. In this first chapter I shall try to summarize the major point we have learned and at the same time point out the problems we still have on the subject.

A. Orderly and Chaotic Motions in Classical Mechanics

Motion in classical mechanics means the evolution of trajectories in configuration space or in phase space.

Classical motion of a Hamiltonian system is governed by Hamilton's equations(in the discussion below we restrict ourselves to systems with time-independent Hamiltonians).[19] There are numerous Hamiltonians, but basically two kinds of motion exist.

On one hand is regular motion. This is the type that is most familar to us. Almost all of the examples and exercises in traditional classical mechanics textbooks represent regular motion.[19] Typical systems which represent this type of motion are the pendulum, harmonic oscillator and the planets. With a pendulum, the motion is repeated after a period. A harmonic motion is perfectly described by a sine function. The orbit of a planet is a ellipse. These motions are stable under small changes in the Hamiltonian or in the initial conditions, and they are models of predictability in classical mechanics.

On the other hand is irregular motion. This type of motion is exhibited by a molecule in a gas. Although the motion is still governed by Hamilton's equations, the complete orbit of such a molecule is not calculable in principle.[18] The reason is that if the initial position or momentum are known to within a small error, then this error grows exponentially with the number of collisions. This motion is therefore unstable, and it illustrates long-term unpredictability in mechanics.

There are also motions with properties that are intermediate between the extreme examples given above. We shall find more in the following pages.

1. Integrable Systems

Integrable systems are the simplest among regular systems and their orbits all have a simple structure in phase space.[17,18]

For an N-dimensional integrable system there exist N independent constants of motion, $C_i(\vec{q},\vec{p})$ $1 \le i \le N$. Thus the phase space motion of the system will be on an N-dimensional surface Σ. Further, it can be proved[20a] by constructing proper vector fields out of these N constants of motion $C_i(\vec{q},\vec{p})$ that the surface Σ takes on a special form---an N-torus.

For a particle moving in a one-dimensional potential well, energy conservation is enough to make the system integrable. Any N-dimensional separable system can be reduced to N one-dimensional systems, so all such systems are integrable. But there also exist integrable systems which are not separable.[20b]

For integrable systems, it is possible to transform to action angle variables, in which the motion is described in a very simple way.

The actions are defined as integrals around certain distinct paths γ_i in phase space:[19]

$$I_i = \frac{1}{2\pi}\oint_{\gamma_i} \vec{p}\, d\vec{q} \qquad (1\text{-}1)$$

The action variables are functions of the constants of the motion $C_i(\vec{q},\vec{p})$, and therefore they are constant themselves. The actions can be regarded as canonical momenta, and the Hamiltonian can be written as a function of the actions only. Therefore the time-

dependence of actions and angles are simply

$$I_i = \text{constant}$$

$$\theta_i = \omega_i(\vec{I})\, t + \theta_i^0 \qquad (1\text{-}2)$$

where $\omega_i(\vec{I})$ and θ_i^0 are constants, depending on the initial condition but not upon time.

A two-dimensional torus corresponding to eqs. (1-2) can be drawn as in Fig. 1.1. The variables θ_1 and θ_2 move on the smaller and lager circle independently. The trajectory $(\theta_1(t), \theta_2(t))$ then winds around the torus.

A canonical transformation between $(\vec{q}, \vec{p})$ and $(\vec{I}, \vec{\theta})$ exists,

$$(\vec{q}, \vec{p}) \rightleftharpoons (\vec{I}, \vec{\theta})$$

and the old variables $(\vec{q}, \vec{p})$ can be written in the action and angle variables as a Fourier series,

$$\vec{q}(\vec{I}, \vec{\theta}) = \sum_{\vec{m}} \vec{q}_{\vec{m}}(\vec{I})\, e^{i\vec{m}\cdot\vec{\theta}}$$

$$\vec{p}(\vec{I}, \vec{\theta}) = \sum_{\vec{m}} \vec{p}_{\vec{m}}(\vec{I})\, e^{i\vec{m}\cdot\vec{\theta}} \qquad (1\text{-}3)$$

It follows that the time-dependence of q(t) and p(t) can be written in the form

$$\vec{q}(t) = \sum_{\vec{m}} \vec{q}_{\vec{m}}(\vec{I})\, e^{i\vec{m}\cdot(\vec{\omega}(\vec{I})\, t + \vec{\theta}^0)}$$

$$\vec{p}(t) = \sum_{\vec{m}} \vec{p}_{\vec{m}}(\vec{I})\, e^{i\vec{m}\cdot(\vec{\omega}(\vec{I})\, t + \vec{\theta}^0)} \qquad (1\text{-}4)$$

These are called multiply-periodic function: the Fourier series contain N fundmental frequencies, and all harmonics and combinations of these frequencies.

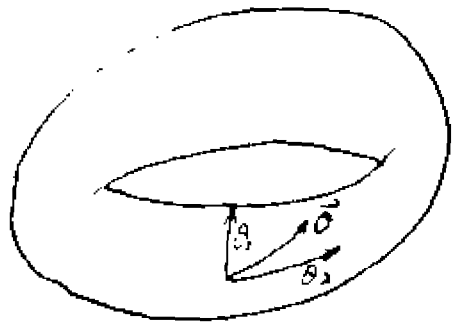

Fig. 1.1 A two dimensional torus. θ_1 and θ_2 move on the smaller and larger circle independently, $\vec{\sigma}$ then winds around the torus.

In general the N frequencies ω_i are not commensurable, and the orbit fills in the torus densely if time is long enough. But when N integers(not all of them zero) exist such that

$$\sum_{i=1}^{N} n_i \omega_i = 0 \qquad (1\text{-}5)$$

the motion is periodic.[19] For all regular systems there are such periodic trajectories.(There are also some systems with high symmetry in which all orbits have commensurable frequencies satisfying (1-5). Familar examples of such systems are the N-dimensional uncoupled harmonic oscillator with commensurable frequencies, and the Coulomb potential. For these systems all the trajectories are closed regardless of the initial conditions and the values of actions. We call these exceptional systems over-integrable.)

2. Irregular Systems

In a general Hamiltonian system there are no other global constants of motion but the energy. The trajectories can in principle explore the 2N-1 dimensional energy surface in phase space.[21]

One important class of irregular systems is the set of so called ergodic systems. In such a system any phase space function averaged along almost any trajectory is equal to the ensemble average of the

function in phase space("almost any" trajectory means all but a zero-measure set of trajectories). Such ergodicity is closely connected with the fundmental principle of statistical mechanics.[22]

Because any one dimensional system is always integrable(as was pointed out earlier), irregular systems must have at least two degrees of freedom.

In fact, even very simple two-dimensional systems can be irregular. It was proved by Sinai[23] that the motion of a particle in a square with a circular reflecting obstacle is ergodic. Another ergodic system is a particle moving in a "stadium", which is formed from two semicircles connected by two straight lines. Ergodicity in these two systems follows from rapid divergence of neighboring trajectories.

Each trajectory in an ergodic system comes arbitrarily close to almost every point on the energy shell if it allowed to run for a sufficient time. Fig.1.2(a) shows one trajectory in the "stadium".[24] We note that at any point the trajectory may pass through in any direction. We also note such system possess closed orbits(isolated or in groups). The consequences of these observations will be explained later.

Typical Hamiltonian systems have motion that are intermediate between ergodic motion and regular motion. An interesting example is the Henon-Heiles system.[25] At low energies, most of the trajectories are mutilply-periodic, like the trajectories of integrable systems.

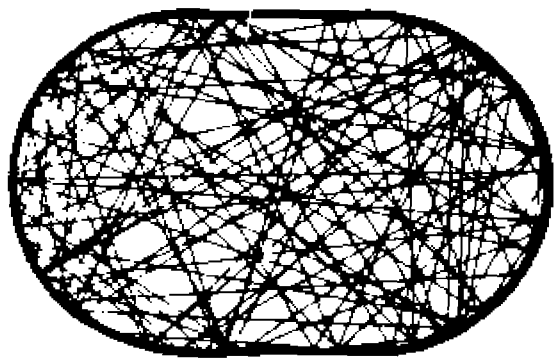

a

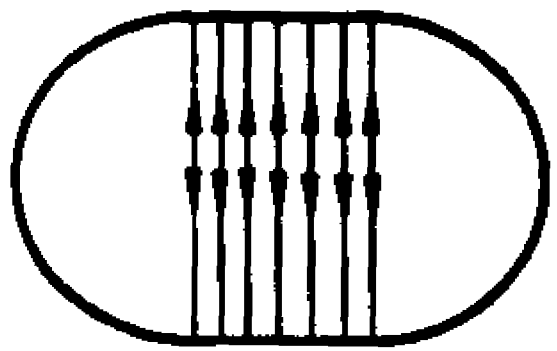

b

Fig. 1.2 One "chaotic" trajectory (a) and a group of periodic orbits (b) in a "stadium".

At higher energies each trajectory occupies a large portion of the energy shell.

The different degrees of irregularity shown by Hamiltonian systems complicate the study, but they are also responsible for the rich behaviours in the Hamiltonian world.

3. Pseudo-Integrable Systems

A pseudo integrable system still possess N constants of motion. But unlike an integrable system, construction of analytic vector fields is not possible.[26] Consequently the trajectories in phase space do not necessarily occupy an N-torus. In fact their structures are usually more exotic.

Richens and Berry[26] have studied some pseudo-integrable systems. One example of this type of system is obtained by replacing the circular obstacle in Sinai's billiard by a square. Obviously v_x^2 and v_y^2 are conserved separately then. The trajectory in phase space was found to occupy a five-handled sphere.

4. Quasi-Integrable Systems

Quasi-integrable systems are neither integrable nor ergodic. They have an integrable Hamiltonian plus a small generic perturbation,

$$H(\theta,P)=H_0(\theta,P)+\epsilon H_1(\theta,P) \tag{1-6}$$

For $\epsilon=0$, $H_0(\theta,P)$ is integrable. so the trajectories occupy tori in phase space. If $\epsilon\neq 0$ what is the structure of the trajectories? The answer is given by the KAM theorem.[11,17] With perturbation, most tori survive, but they are distorted. However, there is always a finite measure of tori that are destroyed. Furthermore, The number of destroyed tori grows with ϵ .

Overall the structure can be very complicated because the surviving and destroyed tori intertwine each other.

5. Mappings

A mapping[16] is a procedure according to which the values of the variables at $(n+1)^{th}$ step can be obtained from those at the n^{th} step. For example a 2-D mapping can be represented by two functions,

$$M:\quad \begin{aligned}\theta_{n+1}&=\theta_{n+1}(\theta_n,P_n)\\ P_{n+1}&=P_{n+1}(\theta_n,P_n)\end{aligned} \tag{1-7}$$

A mapping can be considered as an abstract dynamical system, taking discrete time step instead of continuous one. But in many instances mappings are derived from dynamical systems.

Consider a 2-D Hamiltonian system

$$H = H(x, y, p_x, p_y)$$

(1-8)

Because energy is conserved, the value of fourth variable is determined from the values of any three variables. Now let us select a plane in phase space, for example, x=0. A trajectory will intersect this plane in sequence as shown in Fig. 1.3. This sequence implies a mapping:

$$y^{n+1} = y^{n+1}(y^n, p_y^n)$$
$$p_y^{n+1} = p_y^{n+1}(y^n, p_y^n) \qquad (1\text{-}9)$$

This method of obtaining the mapping above is called the surface of section method.

As a second example let us consider a one dimensional Hamiltonian with periodic time dependence,

$$H(q, p, t) = H(q, p, t + T) \qquad (1\ 10)$$

Suppose we are given q^0, p^0 initially, then from Hamilton's equations we can compute the values of q, p at T, 2T, ...

$$q^0 p^0;\ q^1, p^1, \ldots\ldots \qquad (1\ 11)$$

This is another mapping!

From the way the mappings are deduced we conclude that the properties of the original dynamical system and those of the resulting mapping are closely connected. For example, if the mapping of all

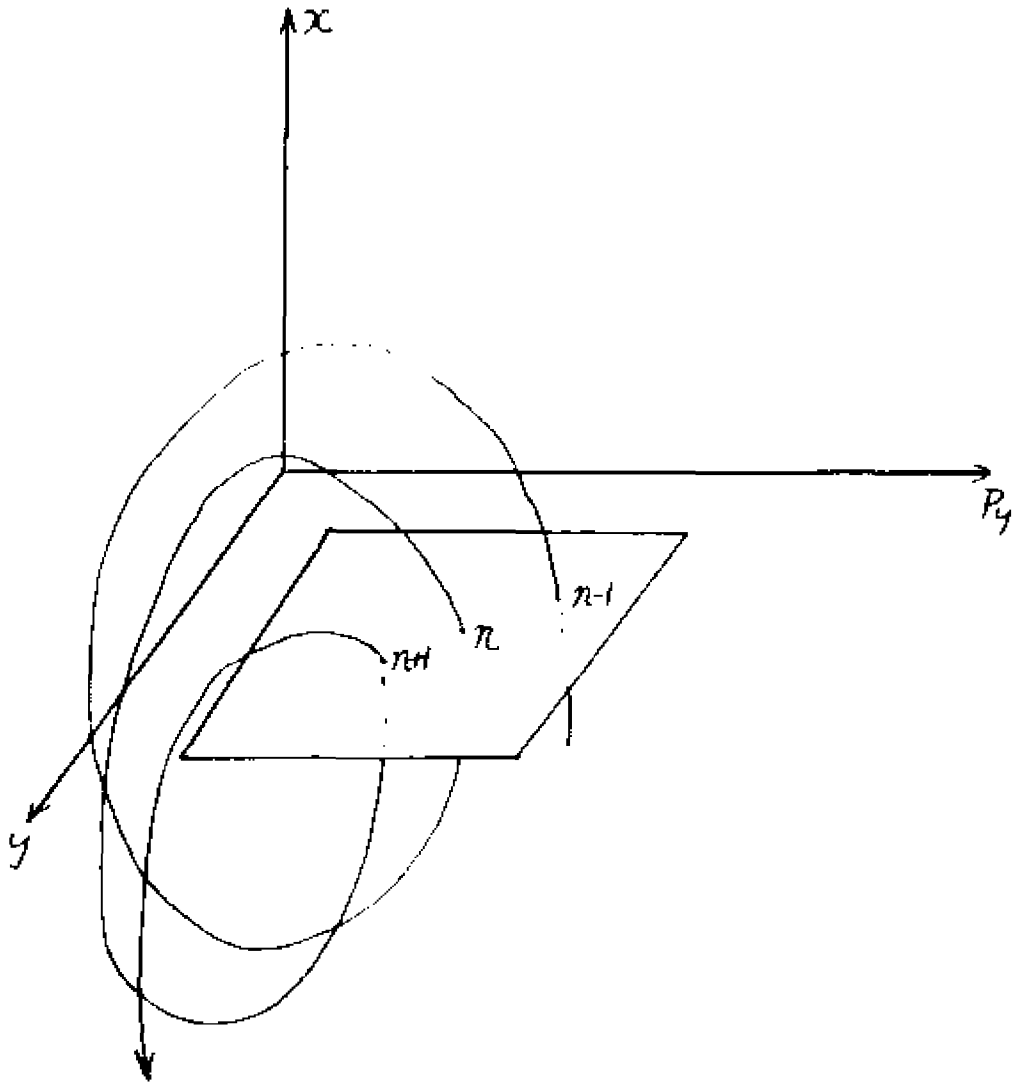

Fig. 1.3 The "surface of section". A trajectory intersects with the x=0 plane and a mapping is produced.

trajectories from the surface of section method form smooth curves, then the original system is either integrable or quasi-integrable.

B. Wave Functions

So far we have seen regular and irregular classical motions. We know that quantum properties of a system are closely associated with classical properties of the system. So the question is again: how will the different types of classical motion be manifested in quantum mechanics?

In quantum mechanics the most important quantities of a system are the energy spectrum, and the wave function of energy eigenstate. We shall see that they are profoundly different when the underlying classical motions are different.

1. Semiclassical Wavefunctions and Family of Trajectories

The relationship between waves and trajectories was realized by Hamilton[19]: light travels along classical trajectories when the wave length is small compared to the scale of objects in the space. Later, when it was realized that all particles have wave properties described by Schroedinger's equation, much effort was devoted to the study of the connection between

waves and trajectories.

Given a family of trajectories, forming a surface in phase space, locally a wave can be associated with the surface Σ by means of two functions S(q) and A(q),

$$\psi(q) = A(q)\, e^{iS(q)/\hbar} \tag{1-12}$$

If A(q) and S(q) are now chosen in a particular way, then $\psi(q)$ will satisfy the Schroedinger equation to first order in Planck's constant $\hbar$.[28]

A(q) represents the probability amplitude, and so its square is required to be proportional to the density of particles at position q. S(q) represents the phase of the wave and is required to be the increase of action of particles along the trajectories. Further detailed formulas are given elsewhere.

2. Eigenfunctions in a Regular System

When the motion of a system is regular, then there is a systematic way to construct eigenfunctions from trajectories.[29]

As pointed out in the discussion of integrable systems, the phase space surface Σ is an N-torus. If this phase space surface is projected on to the q coordinate, we will get the momentum $\vec{p}$ as a multivalued function of $\vec{q}$,

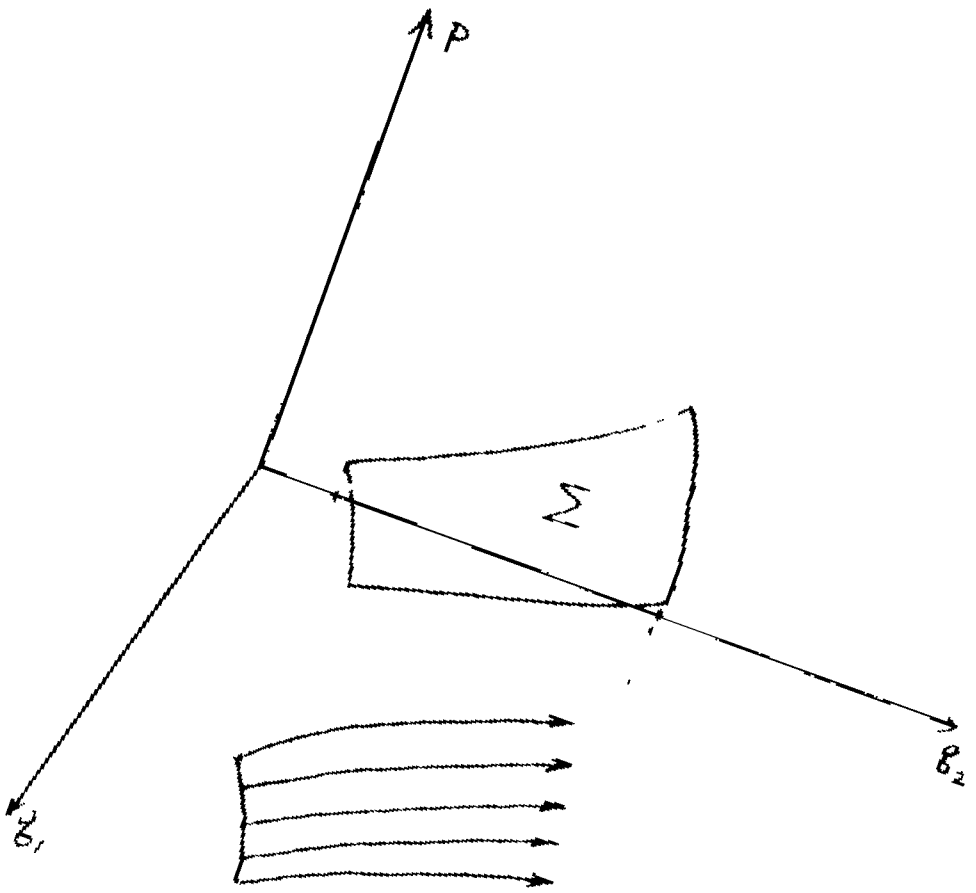

Fig. 1.4 A family of trajectories and the surface Σ in phase space associated with the trajectories.

$$\vec{P}^2 = \vec{P}^2(\vec{q})$$

(1-13)

and at every instant, the trajectory will lie on one of these branches.

Out of these functions $\vec{P}(\vec{q})$ an eigenfunction can be constructed in the following way:

Associate to each branch a wave function of the form

$$\psi^i(\vec{q}) = B^i(\vec{q}) \exp[i(S^i(\vec{q})/\hbar - \frac{\tau^i \pi}{4})]$$

(1-14)

where

$$S^i(\vec{q}) = \int \vec{p}^i \, d\vec{q}$$

and τ^i is the so called Maslov index on each branch, and $B^i(\vec{q})$ is a density function which can be computed from the trajectories.

To make the sum of the above branch-wavefunctions $\psi^i(\vec{q})$ into an eigenfunction, one requires that the branch functions be joined together. The result is that the action change ΔS_{γ_i} around closed path have to be quantized:

$$\Delta S_{\gamma_i} = (n_{\gamma_i} + \frac{\kappa_{\gamma_i}}{4}) 2\pi\hbar, \qquad n_{\gamma_i} = 0, 1, 2$$

(1-15)

where κ_{γ_i} is a constant for each path.
Therefore each eigenfunction is related to one quantized torus, which is sometimes called an eigentrajectory.[30]

Each wavefunction occupies primarily the region of configuration space occupied by its eigentrajectory; typically the eigenfunction has an orderly oscillatory structure, and it is largest near the boundary of the eigentrajectory.

3. Eigenfunctions in an Irregular System

Unlike the regular case, little is known about the precise connection between the eigenfunction and its underlying irregular classical motion.

However from the correspondence principle we can point out some facts. In the regular case the motion is confined to tori. In coordinate space there are only a limited number of directions at each point along which the wave propagates. The resulting wave has simple patterns. On the other hand, if the motion is irregular, trajectory and wave could in principle be propagating in any direction. The resulting wave formed by such a superposition must be very complicated.

A few observations have been made on the eigenfunctions associated with irregular classical motion. First since classical motion explores the whole energy surface, contrary to the regular case, the irregular wave function should occupy the entire energetically allowed region, and the wave function is

expected to be small at the boundary. Berry has called this boundary an "anticaustic".[18,31,32]

Another curious observation is that periodic orbits of the system may have some interesting effects on the eigenfunctions.[33] It was noted that in some of the eigenfunctions, the intensity of the wave along a periodic orbit is very high. But we do not know periodic orbits exist at all energies, but apparently not all eigenfunctions are affected by such orbits. all eigenfunction are affected by such orbits.

Finally although the exact eigenfunction might be extremely complicated, an "averaged" wave function could be simpler.[18,33,34] This average can be an average of the exact wave function in a small area or it can be an average in energy. Both eliminate the fine scale structure.

In this thesis some connections between average quantities and closed orbits will be developed. It will be shown if an energy spectrum is examined at low resolution, averaging over levels in a given range of energy, this averaged spectrum will show oscillations which are correlated with classical closed orbits.

C. Spectra

Having discussed the consequences of different types of motion on the wave function, it is time now to discuss the spectra of different types of motion.

In quantum mechanics when we compute the energy levels, the wave function is usually expanded in a suitable basis, and from Schroedinger's equation a set of algebraic equations is obtained. The energy levels are then determined by zeros of a determinant.

This formal procedure treats all systems the same way. However it does not help us in understanding the structure of the spectrum. And in some cases energy levels become so dense that this procedure may be extremely difficult or even impossible to apply.[34]

A spectrum, if resolved in its finest scale, gives the location of each individual eigenvalue. Calculating each individual eigenvalue can be an ambitious and costly programs which may not always be needed. Then the structure of spectrum in large scale might be more interesting. The large scale structure includes the averaged energy spectrum, statistics of energy levels and clustering of energy levels.[35] These will be discussed in the following sections.

1. Individual Energy Levels

Semiclassical quantization of energy levels began with Sommerfield-Wilson's rule.[3] Later many people have made contributions to the subject.[36]

As we explained earlier, semiclassical quantization is easily realized for a regular system. For such a

systems there are N independent action variables and the energy can be expressed as a function of these action variables. For the allowed energy levels, the action is quantized according to eq. (1-15).

To use this quantization formula the actions at different energies have to be determined. Practical methods for this, including the use of surface of section,[37a] algebraic transformation[37b] and others have been developed.[3]

When the motion is irregular there is no general semiclassical quantization formula to give the energy levels(for example there are no action variables in the irregular case). Such a formula may not exist at all.

However Percival[3] has predicted some general properties of irregular spectra. He argued that, unlike the regular case there is no unambiguous assignment of a set of quantum numbers to a quantum state; a state under weak perturbation is coupled to a large number of states having similar energy; the states in the irregular spectrum are more sensitive to external perturbation than those in the regular spectrum.

2. Small-Scale Structure of Spectrum

Can we say anything about the relationship between neighboring energy levels? Yes, as we shall see, regular and irregular spectra behave very differently

in this regard.[18]

For a regular spectrum energy levels are given by the torus quantization condition. Suppose the Hamiltonian depends upon N actions and also upon one parameter, A: $H=H(\vec{I},A)$, then the quantized energy levels can be regarded as the intersection of an (N-1) dimensional surface $E=H((\vec{n}+\frac{\vec{\alpha}}{4})\hbar,A)$ with the lattice point $\vec{I}=(\vec{n}+\frac{\vec{\alpha}}{4})\hbar$. On changing A and holding E fixed, the surface will evolve in a smooth way and there will be value of A* at which the surface intersects with two different $\vec{n}$'s. That is, at A*, the energies are degenerate. Therefore if the energy spectrum is plotted against the parameter A, typically there will be many crossings of levels.

On the other hand for a general one parameter Hamiltonian, avoided crossings are typical. The argument goes as follows:[18]

Suppose we have a Hamiltonian $\hat{H}^*$ having two orthogonal states $|u\rangle$ and $|v\rangle$ with the same energy E*, or

$$\hat{H}^*|u\rangle=E^*|u\rangle \ , \ \hat{H}^*|v\rangle=E^*|v\rangle \ , \ \langle u|v\rangle=0 \qquad (1\text{-}16)$$

Now consider $\hat{H}=\hat{H}^*+\Delta H$, where ΔH is a small perturbation. The wavefunction of the new Hamiltonian can still be approximated by a combination of $|u\rangle$ and $|v\rangle$,

$$|\psi\rangle=\cos\chi\,|u\rangle+\sin\chi\,|v\rangle \qquad (1\text{-}17)$$

When the Schroedinger's equation

$$\hat{H}|\psi\rangle = E|\psi\rangle \qquad (1\text{-}18)$$

is projected on to states $|u\rangle$ and $|v\rangle$, we obtain a secular equation and the eigenvalues

$$E = F^{x} + \Delta H_{uu} + \Delta H_{vv} \pm \sqrt{\Delta^2 + 4\Gamma^2}$$

where

$$\Delta H_{uu} = \langle u|\Delta H|u\rangle, \quad \Delta H_{vv} = \langle v|\Delta H|v\rangle$$

$$\Delta = \Delta H_{uu} - \Delta H_{vv}$$

$$\Gamma = \langle u|\Delta H|v\rangle$$

(1-19)

For a general perturbation, the quantity under the square root will not be zero, because typically Δ and Γ will not vanish simultaniously. Therefore the perturbed energy levels avoid crossing.(Only if the general Hamiltonian has two or more parameters, then crossings typically occur.[38])

The crossing and avoided crossing profoundly affect the nearest neighbor statistics.[18,39] Let us define the nearest neighbor level distribution as $P(\Delta E)$ where

$$P(\Delta E)d\Delta E = \text{the number of levels having energy difference in the range } (\Delta E - \frac{d\Delta E}{2}, \Delta E + \frac{d\Delta E}{2}) \text{ to its neighbor}$$

(1-20)

For regular spectra a Poisson distribution

$$P(\Delta E) = \lambda\, e^{-\lambda \Delta E}$$

(1-21)

will be found. In contrast, irregular spectrum often possess a Wigner distribution,

$$P(\Delta E) = \frac{\pi}{2} \lambda^2 \Delta E \; e^{-\frac{\pi}{4}\lambda^2 (\Delta E)^2} \tag{1-22}$$

The reasons can be partially understood from the above arguments.

3. Large-Scale Structure of Spectrum

Locating the individual energy levels and finding the nearest neighboring statistics are two ways of studying a spectrum. A third way is to study the large scale structure. By that I mean the spectrum when measured or viewed with a finite resolution, so that within the resolution width there may be many individual energy levels. The large scale structure is believed to be connected to some simple properties of a dynamical system.

The idea is best illustrated with a simple example.[18,40] Suppose the spectrum is a δ-function at each integer n. From Fourier analysis the following expansion can be easily obtained,

$$\sum_{n=-\infty}^{\infty} \delta(E-n) = 1 + 2\sum_{m=1}^{\infty} \cos 2\pi m E \tag{1-23}$$

The sharp peaks on the left are expressed as a sum of a constant plus oscillatory terms; the frequencies of the oscillatory terms increase from 2π to infinity.

Now if we are able to see only the low frequency

terms, after dropping off the higher frequency terms, we get an approximate representation,

$$\sum_{n=-\infty}^{\infty} \delta(E-n) \doteq 1 + 2\sum_{n=1}^{M} \cos 2\pi nE \qquad (1\text{-}24)$$

If more terms are kept, this representation will become more accurate.

Does this example have any similarity with a real spectrum? Suppose we know the energy levels E_j in a system; then the density of states function d(E) can be written as

$$d(E) = \frac{dN(E)}{dE} = \sum_{j=1}^{\infty} \delta(E-E_j) \qquad (1\text{-}25)$$

where N(E) is the number of states with energy below E. If we compare d(E) with the simple example above, we find that they are really similar, only that the locations of the δ-function differ. Therefore it is reasonable to think that a similar expansion in oscillatory terms can be used to described a spectrum.

A beautiful formula of this type for the density of states was developed by Gutzwiller[9], and by Balian and Bloch[44], starting from a semiclassical approach. The result is that d(E) can still be represented as an smooth average term plus oscillatory terms,

$$d(E) = \bar{d}(E) + d_{osc}(E) \qquad (1\text{-}26)$$

Most important, the oscillatory terms are connected

with periodic orbits of the system.

The result could be explained by the Green's function. It is not difficult to show that[18]

$$d(E) = -\frac{1}{\pi} \mathrm{Im} \int d\vec{q}\; G^{+}(\vec{q}, \vec{q}', E)_{\vec{q}=\vec{q}'} \qquad (1\text{-}27)$$

where G^{+} is the outgoing energy-dependent Green's function, satisfying

$$\left[E + i\epsilon - H\left(\vec{q}, -i\hbar \frac{\partial}{\partial \vec{q}}\right)\right] G^{+}(\vec{q}, \vec{q}', E) = \delta(\vec{q} - \vec{q}') \qquad (1\text{-}28)$$

Physically the Green's function G^{+} represents the wave at the point q that is produced by a point source at q'. A semiclassical approximation for the Green's function can be made based on the above observation. In this approximation, the Green's function is a sum of terms which represent waves propagating along different paths from $\vec{q}'$ to $\vec{q}$.[42]

The direct path contributes to the smooth background $\bar{d}(E)$. It has been shown that[19]

$$\bar{d}(E) = \frac{1}{h^{N}} \int d\vec{q}\, d\vec{p}\, \delta(E - H(\vec{q}, \vec{p})) \qquad (1\text{-}29)$$

so $\bar{d}(E)$ is related to the phase space volume accessible to the particle.

The contributions from all other paths to the Green's function can be written as[9,18]

$$G^{+}(\vec{q}, \vec{q}', E) = \frac{1}{i\hbar^{(N+1)/2}} \sum_{j} D_j(\vec{q}, \vec{q}'; E) \exp\left(\frac{i}{\hbar} S_j(\vec{q}, \vec{q}', E)\right) \qquad (1\text{-}30)$$

To find $d_{osc}(E)$, we must let $\vec{q} = \vec{q}'$, and integrate over all space. When $\vec{q} = \vec{q}'$, then only orbits from $\vec{q}$ to

$\vec{q}$ contribute. This includes periodic orbits and other orbits which return to the initial position $\vec{q}$ with a different momentum. One can show, however, that only periodic orbits contribute significantly.

The argument goes as follows: usually when $\vec{q}$ changes, S will change and so G^+ oscillates wildly. Only when S is stationary under small change of $\vec{q}$ can a significant contribution result. This requires

$$P_{\vec{q}} S(\vec{q}, \vec{q}, E) = \lim_{\vec{q}' \to \vec{q}} \left[D_{\vec{q}} S(\vec{q}, \vec{q}', E) + D_{\vec{q}'} S(\vec{q}, \vec{q}', E) \right]$$

$$= \lim_{\vec{q}' \to \vec{q}} \left[\vec{P}(\vec{q}') - \vec{P}'(\vec{q}') \right] \qquad (1\text{-}31)$$

so the initial and final momentum have to be the same. In another words, the orbits must be periodic.

The oscillatory term $d_{osc}(E)$ turns out to be a sum over all periodic orbits

$$d_{osc}(E) = \sum_j A_j(E) \sin\left(\frac{S_j(E)}{\hbar} + \alpha_j \right) \qquad (1\text{-}32)$$

where the amplitude $A_j(E)$ depends on the properties of the particular orbit(stable or unstable, isolated or nonisolated); S_j is the action around the orbit and α_j is associated with the number of focal points on the orbit.

The formula expressing the density of states as a sum over periodic orbits is universal in that it applies to both regular and irregular systems.(The only significant difference between the two cases appears in

the formulas for the amplitudes $A_j(E)$.) Berry and Tabor[43] have applied this approach to regular systems. They showed that the torus quantization condition could be transformed into a sum over periodic orbits. As increasingly more oscillatory terms were included in the sum, δ functions at each energy level emerged.

It is unclear whether this formulation is a practical means to obtain individual energy levels. The problem is that the number of periodic orbits with long periods is very large. Nevertheless if one is interested in the "low resolution" energy spectrum, only a few orbits may give the desired information.

We will use this periodic orbit formulation to study the spectrum of atoms in magnetic fields. We will show that in this case the formulation must be modified in two ways. First, because of the Coulomb singularity in the potential the Green's function can not be approximated semiclassically everywhere, and an appropriate quantum approximation must be used in the singular region. Second, we are not interested in the density of states(which is not what is measured experimently) but the absorption rate. Such quantities can be calculated from the Green's function weighted by the initial quantum state. In such case the argument leading to periodic orbits is modified, and we find that closed orbits, not just periodic ones, will generally be important.

These issues are fully discussed and treated from chapter III to chapter VII.

CHAPTER II

ATOMS IN A MAGNETIC FIELD

It has been recognized since the beginning of atomic physics that atoms interacting with external fields could have radically different behaviour from free atoms.[44] The familar Zeeman and Stark effects are just two examples associated with atoms in magnetic and electric fields respectively.[44]

Undoubtedly the study of atoms interacting with external fields has been very important throughout the development of atomic physics. However, it is only recent that we can engage in this kind of study under more desired conditions. This is for one reason due to the advances in technology. Lasers make it possible to prepare an atom in almost any state; superconducting materials can easily generate a high magnetic field; higher and higher resolution spectrometers are now avilable.[45]

Recently there has been increasing interest in the properties of Ryderberg atoms interacting with strong fields.[46] This arises from the realization that a highly excited atom has many properties that an atom in lower states does not have. For example, a highly excited atom has a long life time, and a large size; its binding energy is small, so any external field could have a large effect. The interaction of the outer electron

with the core of the atom, which usually makes the dynamics more complicated, can often be ignored since the electron spends most of its time far away from the core.

Atoms in magnetic fields are particular important. In the early days "spatial quantization" was demonstrated by the Stern-Gerlach experiment; now atoms in magnetic fields provide us another chance to understand something new. In this Chapter I shall try to present the rich phenomena displayed by an atom in a magnetic field due to the diamagnetic interaction only. First our current understanding is described; then new problems are identified, which are the subject of this thesis.

A. Hamiltonian of the System

Let us consider an electron moving in a potential field $V(\vec{r})$ and a uniform magnetic field $\vec{B}$. The Hamiltonian for the motion of electron is

$$\hat{H} = \frac{1}{2m_e}\left(\vec{P} + \frac{e}{c}\vec{A}\right)^2 + V(\vec{r}) \qquad (2\text{-}1)$$

If the magnetic field is in the z direction and the Coulomb gauge ($\nabla \vec{A} = 0$) is used, we could choose

$$\text{Coulomb gauge } (\nabla \vec{A} = 0$$
$$\vec{A} = \frac{1}{2}\vec{B} \times \vec{r} \qquad (2\text{-}2)$$

After expanding (2-1) and inserting (2-2), we obtain

$$\hat{H} = \frac{\vec{p}^2}{2m_e} + V(\vec{r}) + \frac{eB}{m_e c}\,\vec{r}\times\vec{p} + \frac{e^2}{8m_e c^2}(\vec{B}\times\vec{r})^2$$

$$= \frac{\vec{p}^2}{2m_e} + V(\vec{r}) + \frac{eB}{m_e c}L_z + \frac{e^2B^2}{8m_e c^2}r^2\sin^2\theta \qquad (2\text{-}3)$$

In the above derivation the electron spin is ignored. To include the electron spin and the nuclear spin, we would have to add a few spin-dependent terms. However, such effects have been extensively studied,[44] and we ignore them here. We shall be concerned mainly with the diamagnetic term (the last term in (2-3)) which is proportional to the square of B. In our following discussion we shall consider an electron of Hydrogen in a uniform magnetic field represented by the Hamiltonian,

$$\hat{H} = \frac{\vec{p}^2}{2m_e} - \frac{e^2}{r} + \frac{eB}{m_e c}L_z + \frac{e^2B^2}{8m_e c^2}r^2\sin^2\theta \qquad (2\text{-}4)$$

It is convenient to use atomic units, in which $m_e = e = \hbar = 1$, $c = 137.29$ and $B(\text{a.u.}) = 5.85\times10^{-4}\ B(\text{Tesla})$. The distance is then measured in Bohrs(0.53×10^{-8} cm) and the energy is in Hartrees(27.07ev). With such convention in units, the Hamiltonian in (2-4) is rewritten as

$$\hat{H} = \frac{\vec{p}^2}{2} - \frac{1}{r} + \frac{B}{c}L_z + \frac{1}{8}\left(\frac{B}{c}\right)^2 r^2\sin^2\theta \qquad (2\text{-}5)$$

The first two terms are just the Hydrogen atom without field; the third term is the paramagnetic term; and the fourth and last term is called the diamagnetic term or

quadratic Zeeman term.

We consider states with the same magnetic quantum number ($L_z = m\hbar$), then the paramagnetic term only adds a constant to the energy. Therefore this term is not interesting and can be dropped.[47]

After all these simplifications, we finally arrive at the Hamiltonian we will be using throughout this thesis,

$$\hat{H} = \frac{\vec{P}^2}{2} - \frac{1}{r} + \frac{1}{8}\left(\frac{B}{c}\right)^2 r^2 \sin^2\theta \qquad (2\text{-}6)$$

On examining (2·6), one finds that the parity, the magnetic quantum number, as well as the total energy of the system are conserved quantities. However, this simple looking Hamiltonian is not separable in any known coordinate system. So despite its simplicity in appearence, there seems to be no general solution to quantum or classical equations. It has been argued that this is "the principal remaining problem in the elementary quantum mechanics of one-electron atoms".[44a,49] As we shall see, the rich behaviour displayed by (2·6) is really astonishing.

Now it is helpful to get an idea on the size of the Coulomb term and the diamagnetic term in different states and for varying field strengths.

Let us crudely estimate these quantities on the basis of Hydrogen atom in state $|n\ell m\rangle$. We have

$$\text{Coulomb term} = \langle n\ell m|\frac{1}{r}|n\ell m\rangle \sim \frac{1}{n^2} \qquad (2\text{-}7)$$

but

$$\text{Diamagnetic term} = \langle n\,l\,m | \frac{1}{8}\left(\frac{B}{c}\right)^2 r^2 \sin^2\theta | n\,l\,m \rangle$$

$$= \frac{1}{8}\left(\frac{B}{c}\right)^2 \langle n\,l\,m | r^2 \sin^2\theta | n\,l\,m \rangle$$

$$\sim \frac{1}{8}\left(\frac{B}{c}\right)^2 n^4 \qquad (2\text{-}8)$$

therefore the ratio of the two terms is

$$\frac{\text{Diamagnetic term}}{\text{Coulomb term}} \sim \frac{1}{8}\left(\frac{B}{c}\right)^2 n^6 \qquad (2\text{-}9)$$

Which for highly excited states (n large) and/or high field can be larger than 1. For example if B=6 Tesla, we would get

$$\frac{\text{Diamagnetic term}}{\text{Coulomb term}} \sim 10^{-10} n^6 \qquad (2\text{-}10)$$

Therefore when n $\sim$ 30 the diamagnetic term is comparable with the Coulomb term. We expect something interesting to happen under such conditions!

One can compute classical trajectories from the Hamiltonian (2-6) for various energy and field strength. The result of this will tell us the classical motion of the system. Such calculations have been done.[49] It was found that both regular and irregular motions exist in the system and the parameter region for each different type of motion has been identified.

We are here concerned with the quantum properties of this system. Particularly we want to understand what is the nature of the spectrum under different conditions. Specifically in the following discussion we shall confine ourselves to magnetic field strengths of about a few Tesla where most of the experiments are done.

B. Different Types of Spectrum

Let us examine the experimental spectrum. Fig 2.1 is a typical absorption spectrum, which was obtained by measuring the absorption rate for transitions from ground state of Ba to highly excited states.[50]

Look at the bottom panel first, where the magnetic field B is zero. The energy levels are the familar Rydberg series. The formula for the energy is similar to the Hydrogen atom except a quantum defect correction is needed because of the core interaction. On the right-hand side the energy levels are well separated. As we move to the left the spacing of neighboring levels becomes smaller and smaller. Eventually the spacing is so small that the spectrometer with a finite resolution can not resolve the individual levels. As a result a smooth energy spectrum near the ionization threshold is obtained.

Now look at the second panel from the bottom. On the right side we see that the discrete levels are

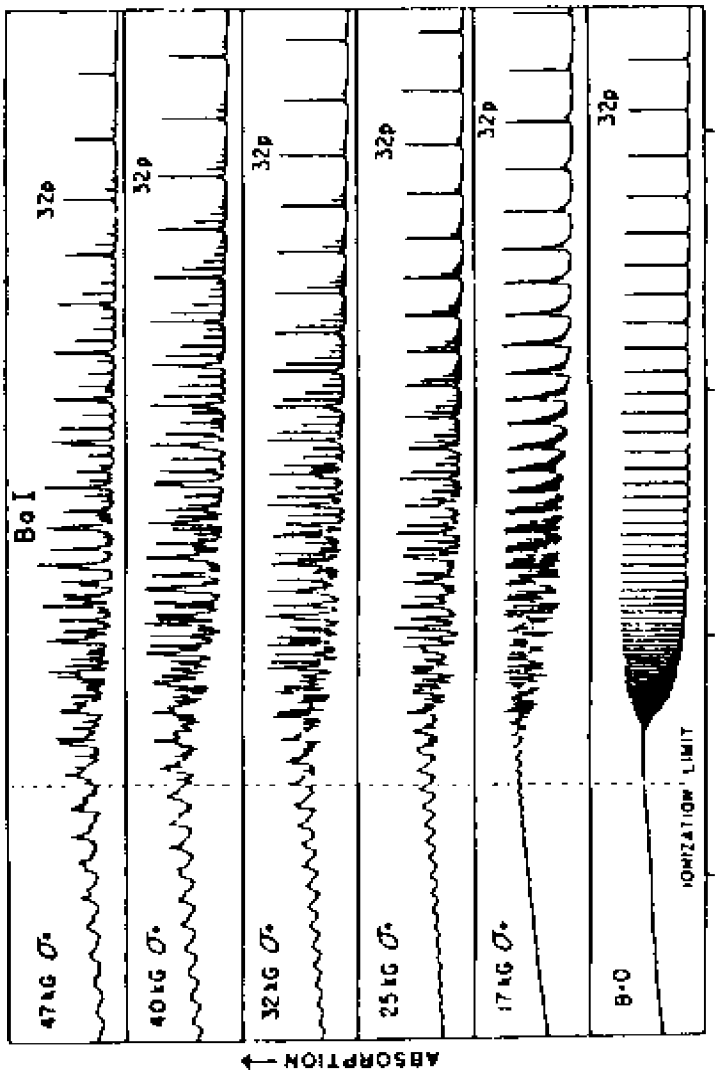

FIGURE 2.1 Absorption spectrum of the Ba I principal series in a magnetic field.

shifted slightly; more importantly each individual line has been split into a family of lines. This part of the spectrum is called low field spectrum. As we move to the left, neighboring groups of lines start to overlap, and the spectrum becomes very complicated. This complicated region of the spectrum is called the intermediate field spectrum. Further as we approach the ionization threshold, we see a simple oscillation imposed on the smooth background. The spectrum in this region is called the ionization threshold spectrum.

The above-described behaviour continues for every higher magnetic field, only that the intermediate field region becomes wider.

Recently the three regions of the spectrum using Hydrogen atom have been studied experimentally with high resolution. Existing theoretical interpretations can account for most of the features in the low field and intermediate field regions. But the seemingly simple spectrum near the ionization threshold has until now been a mystery.

1. Low Field Spectrum

The spectrum in this region can be understood through perturbation theory.

When the field is low, or more precisely when the diamagnetic term is small compared with the Coulomb

term.

$$\frac{\text{Diamagnetic term}}{\text{Coulomb term}} \sim \left(\frac{\beta}{c}\right)^2 n^6 \ll 1 \qquad (2\text{-}11)$$

the diamagnetic term can be considered as a perturbation to the Hydrogen atom.

Let us recall that for a Hydrogen atom, states with given principal number n but with different orbital quantum number ℓ (ℓ=0, 1, ..., n-1) and magnetic quantum number m are degenerate. The lowest order effect of the perturbation is to remove this degeneracy. To obtain the perturbed energy levels and eigenfunctions, one needs to evaluate the matrix elements of Hdiamagnetic between the degenerate states,

$$\langle n\,\ell\,m|H_{diamagnetic}|n\,\ell'\,m\rangle$$

$$= \langle n\,\ell\,m|\frac{1}{8}\left(\frac{\beta}{c}\right)^2 r^2 \sin^2\theta|n\,\ell'\,m\rangle$$

$$\ell,\ell' = |m|, |m|+1, \cdots, n-1 \qquad (2\text{-}12)$$

By diagonalizing the (n-|m|) by (n-|m|) matrix, the shifted energy levels and eigenfunctions can be obtained.[51]

More insight can be gained by using classical perturbation theory.[47 30, 52] We know the electron in a Coulomb field moves on an ellipse which is fixed in space. The shape of the ellipse depends on the energy and angular momentum of the electron. Now if the small diamagnetic term is turned on the ellipse will move and change its

shape in time. We expect the change of the ellipse to be much slower than the electron motion on the instantaneous ellipse. Because of the different time scale of the two motions, an adiabatic approximation can be used to separate these two types of motions. The result of such separation is that the effective equation of motion have only one degree-of-freedom. The motion in this one dimensional problem is a little more complicated than that for a pendulum. Therefore it is not difficult to understand the motion of the system and to obtain the shifted energy levels by semiclassical quantization method.

The results of the above simple descriptions fully account for the spectrum observed experimentally in the low field region.

2. Intermediate Field Spectrum

As we move to higher n states from the low field spectrum, the energy difference between different n manifolds becomes small as

$$\Delta E \sim \frac{1}{n^3} \qquad (2\text{-}13)$$

When this difference is comparable to the energy shifts introduced by the diamagnetic term

$$\langle H_{dia} \rangle \sim \left(\frac{B}{c}\right)^2 n^4 \qquad (2\text{-}14)$$

then the interactions between different manifolds

become important (the matrix elements between different n's can not be ignored any more). We thus obtain the condition for this intermediate region,

$$(\frac{B}{C})^2 n^7 \geq 1 \qquad (2\text{-}15)$$

Classical trajectory calculations have shown a transition from regular motion to irregular motion taking place in this intermediate region.[49d] For example, at field strength B=6 Tesla, trajectories at E=-100cm^{-1} and below are regular, but trajectories above E=-20cm^{-1} are completely chaotic. Trajectories with energies between E=-100cm^{-1} and E=-20cm^{-1} are partially regular and partially chaotic.

The regular and irregular motions displayed by such a system are one of the major reasons that the Hydrogen atom in a magnetic field is a fascinating system to study. Unlike most of the chaotic systems studied so far, this system is experimentally observable!

The quantum spectrum in the intermediate region has not been explained with a simple theory. However, with much effort one can expand the wave functions of the bound states in a carefully chosen basis, then diagonalization of a huge matrix will give the spectrum. This has been done. The computed spectrum is in full agreement with experiment up to 20cm^{-1}.[53]

3. Spectrum Near the Ionization Threshold

So far we have discussed the discrete spectrum of the system. Near and above the ionization threshold, the energy levels become continuous or quasi-continuous. A finite resolution measurement of the spectrum in this region can not fully resolve individual energy levels.

The oscillation in the spectrum shown in Fig. 2.1 was first found experimentally in 1969.[4] Furthermore it was found that the energy spacing(peak to peak) in the spectrum is about 1.5 times that of the energy level spacing (cyclotron frequency) for an electron moving in the same magnetic field only.

This spacing was soon correlated with the motion of the electron perpendicular to the magnetic field.[5] Curiously, the energy spacing is connected with the period of an electron orbit which goes from the nucleus and returns to the nucleus on the z=0 plane,

$$\Delta E = \frac{2\pi\hbar}{T} \qquad (2\ 16)$$

Various arguments were given to explain why this relationship holds.[5,4] However, a quantitative description of the oscillation has never been obtained, a more complete theory is needed.

Not long ago higher resolution experiments on the Hydrogen atom were conducted in this near threshold region.[7] The simple oscillation disappeared and the

observed spectrum becomes extremely oscillatory (It is shown in Fig. 7.4 (f)--page 176)! When a Fourier transform was performed on the spectrum, converting from energy to time as the independent variable, distinct peaks appeared at distinct times. Many of these times were found to correspond to the periods of periodic classical trajectories.[76]

The present theory is developed in view of both the theoretical and experimental situation. The purpose is to understand the oscillatory spectrum near the ionization threshold and to make quantitative calculations of the spectrum. It is also hoped that this study will lead to better understanding of irregular spectra in general.

Here let me describe the physical picture underlying the theory of the spectrum.[1]

When a laser is applied to an atom in the initial localized state, the atom may absorb a photon. When it does so, the electron goes to a near-zero energy Coulomb outgoing wave. This wave propagates away from the nucleus to large distances. At large distances ($r>50a_0$), the outgoing wave-fronts propagate according to semiclassical mechanics, and the wave travels along classical trajectories. Eventually the trajectories and the wave fronts are turned back by the magnetic field; some of the orbits return to the nucleus, and the associated waves (now incoming) interfere with the outgoing wave to produce the observed oscillations.

Since the trajectories are chaotic in this range of energy, the closed orbits that begin and end at the nucleus are isolated. For each closed orbit, i, when the energy changes, the phase difference between the outgoing and incoming waves changes according to

$$\Delta phase_i = \frac{T_i \Delta E}{\hbar} \qquad (2\text{-}17)$$

With this it is easy to understand the empirical formula (2-16).

The above picture can be made complete and quantitative. It is developed in detail with rigorous mathematical formulas in the following Chapters. The results of calculations with this new theory are presented and compared with experimental results in Chapter VII.

CHAPTER III

BASIC FORMULAS FOR SPECTRA

In this chapter, I shall define the theoretical quantities corresponding to the measured absorption spectrum of an atom. These quantities are oscillator strength and transition rate. Their calculation is the goal of this study. The results of this calculation will be compared with experimental observations in later chapters.

In section A, the relevant quantities will be defined, and then in section B, these quantities will be related to matrix elements of propagators and Green's functions. The physical meaning of the resulting formulas will also be discussed.

A. Photon Absorption and Oscillator Strength Density

Suppose we are given a collection of atoms in an initial quantum state ψ_i, and we apply a radiation field to these atoms; at what rate will the atoms make transitions to other quantum states? The rate of absorption of photons, or the rate of production of atoms in excited states is proportional to the intensity of the radiation field $I(\omega)$ and to the number of atoms in the initial stste, N_i:

$$\frac{dN_f}{dt} = B_{fi} \cdot N_i \cdot I(\omega) \qquad (3\text{-}1)$$

Here $I(\omega)d\omega$ is the energy flux density(energy per unit area per unit time) in the frequency range $d\omega$ (It is assumed that the range of energies in the photon beam is large compared to the natural linewidth for the transition.). In many textbooks on quantum mechanics[55], it is shown that B_{fi} is given by

$$B_{fi} = \frac{4\pi^2 e^2}{\hbar^2 C} \cdot |\langle \psi_f | D | \psi_i \rangle|^2 \qquad (3\text{-}2)$$

D is called the dipole operator, and is the projection of the electronic coordinate $\vec{r}$ in the polarization direction of the field; ψ_i and ψ_f are the initial and final quantum states of atom; e is the charge of electron; C is the speed of light; $\hbar$ is the Planck's constant over 2π .

The formulas above are derived by using a classical description of the electromagnetic field and a dipole approximation to the transition matrix element. The classical treatment of the field is a good approximation when the photon density is large. The dipole approximation is accurate if the size of the initial or final atomic wave function is much smaller than the wave length of the electromagnetic field. Both of these conditions are satisfied in the present case.

While the quantities defined above are closely

related to experimental measurement, theoretical calculations most often focus upon the oscillator strength. The reasons are manifold: the oscillator strength is dimensionless; it typically has values close to unity; it is the analogue of a classical quantity; and finally the oscillator strength obeys a well-known sum rule. The oscillator strength is defined as

$$f_{fi} = \frac{2 m_e (E_f - E_i)}{\hbar^2} |\langle \psi_f | D | \psi_i \rangle|^2 \qquad 3\text{-}3)$$

Where m_e is the mass of the electron; E_i and E_f are the energies of the initial and final states. Thus the transition rate and the oscillator strength are proportional to each other.

The oscillator strength is appropriate for transitions from one discrete quantum state to another. However when the final quantum state lies in the continuum, the transition does not go to a particular final state, but to a group of final states in the continuum with energy close to E_f . Similarly, when transitions occur to bound states close to the ionization threshold, the density of states is very high, and the energy spacing between the states is less than the uncertainty in the photon energy. Again, therefore, transitions occur to a group of final states. It is therefore appropriate to define the oscillator strength density(the oscillator strength per unit energy) $Df(E_f)$ as

$$\mathcal{D}f(E_f) = \frac{2me(E_f - E_i)}{\hbar^2} |\langle \psi_f | D | \psi_i \rangle|^2 \rho(E_f) \quad (3\text{-}4)$$

In eq.(3-4), $\rho(E_f)$is the density of final states(Number of distinct quantum states per unit energy).

For discrete, well-resolved transitions, the density of final states is $\rho(E_f) = \delta(E_f - E_n)$, and the integral of the oscillator-strength-density over a narrow range of energy is equal to the oscillator strength:

$$\int_{E_n - \epsilon}^{E_n + \epsilon} \mathcal{D}f(E_f)\, dE_f = f_{fi} \quad (3\text{-}5)$$

For $\int_{E_n - \epsilon}^{E_n + \epsilon} \mathcal{D}f(E_f)\, dE_f = f_{fi}$ of fields, near the ionization threshold, the oscillator strength goes to zero as n^{-3}; on the other hand, the density of states goes to infinity as n^3 . The product of these two, that is, the oscillator strength density, has a finite limit.

For all these reasons, therefore, the oscillator strength density is the proper quantity to pursue. This definition of oscillator strength density in (3-4) is the beginning of our story. In the next section, alternative formulas for the oscillator strength density will be derived, and connections among them will be explored. Later we will find that these alternative formulas lead to natural approximations which provide a means of computing $\mathcal{D}f(E_f)$.

B. Formal Expressions of the Oscillator Strength Density and Their Relationship

The definition of oscillator strength density is given by (3-4) in last section. From the definition, it is clear that if the initial and final wave-functions ψ_i and ψ_f are known, it is then possible to compute the oscillator strength density D_f. For simpler systems than the present one, this procedure can be carried out: for example, the wave-functions could be computed by expansion in a basis, or by a semiclassical approximation. In the present case, neither of these methods can be used. Near the ionization threshold, the density of states goes to infinity, so no finite basis can fully represent the states. Even if expansion in a basis could be used, it would provide little insight(and it wouldn't be much fun). In addition, since the classical motion is irregular, we do not know any formula for the classical limit of the wave-functions ψ_f, and we do not even know whether a classical limit exists at all. Therefore in the present case we are forced to seek alternative formulas and methods for calculating the oscillator strength density. This search will lead to new ideas and understanding of the quantum behavior of classically irregular systems.

In this section, I shall write the oscillator strength density in two forms. One is in terms of the

time-dependent propagator K and the other is in terms of the Green's function G^+.

1. Definition of Time-Dependent Propagator K

Suppose a quantum mechanical Hamiltonian $H_{op}(-i\hbar\frac{\partial}{\partial q}, q)$ is given; then the time dependent propagator $K(q'',t'';q',t')$ is defined as the solution to the Schroedinger equation

$$i\hbar\left(\frac{\partial K(q'',t'';q',t')}{\partial t''}\right)-H_{op}(-i\hbar\frac{\partial}{\partial q''},q'')\cdot K(q'',t'';q',t')=0 \qquad (3\text{-}6a)$$

with the initial condition

$$\lim_{t''\to t'} K(q'',t'';q',t')=\delta(q''-q') \qquad (3\text{-}6b)$$

It is clear that because eq. (3-6a) is a first order differential equation in t'', with the initial condition in (3-6b), the propagator $K(q'',t'';q',t')$ is uniquely defined.

All solutions to the time dependent Schroedinger equation can be found from the propagator. If $\psi(q',t')$ is the wave function at time t', then the wave function at any time t'' is

$$\psi(q'',t'')=\int dq'\cdot K(q'',t'';q',t')\,\psi(q',t') \qquad (3\text{-}7)$$

This is easily checked from (3-6).

A particular result of eq. (3-7) is the group property of the propagator. Taking in (3-7) $\psi(q',t')$ as

$K(\xi',t';\xi,t)$ (Where ξ, t appear as parameters on both sides of eq. (3-7)), then we get

$$K(\xi'',t'';\xi,t)=\int d\xi' K(\xi'',t'';\xi',t') K(\xi',t';\xi,t) \qquad (3\text{-}8)$$

Eq. (3-8) simply states the fact that a wave propagating from t to t'' is equivalent to the wave propagating from t to any intermediate time t' and then from t' to t''.

If all the eigenfunctions of the Hamiltonian H_{op} are known, the propagator K can be expanded as

$$K(\xi'',t'';\xi',t')=\sum_E \psi_E(\xi'')\,\psi_E^*(\xi')\,\rho(E)\,e^{-iE(t''-t')/\hbar}\,dE \qquad (3\text{-}9)$$

Each term in (3-9) satisfies the Schroedinger eq. (3-6a). The completeness relation of the eigenfunction gives the right initial condition for K, the eq. (3-6b).

2. Definition of Time Independent Outgoing Green's Function G^+

If the Hamiltonian H_{op} does not depend on time, then define the outgoing Green's function

$$G^{+}(\beta'',\beta',E)=\frac{1}{i\hbar}\int_0^{\infty}dt\;\; K(\beta'',t;\beta',0)\exp\left[\frac{iEt}{\hbar}\right]$$

(3-10)

Where $E=E+\epsilon i$ and $\epsilon\to+0$.

The equation satisfied by G^{+} is just the time-independent Schroedinger equation with a point source.

$$\begin{aligned}
&\left[E-H_{op}\left(-i\hbar\frac{\partial}{\partial\beta''},\beta''\right)\right]G^{+}(\beta'',\beta',E)\\
&=\frac{1}{i\hbar}\int_0^{\infty}dt\left[E-H_{op}\left(-i\hbar\frac{\partial}{\partial\beta''},\beta''\right)\right]K(\beta'',t;\beta,0)\exp\left[\frac{iEt}{\hbar}\right]\\
&=\frac{1}{i\hbar}\int_0^{\infty}dt\,\exp\left[\frac{iEt}{\hbar}\right]\left[E-i\hbar\frac{\partial}{\partial t}\right]K(\beta',t;\beta',0)\\
&=\int_0^{\infty}dt\left[\frac{-iE}{\hbar}\exp\left[\frac{iEt}{\hbar}\right]K-\exp\left[\frac{iEt}{\hbar}\right]\frac{\partial}{\partial t}K\right]\\
&=-\int_0^{\infty}dt\left[K\frac{\partial}{\partial t}\exp\left[\frac{iEt}{\hbar}\right]+\exp\left[\frac{iEt}{\hbar}\right]\frac{\partial}{\partial t}K\right]\\
&=-\int_0^{\infty}dt\,\frac{\partial}{\partial t}\left[K\exp\left[\frac{iEt}{\hbar}\right]\right]\\
&=-K(\beta'',t;\beta',0)\exp\left[\frac{iEt}{\hbar}\right]\Big|_0^{\infty}\\
&=K(\beta'',0;\beta',0)\\
&=\delta(\beta''-\beta')
\end{aligned}$$

(3-11)

The eigenfunction expansion of the Green's function is well known,

$$G^{+}(\beta'',\beta',E)=\oint\frac{\psi_E(\beta'')\,\psi_{E'}^{*}(\beta')\,\rho(E')\,dE'}{E-E'}\qquad(3-12)$$

Eq. (3-12) can be verified by combining eq. (3-9)

and eq. (3-10), or by using the differential equation for G^+ in (3-11).

3. The Oscillator Strength Density in Terms of the Propagator K

The oscillator strength density is related to matrix elements of the propagator by the formula

$$Df(E_f) = \frac{2m_e(E_f - E_i)}{\hbar^2} \cdot \frac{1}{2\pi\hbar} \int_{-\infty}^{+\infty} dt \, \langle \psi_i D | K | D \psi_i \rangle e^{iE_f t/\hbar} \tag{3-13}$$

To prove this, we recall the definition of the oscillator strength density in (3-4) and compare it with (3-13). Then all I need to prove is the following relation,

$$|\langle \psi_f | D | \psi_i \rangle|^2 \rho(E_f) = \frac{1}{2\pi\hbar} \int_{-\infty}^{+\infty} \langle \psi_i D | K | D \psi_i \rangle e^{iE_f t} dt \tag{3-14}$$

To prove (3-14), we assume the Hamiltonian is time-independent, so the eigenfunction expansion of the propagator $K(\xi'', t; \xi', 0)$ can be used. Further the δ-function relation is valid,

$$\frac{1}{2\pi\hbar} \int_{-\infty}^{+\infty} \exp\left[i(E_f - E)t/\hbar \right] dt = \delta(E_f - E) \tag{3-15}$$

Now start from the right hand side of eq. (3-14), use the eigenfunctionn expansion of K, and integrate

over t first, and then over E *:

$$\frac{1}{2\pi\hbar}\int_{-\infty}^{+\infty}\langle\psi_i D|K(\vec{\delta}'',t;\vec{\delta}',0)|D\psi_i\rangle e^{iE_f t/\hbar}\,dt$$

$$=\frac{1}{2\pi\hbar}\int_{-\infty}^{+\infty}\langle\psi_i D|\sum_E \psi_E(\vec{\delta}'')\,\psi_E^*(\vec{\delta}')\,\rho(E)\,e^{-iEt/\hbar}\,dE|D\psi_i\rangle e^{iE_f t/\hbar}dt$$

$$=\langle\psi_i D|\sum_E \psi_E(\vec{\delta}'')\,\psi_E^*(\vec{\delta}')\,\rho(E)\,\delta(E_f-E)\,dE\,|D\psi_i\rangle$$

$$=\langle\psi_i D|\psi_{E_f}(\vec{\delta}'')\,\psi_{E_f}^*(\vec{\delta}')\,\rho(E_f)|D\psi_i\rangle$$

$$=\langle\psi_i D|\psi_f\rangle\langle\psi_f|D\psi_i\rangle\,\rho(E_f)$$

$$=|\langle\psi_f|D|\psi_i\rangle|^2\,\rho(E_f)$$

Q.E.D

(3-16)

Eq. (3-13) involves integration over time from minus infinity to plus infinity. A simpler form can be obtained by using the time-reversal symmetry of the propagator K.

I will first prove the time-reversal relation on K.

$$K(\vec{\delta}'',-t;\vec{\delta}',0)=K^*(\vec{\delta}',t;\vec{\delta}'',0) \qquad (3\text{-}17)$$

---

* We use a slightly unconventional but very clear notation:

$$\langle\psi_i D|K|D\psi_i\rangle$$

$$\equiv\langle\psi_i D|K(\vec{\delta}'',t;\vec{\delta}',0)|D\psi_i\rangle$$

$$\equiv\langle\psi_i D(\vec{\delta}'')|K(\vec{\delta}'',t;\vec{\delta}',0)|D\psi_i(\vec{\delta}')\rangle$$

$$\equiv\iint d\vec{\delta}''d\vec{\delta}'\,\psi_i^*(\vec{\delta}'')D^*(\vec{\delta}'')\,K(\vec{\delta}'',t;\vec{\delta}',0)\,\psi_i(\vec{\delta}')D(\vec{\delta}')$$

Note also

$$\langle D\psi_i| = \langle\psi_i D|$$

This can be accomplished by examining the eigenfunction expansion (3-9),

$$
\begin{aligned}
&K(\xi'', -t; \xi', 0) \\
&= \int \psi_E(\xi'')\, \psi_E^*(\xi')\, \rho(E)\, e^{+iEt/\hbar}\, dE \\
&= \left[\int \psi_E(\xi')\, \psi_E^*(\xi'')\, \rho(E)\, e^{-iEt/\hbar}\, dE \right]^* \\
&= K^*(\xi', t; \xi'', 0)
\end{aligned}
$$

Q.E.D

From this symmetry, $D_f(E_f)$ can be written as an integration over positive time only:

$$
\begin{aligned}
&\int_{-\infty}^{0} \langle \psi_i(\xi'') D | K(\xi'', t; \xi', 0) | D \psi_i(\xi') \rangle e^{iE_f t/\hbar}\, dt \\
&= \int_{+\infty}^{0} \langle \psi_i(\xi'') D | K(\xi'', -\tau; \xi', 0) | D \psi_i(\xi') \rangle e^{-iE_f \tau/\hbar}\, d(-\tau) \\
&= \int_{0}^{\infty} \langle \psi_i(\xi'') D | K(\xi'', -\tau; \xi', 0) | D \psi_i(\xi') \rangle e^{-iE_f \tau/\hbar}\, d\tau \\
&- \left[\int_0^{\infty} \langle \psi_i(\xi') D | K(\xi', \tau, \xi'', 0) | D \psi_i(\xi'') \rangle e^{iE_f \tau/\hbar} \right]^*
\end{aligned}
$$

(3-18)

With the help of (3-18),

$$
\begin{aligned}
D_f(E_f) &= \frac{2m_e(E_f - E_i)}{\hbar^2} \frac{1}{2\pi\hbar} \left[\int_0^{\infty} + \int_0^{\infty *} \right] \\
&= \frac{2m_e(E_f - E_i)}{\pi\hbar^3} \mathrm{Re} \int_0^{\infty} \langle \psi_i D | K | D \psi_i \rangle e^{iE_f t/\hbar}\, dt
\end{aligned}
$$

(3-19)

To see the meaning of eq. (3-19), consider the

action of the propagator on the function $D\psi_i(\theta)$:

$$\psi(\theta,t) = \int d\theta' K(\theta,t;\theta',0) D\psi_i(\theta') \qquad (3\text{-}20)$$

So $\psi(\theta,t)$ is a solution to the time-dependent Schroedinger equation with the initial condition

$$\psi(\theta,0) = D\psi_i(\theta) \qquad (3\text{-}21)$$

These formulas (3-19)-(3-21) suggest a procedure for computing the oscillator strength density: for the given initial wave function and polarization of light, solve the time-dependent Schroedinger equation for the wave function $\psi(\theta,t)$ with initial condition $D\psi_i(\theta)$; then compute the "correlation function" $\langle \psi_i D | \psi(\theta,t) \rangle$, finally do the half Fourier transformation of this "correlation function". The result will be the desired oscillator strength density.

It is clear from this procedure that the initial wave packet $D\psi_i$ propagates and evolves in space. Those parts of the wave ψ which come back and overlap with $D\psi_i$ at a later time will contribute to the oscillator strength density.

As mentioned above, $Df(E\hbar)$ is a half Fourier transform of the correlation function, and in principle the integration should involve an infinite range of t. If the integration is cut off at some finite upper limit, T, the effect is that an averaged or smoothed oscillator strength density is computed. In Appendix A

it is shown that the resulting averaged oscillator strength density $\overline{Df}(E_f)$ is equal to the exact oscillator strength density averaged with a weighting function over a range of energies of width $\hbar/T$.

$$\overline{Df}(E_f) = \int Df(E') \cdot \mathcal{J}_T(E_f - E')\, dE' \qquad (3\text{-}22)$$

The measured spectrum involves just such an average: the width in energy of the photon beam is large compared to the spacing between the states. It follows that we can account for the observations using a correlation function defined only over finite times. If the experimental resolution is ΔE, then the required upper time limit T for computing the correlation function is approximately $\hbar/\Delta E$.

However, following the evolution of a time-dependent wave packet is not easy, and in general it is impossible to do this in a satisfactory way. Wave packets spread and become very complicated in a short time.

In the next section, a time-independent formulation based on the Green's function is derived. It will be seen that much of the physical meaning of the time-dependent formulas is retained. But the time-independent formulation is clearer, more complete, more in accord with the experimental situation, and much easier to use.

4. The Oscillator Strength Density in Terms of the Green's Function G^+

At this point, it takes no effort to find the desired Green's function formula. In fact, combining eq. (3 10) and eq. (3 19) gives us the result:

$$D\mathcal{H}(E_f) = -\frac{2m_e(E_f - E_i)}{\pi\hbar^2}\, Im\langle \psi_i D | G^+ | D\psi_i \rangle \qquad (3\text{-}23)$$

To understand eq. (3·23), one needs to understand the meaning of Green's function $G^+(\vec{s}'', \vec{s}', E_f)$ in configuration space. It can be shown[42] that $G^+(\vec{s}'', \vec{s}', E_f)$ represents the probability amplitude of finding the particle at $\vec{s}''$ for a particle launched at $\vec{s}'$ in all directions with energy E_f.

This interpertation becomes much more clear if the semiclassical approximation for G^+ is used. In this approximation, each classical trajectory of energy connecting $\vec{s}'$ to $\vec{s}''$ contributes a term

$$\mathcal{B}(\vec{s}'', \vec{s}')\exp[i\mathcal{S}(\vec{s}'', \vec{s}')/\hbar] \qquad (3\text{-}24)$$

to the Green's function($\mathcal{S}$ is the classical action for the trajectory and $\mathcal{B}$ is an amplitude that will be defined later).

Now ψ_i is a wave function localized around the nucleus, so let us imagine the extreme case in which $D\psi_i$ is very localized and can be regared as a δ-function,

then from (3-23) we have

$$D_f(E_f) \sim G^+(0,0,E_f) \qquad (3\text{-}25)$$

The oscillator strength density in this extreme case would be the probability amplitude that the electron is emitted from the nucleus, travels along a classical trajectory, and subsequently returns to the nucleus.

More generally, we may regard $D\psi_i$ as a "source" of waves. The Green's function G^+ propagates those waves forward at fixed energy; in the semiclassical approximation, the waves propagate along classical trajectories. Some of those trajectories subsequently return, with their associated waves, to the vicinity of the nucleus, and they overlap with the source. Eq. (3-23) tells us that the oscillator strength density $D_f(E_f)$ is proportional to the overlap of the source with these propagated waves. In particular the observed oscillations in the spectrum result from interference of outgoing waves of the source with returning waves propagated by G^+.

More detailed formulas and explanation will be given later.

C. Summary

1. The observed absorption spectrum(rate of absorption of photons, or rate of production of the excited atoms or ions) is proportional to the oscillator strength density $Df(E_f)$ defined in eq. (3-4).

$$Df(E_f) = \frac{2m_e(E_f - E_i)}{\hbar^2} |\langle \psi_f | D | \psi_i \rangle|^2 \rho(E_f) \qquad (3\text{-}4)$$

2. The oscillator strength density is related to the initial state of the system ψ_i, to the projection of the dipole operator onto the direction of polarization of light, D, and to the Green's function G^+ of the system, through eq. (3 23)

$$Df(E_f) = -\frac{2m_e(E_f - E_i)}{\pi\hbar^2} Im\langle \psi_i D | G^+ | D \psi_i \rangle \qquad (3\text{-}23)$$

The work in the next two chapters will be oriented toward calculation of the matrix element in eq. (3-23). First it is necessary to study the Hydrogen atom in the absence of magnetic fields; second, we need to learn some semiclassical mechanics to construct G^+. These will be the topics of chapters IV and V.

CHAPTER IV

HYDROGEN ATOM WITHOUT FIELDS

In chapter III, I have related the experimentally measured spectrum to the oscillator strength density, and further I have expressed the oscillator strength density in terms of the time-independent Green's function. My task in this chapter and the next one is to construct the Green's function for the particular system.

To make further progress, appropriate approximations have to be considered. As I have said in section 0.A. , the central idea is the division of space into two regions: close to the nucleus the magnetic field can be neglected, and the wave-functions are those associated with a pure Coulomb field; far from the nucleus, the wavelength is short compared to the range over which the potential energy changes, and a semiclassical approximation to the wave functions can be used.

In this chapter, I will discuss the first of these two approximations. The justification of the approximation is discussed first; then partial wave analysis and scattering in a Coulomb field follow; and finally, a summary is given.

A. Justification for the Neglect of Magnetic Field Close to Nucleus

In general the effects of magnetic field and those of the Coulomb field are comparable, and in the Hamiltonian

$$H = \frac{\vec{p}^2}{2} - \frac{1}{r} + \frac{1}{8}\left(\frac{B}{c}\right)^2 (x^2+y^2) \tag{4-1}$$

neither term can be neglected. But if the contribution of each term is examined more carefully, we find that the Coulomb field dominates the magnetic field close to the nucleus. For example, if the magnetic field is 6 Tesla, and if the electron stays within 100 Bohrs of the nucleus, then the ratio of magnetic term to the Coulomb term would be

$$\begin{aligned} \frac{\text{diamagnetic term}}{\text{Coulomb term}} &= \frac{\frac{1}{8}\left(\frac{B}{c}\right)^2 (x^2+y^2)}{\frac{1}{r}} \\ &\leq \frac{B^2 r^3}{8c^2} \\ &= \frac{1}{8}\,\frac{\left(\frac{6}{1\,2\,0}\right)^2 100^3}{137^2} \\ &\approx 8.2 \times 10^{-4} \end{aligned} \tag{4-2}$$

(which is much smaller than 1.) Therefore we think the neglect of the diamagnetic term close to the nucleus is

well justified. (Of course, the ultimate justification rests upon the comparison between experimental measurements and theoretical predictions. We will make these comparisons in the last two chapters.).

In the rest of this chapter, the discussions will consider the Hydrogen atom in the absence of fields. In particular we need formulas for the wave-function of a near-zero energy electron as it escapes and later returns to the nucleus.

B. Initial Wave Function and Coulomb Green's Function Near the Ionization Threshold

In this section B, solutions of the Hydrogen atom, both bound and near the ionization threshold, are found. From them the initial quantum wave function and the Green's function in a Coulomb field at the ionization threshold are constructed.

1. Bound State Solutions: Initial Quantum Wave Function

The full Hamiltonian in (4.1), after dropping the diamagnetic term, is the Hamiltonian of a Hydrogen atom, denoted H_c,

$$H_c = \frac{1}{2}\vec{p}^{\,2} - \frac{1}{r} \qquad (4.3)$$

The solutions to the eigenvalue equation

$$H_c \phi = E \phi \qquad (4\text{-}4)$$

are discussed in detail in standard Quantum Mechanics textbooks[55] . The eigenfunctions can be written as a product of a radial wave function and a spherical harmonic function

$$\phi_{nlm} = R_{nl}(r)\ Y_{lm}(\theta, \varphi) \qquad (4\text{-}5)$$

The definitions and phase conventions we use for these functions are the ones given by Bethe and Salpeter[56] . For convenience, some of them are listed explicitly in Appendix B.

As discussed in chapter III, the Hydrogen atom is excited with a laser beam from initial state ψ_i to states near the ionization threshold. What are these states ψ_i ? They are precisely these bound quantum state ϕ_{nlm} in (4-5) (in atomic beam, essentially all of the Hydrogen atoms are in the ground state ϕ_{100} . The atoms are excited with one laser from the ground state to a low excited state, such as $2P_z$; then with a second laser, they are excited to states near the ionization threshold. It is the low excited state that we call the "initial" state ψ_i).

One point to mention here is a restriction on these initial states. We know that for quantum state

$\phi_{n\ell m}$, the average radius of the electron is n^2. To have consistency with the neglect of the magnetic field close to nucleus, n can not be too large ($n<10$). Since we are really interested in those first few quantum states as the initial state ψ_i, the restriction is not a problem.

2. Solution Near Ionization Threshold

In general the radial wave functions $R_{n\ell}(r)$ in eq. (4-5) can be written in terms of confluent hypergeometric functions. However, the solution near the ionization threshold is much simpler.

We shall show that the zero-energy radial wave functions are given by the simple formula,

$$R_\ell^{0,reg}(r) = J_{2\ell+1}(\sqrt{8r})/\sqrt{8r} \qquad (4\text{-}6a)$$

$$R_\ell^{0,irreg}(r) = H_{2\ell+1}^{(1)}(\sqrt{8r})/\sqrt{8r} \qquad (4\text{-}6b)$$

Proof of this is given below; those who accept the result can skip to section IV.B.3

The radial wave function R_ℓ^E satisfies

$$\left[E + \frac{1}{2}\frac{1}{r^2}\frac{d}{dr}r^2\frac{d}{dr} - \frac{\ell(\ell+1)}{2r^2} + \frac{1}{r}\right]R_\ell^E(r) = 0 \qquad (4\text{-}7)$$

When E is set to zero, and the derivatives are written out in eq. (4-7), we obtain

$$\left[\frac{1}{2}\frac{d^2}{dr^2} + \frac{1}{r}\frac{d}{dr} - \frac{l(l+1)}{2r^2} + \frac{1}{r}\right] R_l^0(r) = 0 \tag{4-8}$$

To find solutions for eq. (4 8), we make a change of variables: let

$$R_l^0(r) \equiv \frac{B_l(x)}{x} \tag{4-9a}$$

and

$$x \equiv \sqrt{8r} \tag{4-9b}$$

The following relations on derivatives are not difficult to find from (4 9):

$$\frac{dR_l^0(r)}{dr} = \frac{4}{x^3}\left[x\frac{dB_l(x)}{dx} - B_l(x)\right] \tag{4-10a}$$

$$\frac{d^2R_l^0(r)}{dr^2} = \frac{16}{x^7}\left[x^4\frac{d^2B_l(x)}{dx^2} - 3x^3\frac{dB_l(x)}{dx} + 3x^2B_l(x)\right] \tag{4-10b}$$

Combining eqs. (4-8) and (4-10), we have the differential equation for the function $B_l(x)$:

$$x^2\frac{d^2B_l(x)}{dx^2} + x\frac{dB_l(x)}{dx} + (x^2 - \nu^2)B_l(x) = 0 \tag{4 11a}$$

with

$$\nu = 2\ell + 1 \qquad (4\text{-}11b)$$

Eq. (4-11a) is the standard equation of Bessel functions[57]. The solutions for $B_\ell(\chi)$ are the regular Bessel function $J_{2\ell+1}(x)$ and the irregular function such as $H^{(1)}_{2\ell+1}(x)$ (called the Hankel function). Transforming back to variable r, the solutions to (4-8) are (4-6).

3. Estimate of Accuracy for $E \neq 0$

Eq. (4-6) are exact at E=0. We will use these formulas as approximations also for other E near zero. As we shall show below, for energy not too different from zero, the error made by replacing the exact wave function at energy E with the wave function at zero-energy is quite small.

Our formulas will involve a dipole matrix element between the regular Bessel function and the initial radial function. Therefore we are concerned about the difference between the exact regular wave function $R^E_\ell(r)$ and the zero-energy regular wave function $R^0_\ell(r)$ for $r \leq r_c = n^2 = 4$.

From the asymptotic formula for the Bessel function $J_\nu(x)$,

$$J_\nu(x) \sim \sqrt{\frac{2}{\pi x}} \cos\left(x - \frac{\nu}{2}\pi - \frac{\pi}{4}\right) \qquad (4\text{-}12)$$

we obtain the asymptotic formula for $R^0_{\ell}(r)$,

we obtain the asymptotic formula for $R^0_{\ell}(r), -\frac{\pi}{4})$

$$\sim \frac{1}{2^{\frac{1}{4}}\cdot\pi^{\frac{1}{2}}}\ \frac{1}{r^{\frac{1}{4}}}\cos\left(\int_0^r p_r dr - \frac{(2\ell+1)\pi}{2} - \frac{\pi}{4}\right)$$

(4-13a)

When $E \neq 0$, the phase of $R^E_{\ell}(r)$ would differ from that of $R^0_{\ell}(r)$, by

$$\Delta\text{phase} = \int_0^{r_0} (p_r^E - p_r^0)\,dr$$

$$= \int_0^{r_0} \left(\sqrt{2E + \frac{2}{r}} - \sqrt{\frac{2}{r}}\right) dr \qquad (4\text{-}13b)$$

If r_0 is taken as 5 au, then expanding the integrand in powers of energy E, the phase difference is estimated as

$$\Delta\text{phase} \sim \frac{\sqrt{2}}{3} r_0^{\frac{3}{2}} \cdot E$$

$$\sim 5.27 \cdot E$$

(4-13c)

For $|E| \leq 100\,cm^{-1}$, for example, the phase difference would be smaller than 2.4×10^{-3}. This number gives us an absolute error estimate for the dipole matrix element. These matrix elements have magnitudes between 1 and 20 (atomic units), and therefore the relative error in the matrix elements should be no more than a few tenths of a percent.

4. Coulomb Green's Function $G_c^+(\vec{r},\vec{r}')$ Near the Ionization Threshold

The Green's function in a Coulomb field at the ionization threshold $G_c^+(\vec{r},\vec{r}')$ is important in constructing the general Green's function for the atom in strong magnetic field as we shall see in chapter VI. In this section, $G_c^+(\vec{r},\vec{r}')$ will be found explicitly.

Recall the differential equation (3-11) that a Green's function satisfies. If the Hamiltonian is chosen as H_c in (4-3) and the energy E is set to zero, we have the equation for $G_c^+(\vec{r},\vec{r}')$,

$$-H_c \cdot G_c^+(\vec{r},\vec{r}') = \delta(\vec{r}-\vec{r}') \qquad (4\ 14)$$

Again because of the rotational symmetry in H_c, the Green's function $G_c^+(\vec{r},\vec{r}')$ can be decomposed into angular functions and radial functions,

$$G_c^+(\vec{r},\vec{r}') = \sum_{lm} Y_{lm}^*(\theta',\varphi') \cdot g_l(r,r')\, Y_{lm}(\theta,\varphi) \qquad (4\ 15a)$$

In this summation, $g_l(r,r')$ is a function of the radial variables r and r', but not of the angular variables; it depends upon the angular momentum l, but not on m. I shall show that $g_l(r,r')$ is given by

$$g_\ell(r,r') = -2\pi i \frac{J_{2\ell+1}(\sqrt{8}r_<)\, H^{(1)}_{2\ell+1}(\sqrt{8}r_>)}{\sqrt{r_< r_>}}$$

(4-15b)

To prove this, write the δ-function in polar coordinate r, θ, φ.

$$\delta(\vec{r}-\vec{r}') = \frac{1}{r^2}\,\delta(r-r')\,\delta(\cos\theta-\cos\theta')\,\delta(\varphi-\varphi')$$

(4-16)

and use the orthogonality relation for the spherical harmonics[58],

$$\sum_{\ell m} Y^*_{\ell m}(\theta',\varphi')\, Y_{\ell m}(\theta,\varphi) = \delta(\cos\theta-\cos\theta')\,\delta(\varphi-\varphi')$$

(4-17)

We can obtain an equation for $g_\ell(r,r')$ from (4-14). On the left side,

$$\begin{aligned} &-H_c\; G_c^+(\vec{r},\vec{r}') \\ &= \sum_{\ell m} Y^*_{\ell m}(\theta',\varphi')\,[-H_c]\cdot g_\ell(r,r')\, Y_{\ell m}(\theta,\varphi) \\ &= \sum_{\ell m} Y^*_{\ell m}(\theta',\varphi')\, Y_{\ell m}(\theta,\varphi)\left[\frac{1}{2}\frac{d^2}{dr^2} + \frac{1}{r}\frac{d}{dr} - \frac{\ell(\ell+1)}{2r^2} + \frac{1}{r}\right] g_\ell(r,r') \end{aligned}$$

(4-18)

and on the right side,

$$\delta(\vec{r}-\vec{r}') = \frac{\delta(r-r')}{r^2}\,\delta(\cos\theta-\cos\theta')\,\delta(\varphi-\varphi')$$

$$= \frac{\delta(r-r')}{r^2}\sum_{lm} Y^*_{lm}(\theta',\varphi')\,Y_{lm}(\theta,\varphi)$$

(4-19)

Since each Y_{lm} is independent of every other, the coefficients of Y_{lm} in (4 18) and (4 19) must be all equal. Hence we have equation for $g_l(r,r')$,

$$\left[\frac{1}{2}\frac{d^2}{dr^2}+\frac{1}{r}\frac{d}{dr}-\frac{l(l+1)}{2r^2}+\frac{1}{r}\right]g_l(r,r') = \frac{\delta(r-r')}{r^2}$$

(4-20)

This is the radial Schroedinger equation with a point source at r'. Now let me show that the solutions to (4-20) can be found from the solutions of the radial Schroedinger equation (4 8).

If G_c^+ is required to be an outgoing Green's function, then $g_l(r,r')$ must be an outgoing function. Further $g_l(r,r')$ is required to be finite everywhere. It is not difficult to see that

$$g_l(r,r') = A\cdot\frac{J_{l+1/2}(\sqrt{8}r_<)}{\sqrt{8}r_<}\;\frac{H^{(1)}_{l+1/2}(\sqrt{8}r_>)}{\sqrt{8}r_>}$$

(4 21)

is a possible solution. In (4-21),

$$r_< = \min(r,r')$$

(4-22a)

$$r_> = \max(r,r')$$

(4-22b)

and A is a constant.

When $r \neq r'$, then the right hand side of eq. (4-20) is zero, so the expression in (4-21) satisfies (4 20) since $J_{l+\frac{1}{2}}(\sqrt{8}r)/\sqrt{8}r$ and $H^{(1)}_{l+\frac{1}{2}}(\sqrt{8}r)/\sqrt{8}r$ are solutions of (4 8). Also $J_{l+\frac{1}{2}}(\sqrt{8}r)/\sqrt{8}r$ is regular at small distances and $H^{(1)}_{l+\frac{1}{2}}(\sqrt{8}r)/\sqrt{8}r$ has outgoing behavior at large distances. Now the constant A has to be determined. To do that, Eq. (4 20) is integrated from r'-0 to r'+0.

The right hand side integration yields

$$RHS = \frac{1}{(r')^2} \tag{4-23a}$$

More work is required to integrate the left hand side. Because $g_l(r,r')$ is continuous, only the second derivative survives:

$$LHS = \int_{r'-0}^{r'+0} \left[\frac{1}{2}\frac{d^2}{dr^2} + \frac{1}{r}\frac{d}{dr} - \frac{l(l+1)}{2r^2} + \frac{1}{r} \right] g_l(r,r')$$

$$= \frac{1}{2}\frac{d}{dr} g_l(r,r') \Big|_{r'-0}^{r'+0} \tag{4-23b}$$

From (4 21), after a minute of calculus, we get

$$LHS = \frac{A}{4\sqrt{8r'}\, r'} W(\sqrt{8}r') \tag{4 23c}$$

where

$$W(x) = J_{l+\frac{1}{2}}(x)\frac{dH^{(1)}_{l+\frac{1}{2}}(x)}{dx} - H^{(1)}_{l+\frac{1}{2}}(x)\frac{dJ_{l+\frac{1}{2}}(x)}{dx} \tag{4-23d}$$

To find A, we use the asymptotic form[57] of $J_\nu(x)$ and $H^{(1)}_\nu(x)$:

$$J_\nu(x) \sim \sqrt{\frac{2}{\pi x}} \cos\left(x - \frac{\nu}{2}\pi - \frac{\pi}{4}\right) \qquad (4\text{-}24a)$$

$$H_\nu^{(1)}(x) \sim \sqrt{\frac{2}{\pi x}} \exp\left[i\left(x - \frac{\nu}{2}\pi - \frac{\pi}{4}\right)\right] \qquad (4\text{-}24b)$$

and

$$J_\nu'(x) \sim -\sqrt{\frac{2}{\pi x}} \sin\left(x - \frac{\nu}{2}\pi - \frac{\pi}{4}\right) \qquad (4\text{-}24c)$$

$$H_\nu^{(1)}(x)' \sim \sqrt{\frac{2}{\pi x}} \cdot i \exp\left[i\left(x - \frac{\nu}{2}\pi - \frac{\pi}{4}\right)\right] \qquad (4\text{-}24d)$$

Combining (4-23) and (4 24) and equating left and right sides, we find

$$A = -16\pi i \qquad (4\ 25)$$

So we arrive at (4-15b).

5. The Overlap Radial Integrals

When the oscillator strength density is computed in the next few chapters, or to be more specific, when $\langle \psi_i D | G^+ | D \psi_i \rangle$ is being evaluated, a special type of overlap integral arises frequently. I discuss them here.

The integrals $\langle \psi_i D | G^+ | D \psi_i \rangle$ involve, besides the angular overlap integral, the overlap of the radial wave function of the initial state $R_{n\ell}(r)$ with the zero-energy radial energy wave function $\frac{J_{2\ell+1}(\sqrt{8r})}{\sqrt{8r}}$. So let me define

$$I_{nl}^{\pm} = \int_0^\infty R_{nl}(r)\ r^3\ \frac{J_{2(l\pm1)+1}(\sqrt{8}r)}{\sqrt{r}}\ dr$$

(4 26)

As is whown in Appendix C, $I_{nl}^{\pm}$ can be expressed as an analytic function of n and l . Details are given in Appendix C. Here in table 4.1, the first few $I_{nl}^{\pm l}$ are listed.

Table 4.1 Integrals $I^{\pm}_{n\ell}$

n	l	$I^{+}_{n\ell}$	$I^{-}_{n\ell}$
1	0	1.5311	
2	0	4.6888	
2	1	5.4142	1.3535
3	0	9.1804	
3	1	11.1283	-1.2365
3	2	9.9535	1.6589
4	0	16.8411	
4	1	17.9633	7.1497
4	2	18.5393	4.0555
4	3	14.0144	1.7518

C. Scattering in a Coulomb Field

As I have said before, our picture of the ionization of atoms in a strong magnetic field is that the laser acts on the initial state ψ_i, producing a source which generates outgoing waves in the Coulomb field; these outgoing waves travel in space, and some of them are turned back by the magnetic field and return to the location of initial state ψ_i, in the vicinity of the nucleus. The overlap or interference of these returning waves with the initial state gives rise the oscillations in the observed spectrum. The process is represented in Fig. 4.1, where the initial outgoing waves are called stage 1, the propagation of these waves in the combined fields are called stage 2, and the scattering from the Coulomb field near the nucleus are called stage 3.

In sections A and B of this chapter, the Green's function $G_C^+(\vec{r},\vec{r}')$ in a Coulomb field near ionization threshold was found. With this Green's function, the outgoing waves from the initial state ψ_i can be found easily(stage 1). This will be explained in chapter VI, when all the necessary tools are ready. The semiclassical propagation of these waves at large distances from the nucleus(stage 2) is the subject of the next chapter.

Here I will discuss the final stage of the physical process---what happens when the waves come

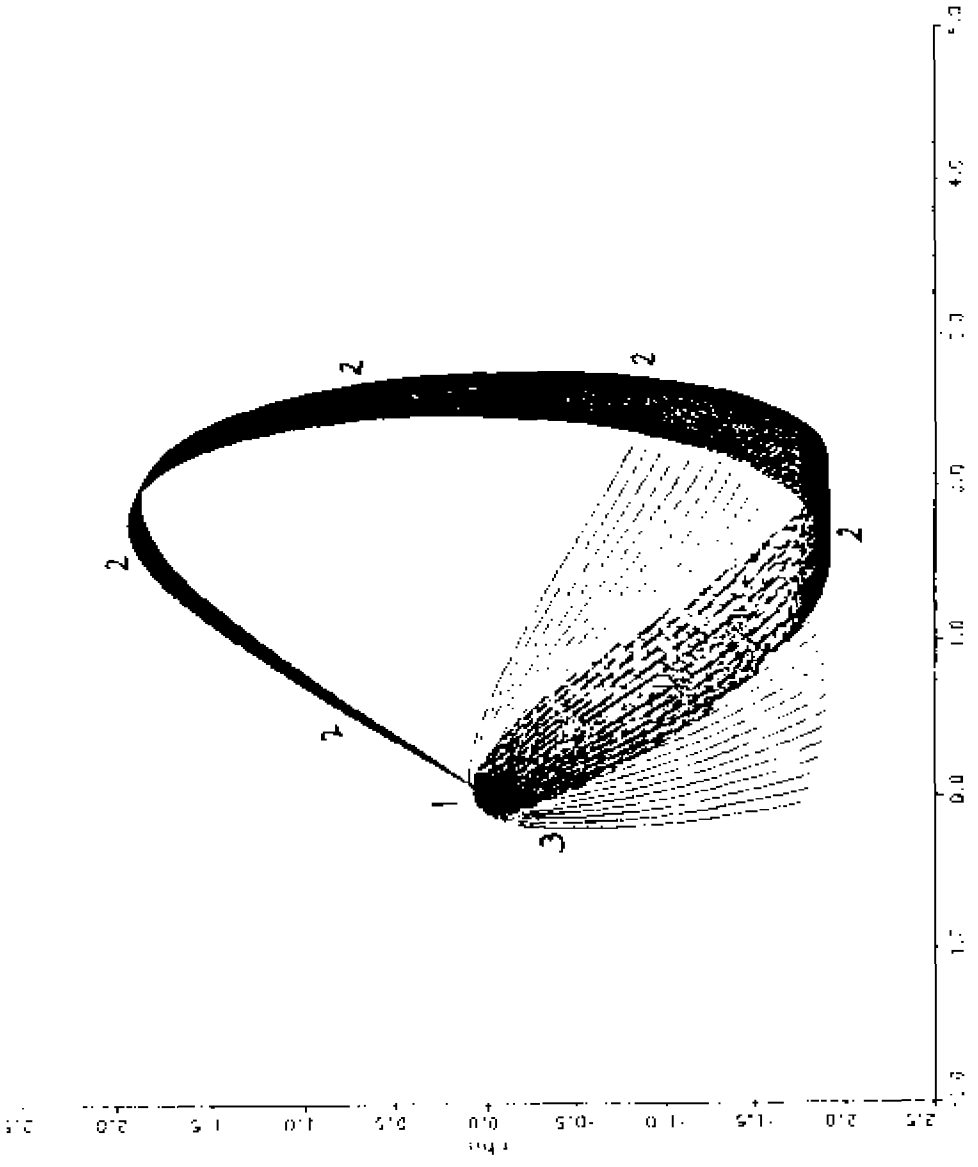

Fig. 4.1 Scattering of waves associated with the family of trajectories. The wave is initially outgoing from the nucleus, then the wave fronts follow the trajectories, and finally it returns to the nucleus being scattered by the Coulomb field.

back from large distances to the vicinity of the nucleus. Clearly this process is a scattering of waves in a Coulomb field.

Our process is a little more complicated than the figure suggests. First, the true waves are three dimensional. However because of the cylindrical symmetry of the problem, the magnetic quantum number m is conserved when the wave is propagated. This must be taken into account. Second, the waves can return from any direction, as against the usual situation that the wave comes in from the negative z axis. Third, the waves possess nearly zero energy; this in fact simplifies the formalism.

In the following discussion, I shall briefly review the already solved case, in which the electron comes in along the negative z axis. From that, the solution for the electron coming from an arbitrary direction is obtained. Then finally, cylindrical waves with given magnetic quantum number are constructed. In all the cases, the wave function is written as a partial wave expansion, and its asymptotic form is expressed compactly. Later (in chapter VI), the asymptotic form will be joined to the semiclassical incoming waves at large distances, and the resulting partial wave expansion will be used to calculate the overlap with the initial state.

1. Incident Electron from Negative z Axis with Zero-Energy

Scattering of electrons from a Coulomb field is well understood. Although the long range Coulomb interaction needs some special attention, the solution is still analytic. In this section, the general formula for the wave function is simplified by considering the zero energy limit.

Imagine a proton sitting at the origin of the coordinate system, and an electron at infinite distance approaching along the negative z axis with velocity v. The complete solution of the wave equation including the incoming wave and the scattered wave can be written[55] as

$$\psi = e^{ikz}\, F(-i\eta, 1, ik\xi) \qquad (4\ 27a)$$

$$= \frac{1}{\Gamma(1+i\eta)} \sum_l d_l (2ikr)^l e^{ikr} F(l+1+i\eta, 2l+2, -2ikr) P_l(\cos\theta) \qquad (4\ 27b)$$

in (4 27b),

$$d_l = \frac{\Gamma(l+1+i\eta)}{(2l)!}$$

$$\eta = -\frac{\hbar k e^2}{\hbar^2 k} = -\frac{e^2}{\hbar v}$$

$\xi = r - z$, and is one of the parabolic variables.

F is the confluent hypergeometric function.

The solution in (4 27) is particularly interesting

to us when the velocity v (or collision energy E) goes to zero.

To find the solution in this limit, an expansion formula for the confluent hypergeometric function in terms of Bessel functions is useful[57].

$$\frac{F(a,b,z)}{\Gamma(b)} = z^{\frac{1-b}{2}} \sum_{n=0}^{\infty} C_n z^n (-az)^{\frac{b-1}{2}+n} J_{b-1+n}(2\sqrt{(-az)})$$

where

$$C_0 = 1,\quad C_1 = -b\lambda,\quad C_2 = -\tfrac{1}{2}(2\lambda-1)a + \tfrac{1}{2}b(b+1)\lambda^2,$$

$$(n+1)C_{n+1} = [(1-2\lambda)n - b\lambda]C_n + \{(1-2\lambda)a - \lambda(\lambda-1)(b+n-1)\}C_{n-1} - \lambda(\lambda-1)aC_{n-2} \qquad (\lambda \text{ real})$$

$$F(a,b,z) = \sum_{n=0}^{\infty} C_n(a,b) I_n(z) \qquad (4\text{-}28)$$

Using this expansion in (4-27), it is straightforward to prove that as $v \to 0$, the wave function ψ turns to

$$\psi \to J_0(2\sqrt{\xi}) \qquad (4\text{-}29a)$$

$$= \sum_l \frac{(2l+1)}{\sqrt{2}} P_l(\cos\theta)\, \frac{J_{2l+\frac{1}{2}}(\sqrt{2}r)}{\sqrt{r}} \qquad (4\text{-}29b)$$

Not surprisingly, the partial wave expansion involves the regular zero-energy radial function $\frac{J_{2l+\frac{1}{2}}(\sqrt{2}r)}{\sqrt{r}}$ found earlier in this chapter.

2. Incident Electron Coming from an Arbitrary Direction

The above describes the complete zero energy Coulomb wave function for the electron coming from infinite negative z. Now we need the solution for the electron coming in from any arbitrary direction.

As long as the solution for electron coming from one direction is known, the solution for an electron coming from any other direction is obtained by a proper rotation.

Let $\hat{k}$ be the unit vector representing the direction of motion of the incoming electron long before the collision. Then eqs. (4 29) still describe parabolic coordinate, and θ becomes the angle between $\hat{k}$ and the electron position vector $\vec{r}$, so $\cos\theta = \hat{k}\cdot\vec{r}/r$.

and the electron position vector $\vec{r}$, so $\cos\theta = \hat{k}\cdot\vec{r}/r$.

Eqs. (4 29) now become

$$J_0(2\sqrt{r-\hat{k}\vec{r}}) \qquad (4\ 30a)$$

$$=\sum_{\ell}\frac{(2\ell+1)}{\sqrt{2}}P_\ell\left(\frac{\hat{k}\cdot\vec{r}}{r}\right)\frac{J_{2\ell+1}(\sqrt{8r})}{\sqrt{r}} \qquad (4\cdot 30b)$$

To write (4·30) explicitly in terms of the spherical polar coordinates of $\vec{r}_1$ the following relation[58] is used. Let two vectors have directions defined by polar angles θ_1, ϕ_1 and θ_2, ϕ_2, and let γ be the angle between the two vectors; then

$$P_\ell(\cos\gamma) = \frac{4\pi}{2\ell+1} \sum_m Y^*_{\ell m}(\theta_1,\phi_1)\, Y_{\ell m}(\theta_2,\phi_2)$$

(4 31)

(This relationship is independent of the phase conventions for $Y_{\ell m}$'s.)

Using (4 31), if θ_k, ϕ_k denote the spherical polar angles of $\hat{k}$, and θ, ϕ, r denote the spherical coordinates of $\vec{r}$, then the solution in (4-30) can be written as

$$J_0\left(2\sqrt{r(1-\cos\theta_k\cos\theta - \sin\theta_k\sin\theta\cos(\phi-\phi_k))}\right)$$

$$= \sum_{\ell m} \frac{4\pi}{\sqrt{2}} Y^*_{\ell m}(\theta_k,\phi_k)\, Y_{\ell m}(\theta,\phi)\, \frac{J_{2\ell+1}(\sqrt{8r})}{\sqrt{r}} \qquad (4\text{-}32a)$$

$$= \sum_{\ell m} \qquad \frac{}{\sqrt{r}} \qquad (4\text{-}32b)$$

3. Cylindrical Coulomb Wave

Because of the cylindrical symmetry in the system, $L_z = m\hbar$ is conserved at every stage of the process, and the waves depend upon the azimuthal angle as $e^{im\phi}$.

Now let us imagine what happens if the two dimensional family of trajectories in Fig. 4.1 is rotated about the z axis to produce a three dimensional family. Then at moderate distances from the nucleus ($r \sim 50$ a$_0$) electrons approach the nucleus from direction specified by a fixed polar angle θ_k, but from all azimuthal angles ϕ_k ($0 \le \phi_k < 2\pi$). What is the

wave-function corresponding to this situation?

We already know the wave function for an electron coming in from a definite direction (θ_k, ϕ_k), it is the Bessel function given in eq. (4 32a), or the partial-wave expansion (4 32b). We also know that the superposition principle applies to waves. So the total wave for electrons coming in from all directions is the superposition of the waves for electron coming from each particular direction. Therefore this cylindrical wave is

$$\int_0^{2\pi} \frac{d\phi_k}{2\pi} J_0\left(2\sqrt{\pi}\sqrt{1-\cos\theta_k\cos\theta-\sin\theta_k\sin\theta\cos(\phi-\phi_k)}\right) \tag{4 33a}$$

which is also equal to (from 4 33b)

$$\int_0^{2\pi} \frac{d\phi_k}{2\pi} \left[\sum_{lm} \frac{4\pi}{\sqrt{2}} Y_{lm}^*(\theta_k,\phi_k)\, Y_{lm}(\theta,\phi)\, \frac{J_{lm}(\sqrt{8}r)}{\sqrt{r}}\right] \tag{4 33b}$$

Before launching into the evaluation of the cylindrical wave in (4 33), I point out that these waves are waves with zero magnetic quantum number, that is $m=0$ (They are obviously independent of ϕ .).

We would like to have a cylindrical wave associated with a given magnetic quantum number m. Remembering that the magnetic quantum number m represents a rotational motion about the z axis, with corresponding wave function $e^{im\phi}$, then a minor

modification to (4-33) will give us the right answer. We merely have to add the wave coherently, with the factor $e^{im\phi_k}$, to reflect this rotation about the z axis. Let us call those waves ψ_c^m, then

$$\psi_c^m = \int_0^{2\pi} \frac{d\phi_k}{2\pi} e^{im\phi_k} J_0\left(2\sqrt{T(1-\cos\theta_k\cos\theta - \sin\theta_k\sin\theta\cos(\phi-\phi_k))}\right)$$

(4-34a)

which is equal to

$$\psi_c^m = \int_0^{2\pi} \frac{d\phi_k}{2\pi} e^{im\phi_k} \sum_{lm'} \frac{4\pi}{\sqrt{2}} Y^*_{lm'}(\theta_k,\phi_k)\, Y_{lm}(\theta,\phi)\, \frac{J_{2l+1}(\sqrt{8T})\sqrt{8T}}{\sqrt{T}}$$

$$= \frac{4\pi}{\sqrt{2}} \sum_l Y^*_{lm}(\theta_k, 0)\cdot Y_{lm}(\theta,\phi)\cdot \frac{J_{2l+1}(\sqrt{8T})}{\sqrt{T}}$$

(4-34b)

Eq. (4-34b) is exact. That ψ_c^m is a wave with given magnetic quantum number m is clear, since only those spherical harmonics with the given m appear in the sum.

To find a compact closed form from (4-34a) is more difficult. We shall find the asymptotic form for the incoming part only, using the stationary phase method (see Appendix D) and use the asymptotic form for the Bessel function

$$J_\nu(z) = \sqrt{\frac{2}{\pi z}}\cos\left(z - \frac{1}{2}\nu\pi - \frac{\pi}{4}\right)$$

(4-35)

so the incoming part of ψ_c^m is

$$\text{Inc}\,\psi_c^m = \int_0^{2\pi} \frac{d\phi_k}{2\pi} e^{im\phi_k} \frac{1}{2}\sqrt{\frac{2}{\pi}} \cdot$$

$$\frac{1}{\left[2\sqrt{\pi(1-\cos\theta_k\cos\theta - \sin\theta_k\sin\theta\cos(\phi_k-\phi))}\right]^{1/2}}$$

$$\cdot \exp\left[i\left(-2\sqrt{\pi(1-\cos\theta_k\cos\theta - \sin\theta_k\sin\theta\cos(\phi_k-\phi))} + \frac{\pi}{4}\right)\right]$$

(4-36)

There are two stationary points for this integral, namely

$$\phi_k - \phi = 0 \quad \text{and} \quad \phi_k - \phi = \pi \tag{4-37}$$

For the incoming wave, only the second $\phi_k - \phi = \pi$ contributes(Remember that θ_k, ϕ_k is the polar angle of the incoming velocity, which is on the opposite side from the position of electron, so $\phi_k = \phi + \pi$ and $\theta_k = \pi - \theta$). Using the stationary phase formula, the result is

$$\text{Inc}\,\psi_c^m = (-1)^m e^{i\frac{\pi}{2}} \frac{1}{2^{\frac{1}{2}}\pi} \frac{1}{\sqrt{\sin\theta_k}}$$

$$\cdot \frac{e^{-i2\sqrt{\pi(1-\cos(\theta+\theta_k))}}}{\sqrt{r\sin\theta}} e^{im\phi}$$

(4 38)

For future use, it is more convenient to write both (4-34b) and (4 38) in terms of the incoming electron position $\theta_f = \pi - \theta_k$,

$$\psi_c^m = \frac{4\pi}{\sqrt{2}} \sum_l (-1)^{l-m} Y_{lm}^*(\theta_f, 0)\, Y_{lm}(\theta, \phi) \frac{J_{l+\frac{1}{2}}(\sqrt{8}r)}{\sqrt{r}}$$

(4 39)

$$\psi_{inc}^{m} = (-1)^m e^{i\frac{\pi}{2}} \frac{1}{2^{3/4}\pi} \cdot \frac{1}{\sqrt{\sin\theta_f}} \cdot \frac{e^{-i2\sqrt{r}(1+\cos(\theta-\theta_f))}}{\sqrt{r\sin\theta}} e^{im\phi} \qquad (4\ 40)$$

From (4-39), using the asymptotic form for $J_{2m}(\sqrt{8r})$, we also have

$$\psi_{inc}^{m} = \frac{4\pi}{\sqrt{2}} \sum_{\ell} (-1)^{\ell-m} \frac{1}{2^{3/4}\pi^{1/2}} Y_{\ell m}^{*}(\theta_f, 0) Y_{\ell m}(\theta,\phi) \cdot \frac{e^{i[\rho/2(-\sqrt{8r} + \ell\pi + \frac{3}{4}\pi)]}}{r^{3/4}} \qquad (4\text{-}41)$$

Eqs. (4-40) and (4-41) are two asymptotic expressions for the desired cylindrical Coulomb zero-energy wave with given magnetic quantum number m. The first is an asymptotic form of a compact expression, and the second is the corresponding partial wave expression. These two formulas will enable us to find the partial wave coefficients close to the nucleus once the incoming wave is known far from the nucleus.

D. Summary

1. The initial quantum wave functions ψ_2 are the eigenfunctions of the Hydrogen atom $R_{n\ell}(r)\ Y_{\ell m}(\theta\phi)$. Some of them are listed in Appendix B.

2. The Green's function for the Hydrogen atom at the ionization threshold (E 0) G_C^+ is found in eq. (4 15):

$$G_C^+(\vec{r},\vec{r}') = \sum_{\ell m} Y_{\ell m}^{*}(\theta',\phi')\, g_\ell(r,r')\, Y_{\ell m}(\theta,\phi) \qquad (4\ 15a)$$

$$g_\ell(r,r') = -2\pi i \frac{J_{2\ell+1}(\sqrt{8}r_<)\, H^{(1)}_{2\ell+1}(\sqrt{8}r_>)}{\sqrt{r_< r_>}}$$

(4-15b)

where $J_{2\ell+1}$ is the Bessel function and $H^{(1)}_{2\ell+1}$ is the Hankel function.

3. Oscillator strength computed in a later chapter will involve an overlap integral between the initial state and the zero energy Coulomb radial wave function:

$$I^{\pm}_{n\ell} = \int_0^\infty R_{n\ell}(r)\, r^3 \frac{J_{2(\ell\pm1)+1}(\sqrt{8}r)}{\sqrt{r}}\, dr \qquad (4\text{-}26)$$

The ones needed are listed in Table 4.1.

4. Excitation by the laser produces outgoing waves, which propagate in the combined Coulomb and magnetic fields, and which later return to the vicinity of the nucleus. These returning waves can be described (in a good approximation) as a superposition of zero-energy Coulomb waves approching from polar angle θ_f with all azimuthal angles. The asymptotic form of the incoming part of these waves is given in compact form by

$$\psi^{(-)}_{inc} = (-i)^m e^{i\frac{\pi}{2}} \frac{1}{2^{3/4}\pi} \frac{1}{\sqrt{\sin\theta_f}} \cdot \frac{e^{-i2\sqrt{r}(1+\cos(\theta-\theta_f))}}{\sqrt{r\sin\theta}} e^{im\phi}$$

(4 40)

and in partial wave expansion by

$$\mathrm{Inc}\,\psi_c^m = 2^{1/4}\sqrt{\pi}\sum_l (-1)^{l+m} Y_{lm}^*(\theta_r, 0)\, Y_{lm}(\theta,\phi)$$

$$\cdot \exp(-i\sqrt{8r})\exp(i(l+\tfrac{3}{4})\pi)/r^{1/4}$$

(4 41)

In this chapter, we have gathered everything we need to describe the outgoing wave function (stage 1) and returning wave function (stage 3) near the nucleus. In the next chapter, a different subject is taken up: the semiclassical propagation of waves in stage 2 will be discussed.

CHAPTER V

PROPAGATION OF WAVES IN SEMICLASSICAL MECHANICS

After the outgoing waves are produced by the laser from the initial state ψ_i, these waves propagate forward in the combined Coulomb and magnetic fields. The only presently available way of propagating the waves is the semiclassical method. This semiclassical method is a generalization of the familar WKB method, and it is a good approximation in the present case. The method is easy to use, and it also provides an intuitive physical picture.

This chapter is entirely devoted to the discussion of the semiclassical method of propagation of waves. I shall show how to use the formulas of the semiclassical method primarily, explain their meanings and justify their validity on physical grounds (A proof of one important result is given in Appendix E.).

The plans for this chapter are the following: first I discuss the role of semiclassical mechanics in general; then the conditions for the semiclassical formulas to be valid follow; after these, the general formulas are introduced and discussed; finally these general formulas are simplified using the cylindrical symmetry of the system.

Those who are interested in semiclassical mechanics,

and those who want more mathematical rigor should consult some excellent references[28,29].

A. Semiclassical Mechanics

One time when I talked about semiclassical mechanics, I was asked why should there be semiclassical mechanics at all? The person asked this question because he thought that quantum mechanics is the only correct mechanics needed to describe the microworld. It is true that quantum mechanics has been proven to be the right mechanics to describe atoms, molecules, even the motion of the earth around the sun. But as we know, the motion of the earth is much more simply and very accurately described by classical mechanics.

The connection between quantum mechanics and classical mechanics is stated in Bohr's correspondence principle: when the quantum numbers of the system become large, the system becomes more like a classical system - a system governed by classical mechanics.

So what is the role of semiclassical mechanics? In essence, semiclassical mechanics serves as a bridge between quantum and classical mechanics. It attempts to get quantum quantities, such as energy levels and wave functions, from the classical quantities. Of course this can only be an approximation, but this approximation in many cases not only greatly simplifies

the computation, but also captures the essence of the physical problem. In some cases (like the one we have now) the semiclassical method may be the only available way to solve the problem, since we do not yet know how to use a full quantum formalism.

We regard semiclassical mechanics as an approximation to quantum mechanics which combines classical mechanics together with the superposition principle; it therefore gives an approximate description of distinctively quantum phenomena, such as interference, and in its most general forms, it can also be used to describe tunneling and diffraction. I shall use semiclassical mechanics to propagate the outgoing waves forward under the influence of Coulomb and magnetic fields.

B. Conditions for Semiclassical Mechanics

In order to get sensible results from semiclassical approximations, the system has to satisfy some conditions.

Usually the semiclassical approximation is derived by assuming that the wave function ψ can be written as a product of amplitude and phase,

$$\psi \sim A e^{iS/\hbar} \tag{5.1}$$

Then, inserting this particular form of wave function

into the Schroedinger equation, and dropping terms of order $\hbar$ and higher, one obtains separate equations for A and S. Necessary condition for the validity of the semiclassical approximation is that the terms neglected must be smaller than the terms kept.

Take the familar one dimensional WKB approximation as an example. Going through the above procedure, one finds that the WKB approximation is good when the fractional change in k ($= \frac{2\pi}{\lambda}$, λ is the de Broglie wave length) in the distance $\lambda/4\pi$ is small compared to unity:[15]

$$\frac{\lambda}{4\pi}\left|\frac{dk}{dx}\right| \ll k \tag{5-2}$$

If the potential energy of the system is $V(x)$, condition (5-2) can be transformed into

$$\left|\frac{dV(x)}{dx}\right| \ll \frac{4\sqrt{2m_e}}{\hbar}(E-V)^{3/2} \tag{5-3}$$

This requires that the potential energy be very flat, or that the state under consideration is a highly excited state. In either of the two cases, the wave function behaves like a plane wave locally, so the approximation to the wave function in (5-1) makes sense. Discussion of multidimensional semiclassical approximations are more involved. But the results are similar to the one dimension result.

In our problem, the effective potential energy is

$$V(r) = -\frac{1}{r} + \frac{1}{8}\left(\frac{B}{c}\right)^2 (x^2+y^2) \qquad (5\ 4)$$

For simplicity, we discuss the condition only for ρ motion. Set $z=0$ in (5 4), then

$$V(\rho) \sim -\frac{1}{\rho} + \frac{1}{8}\left(\frac{B}{c}\right)^2 \rho^2 \qquad (5\ 5)$$

The potential in (5 5) and ionization energy are shown in Fig. 5.1. Semiclassical approximation is used in region I and region II. But the reasons for the validity of semiclassical approximation in the two regions are different.

In region I, the Coulomb term is still greater than the magnetic term, so we have

$$\frac{1}{\rho} \gg \frac{1}{8}\left(\frac{B}{c}\right)^2 \rho^2 \qquad (5\text{-}6a)$$

which gives us an upperlimit of region I,

$$\rho_{max}^{I} \sim 2\left(\frac{c}{B}\right)^{2/3} \sim 10^3\, a_0 \qquad (5\ 6b)$$

When the magnetic term is neglected,

$$V(\rho) \sim -\frac{1}{\rho} \qquad (5\ 7a)$$

$$\frac{dV(\rho)}{d\rho} \sim \frac{1}{\rho^2} \qquad (5\text{-}7b)$$

Using (5-7) in (5 3), we find that the condition for the validity of the semiclassical approximation

$$\rho \gg \frac{1}{32}\, a_0 \qquad (5\ 8)$$

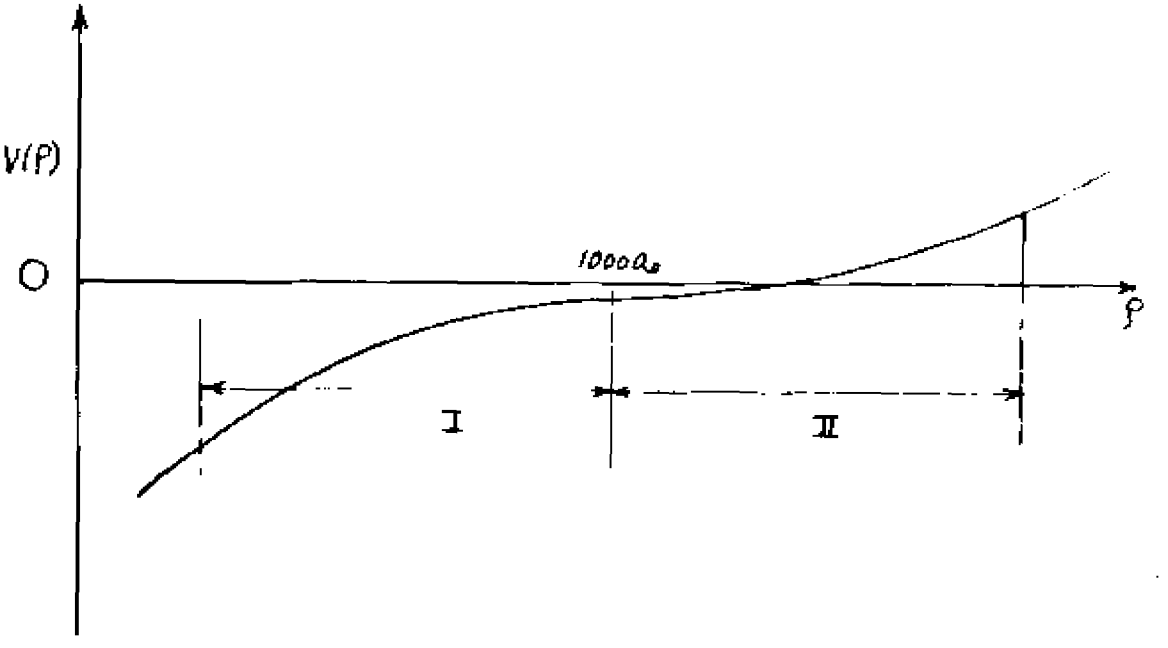

Fig. 5.1 Semiclassical approximation is used in region I and II which are away from the nucleus.

What is happening here is the following: as p increases, $E - V(p)$ gets small and the de Broglie wave length gets large. This seems to suggest that the semiclassical approximation should fail. However, dV/dp decreases even more rapidly than $E - V(p)$; therefore the fractional change of k in a wave length gets smaller as p increases.

In region II, condition (5 3) is violated, since the region is in the neighborhood of a turning point ($E - V \sim 0$). Nevertheless the semiclassical approximation can still give good results, because the approximation can be made in momentum space instead of in configuration space. By means of a long analysis[59] (which is not presented here) one can show that a condition for validity of the momentum space semiclassical approximation is

$$\left| \frac{\frac{\hbar}{2} \frac{d^2V}{dx^2} \frac{dx}{dp}}{\frac{dV}{dx}} \right| << 1 \qquad (5\text{-}9)$$

At the turning point, dx/dp , so the condition is certainly satisfied. At $p \sim 1000 a_0$, the left hand side turns out to be 1/30. Therefore the momentum space form of the semiclassical approximation is valid in region II.

Since the configuration space form of the semiclassical approximation is valid in region I, and the momentum space form of it is valid in region II, we conclude that the approximation is valid everywhere

except close to the nucleus (There we use the Coulomb approximation described in Chapter III.).

C. The Method for Propagating Semiclassical Waves

Even this narrow title demands many pages to answer all the relevant questions. I shall be content to explain the necessary steps in carrying out the procedure. A partial proof of the validity of this procedure is given in Appendix E. Any person who is interested in more complete and detailed proofs is urged to read Refs.[28] .

1. Procedure

First we state as briefly as possible the procedure for propagation of waves; then we discuss the meanings of the quantities that enter the formulas.

Suppose a Hamiltonian $H(q,\beta)$ is given (q is the set of coordinates xyz). Then in quantum mechanics the wave function $u(\beta)$ satisfies the Schroedinger equation,

$$[E - H(-i\hbar\frac{\partial}{\partial\beta}, \beta)]\, u(\beta) = 0 \qquad (5\text{-}10)$$

We suppose that the wave function $u(\beta)$ is known on a two dimensional initial surface

$$\beta = \beta^c(\alpha) \qquad (5\text{-}11)$$

as

$$U(\beta^0) = A(\beta^0)\, e^{iS(\beta^0)/\hbar} \tag{5-12}$$

α represents the coordinates parameterizing the initial surface. Then in semiclassical approximation the wave can be obtained in the following way:

(a) Compute classical trajectories according to

$$\frac{dq}{dt} = \frac{\partial H}{\partial p} \tag{5-13a}$$

$$\frac{dp}{dt} = -\frac{\partial H}{\partial q} \tag{5-13b}$$

with initial positions on the surface

$$q(t=0) = q^0(\alpha) \tag{5-13c}$$

The initial momentum is taken such that the components tangent to the initial surface are equal to

$$P(t=0) = p^0(\alpha) = \frac{\partial S(q^0(\alpha))}{\partial q^0} \tag{5-13d}$$

The component of P normal to the surface is determined by the energy condition

$$H(P,q) - E = 0 \tag{5-13e}$$

Integration of the family of trajectories from the initial surface determines a function $q(t,\alpha)$.

(b) Compute the amplitude factor A(q)

The amplitude factor A(q) is

$$A(q(t,\alpha)) = \sqrt{\frac{J(t=0,\alpha)}{J(t,\alpha)}} \tag{5-14a}$$

and $$J(t,\alpha) = \left| \det\left(\frac{\partial^2 q(t,\alpha)}{\partial t\, \partial \alpha} \right) \right| \tag{5-14b}$$

(c) Compute the phase increase S(q) along each trajectory

$$S_k(q(t,x)) = \int_{t=0}^{t} p\,dq/dt\;dt \qquad (5\text{-}15)$$

(d) Compute the Maslov index μ_k along each trajectory

The complete definition of the Maslov index μ is given in refs. 28 . In the present case, it appears that the Maslov index is equal to the number of caustics through which the trajectory passes.

Then the wave function at point q is equal to

$$u(q) = \sum_k u(q^0)\, A_k(q)\, e^{i[S_k(q) - \mu_k \pi/2]/\hbar} \qquad (5\text{-}16)$$

where q is the point at time t evolved from q^0 at time t=0. The sum is over all trajectories which arrive at the point q from different points on the initial surface.

This procedure is not hard to implement. Some explanation helps to clarify the procedure.

2. Discussion

(a) The Amplitude Factor A(q)

$A^k(q)$ is a solution of a first order transport equation. It represents a classical probability of finding the particle near the point q.

Imagine a system in which particles are distributed over the initial surface $q=q^0(\alpha)$ with a density

$\rho(q_0)$. Those particles will move according to classical mechanics along trajectories (5-13). If neighboring trajectories separate as they move, the density of particles will decrease and vice versa. $A^2(q)$ given in eq. (5-14) measures the relative density of particles along the trajectory if the initial density is unity. Therefore $\rho(q_0)A^2(q)$ is the absolute density of particles, accounting for the initial density.

(b) Classical Action S(q)

It would be a terrible approximation to the quantum wave function if only the classical probability $A^2(q)$ were used, since the interferences of waves would not be correcly described. Interference is important when different trajectories lead to the same final point. The combination of terms in eq. (5-16) gives interference.

The action S(q) along a classical trajectory is the phase accumulated while the wave is propagating forward.

(c) Caustics

Caustics are those singular points where A(q) goes to infinity, because J(q) goes to zero. Some caustics are envelopes or boundaries of the family of trajectories, and others are focal points of the family.

When going through either type of caustic, the wave lose a phase of $\pi/2$. Two methods can be used to

find the caustic. The first one monitors the sign of $J(t,\alpha)$ along the trajectories. Every time a trajectory passes through a caustic the sign of J changes. Another method examines the family of trajectories. At the caustic, neighboring trajectories cross over each other. One can prove that these two methods are in fact the same.

D. Simplified Formulas under Cylindrical Symmetry

The discussions and the formulas given above for the propagation of waves forward in semiclassical approximation are quite general. These formulas can be simplified for a system possessing symmetry.

In this section, I shall write down the formulas for S and J that apply under cylindrical symmetry. It is natural to describe the system in cylindrical coordinates (ρ, ϕ, z).

The z component of the angular momentum $L_z = m\hbar$ is conserved in such a case. The wave function depends upon the angular variable as $e^{im\phi}$. Given the magnetic quantum number m, the classical motion of ϕ is completely determined by the motion in ρ and z.

If a trajectory of given energy is launched from a sphere with initial polar angle θ_0 and azimuthal angle ϕ_0, the time development of ρ and z depends upon the initial polar angle θ_0, but not upon the initial azimuthal angle ϕ_0, and $\phi(t)$ can be calculated from $f(t)$ by

integration

$$\rho = \rho(t, \theta_0) \tag{5-17a}$$

$$z = z(t, \theta_0) \tag{5-17b}$$

$$\phi = \phi(t, \theta_0) + \phi_0 = \int \frac{m_t}{\rho^2} dt + \phi_0 \tag{5-17c}$$

The relationship between Cartesian coordinate (x, y, z) and cylindrical coordinates (ρ, ϕ, z) is

$$x = \rho \cos\phi \tag{5-18a}$$

$$y = \rho \sin\phi \tag{5-18b}$$

$$z = z \tag{5-18c}$$

The momenta in the two coordinate systems are related by

$$P_x = P_\rho \cos\phi - \frac{L_z}{\rho} \sin\phi \tag{5-19a}$$

$$P_y = P_\rho \sin\phi + \frac{L_z}{\rho} \cos\phi \tag{5-19b}$$

$$P_z = P_z \tag{5-19c}$$

We want to evaluate

$$J = \begin{vmatrix} \frac{\partial x}{\partial \theta_0} & \frac{\partial y}{\partial \theta_0} & \frac{\partial z}{\partial \theta_0} \\ \frac{\partial x}{\partial \theta_0} & \frac{\partial y}{\partial \theta_0} & \frac{\partial z}{\partial \theta_0} \\ \frac{\partial x}{\partial \theta_0} & \frac{\partial y}{\partial \theta_0} & \frac{\partial z}{\partial \theta_0} \end{vmatrix} \tag{5-20}$$

in cylindrical coordinates. First we need to express all the derivatives in (5-20) in terms of cylindrical variables. Eq. (5-19) is one set of such relation.

Others are obtained from (5-17) and (5-18). They are

$$\frac{\partial x}{\partial \theta_0} = \frac{\partial r}{\partial \theta_0}\cos\phi - \rho \sin\phi \frac{\partial \phi}{\partial \theta_0} \qquad (5\text{-}21a)$$

$$\frac{\partial y}{\partial \theta_0} = \frac{\partial r}{\partial \theta_0}\sin\phi + \rho\cos\phi \frac{\partial \phi}{\partial \theta_0} \qquad (5\text{-}21b)$$

$$\frac{\partial z}{\partial \theta_0} = \frac{\partial z}{\partial \theta_0} \qquad (5\ 21c)$$

and

$$\frac{\partial x}{\partial \phi_0} = -\rho \sin\phi \qquad (5\text{-}22a)$$

$$\frac{\partial y}{\partial \phi_0} = \rho\cos\phi \qquad (5\text{-}22b)$$

$$\frac{\partial z}{\partial \phi_0} = 0 \qquad (5\ 22c)$$

Combining (5 20), (5 19), (5-21) and (5 22), after about one page of straightforward algebra, we find

$$J = \rho \begin{vmatrix} \frac{\partial z}{\partial r} & \frac{\partial \rho}{\partial r} \\ \frac{\partial z}{\partial \theta_0} & \frac{\partial \rho}{\partial \theta_0} \end{vmatrix} \qquad (5\text{-}23)$$

So the amplitude factor A(q) is independent of ϕ.

By a similar calculation, J can be expressed in spherical coordinates, which are more convenient for joining the semiclassical wave to the Coulomb wave near the nucleus. The result is

$$J = r^2 \sin\theta \begin{vmatrix} \frac{\partial r}{\partial \theta} & \frac{\partial \rho}{\partial \theta} \\ \frac{\partial r}{\partial \theta_0} & \frac{\partial \rho}{\partial \theta_0} \end{vmatrix} \qquad (5\text{-}24)$$

Now let us discuss the phase, first the action S. In Cartesian coordinates (x,y,z),

$$S = \int p_x dx + p_y dy + p_z dz \qquad (5\ 25a)$$

Using (5-16) and (5-17), this can be written as

$$S = \int p_\rho d\rho + p_z dz + m\hbar\, d\phi$$
$$= m\hbar\,[\phi(t) - \phi(t=0)] + \int p_\rho d\rho + p_z dz \qquad (5\text{-}25b)$$

The initial wave function $u(\rho^0)$ depends upon ϕ_0 as $\exp(i m\phi_0)$; therefore the contribution to the full wave function from the ϕ motion is $\exp(im\phi)$ (as is expected). We then just have to compute a reduced action

$$S_r = \int p_r dr + p_z dz \qquad (5\text{-}25c)$$

or, in (r, θ) variables

$$S_r = \int p_r dr + p_\theta d\theta \qquad (5\text{-}25d)$$

Next let us consider the caustics for cylindrically symmetric system. In our calculations, we have seen two type of caustics, shown schematically in Fig. 5.2.

The caustic at large ρ represents a very common type: the trajectories curve back over each other, leaving a boundary between a classically allowed and a classically forbidden region. (The forbidden region is not energetically inaccesible; the trajectories may have enough energy to go into this region, but much of this energy is associated with z motion, so the motion is limited.) This is the simplest type of caustic, and it has been extensively studied.[60] It is

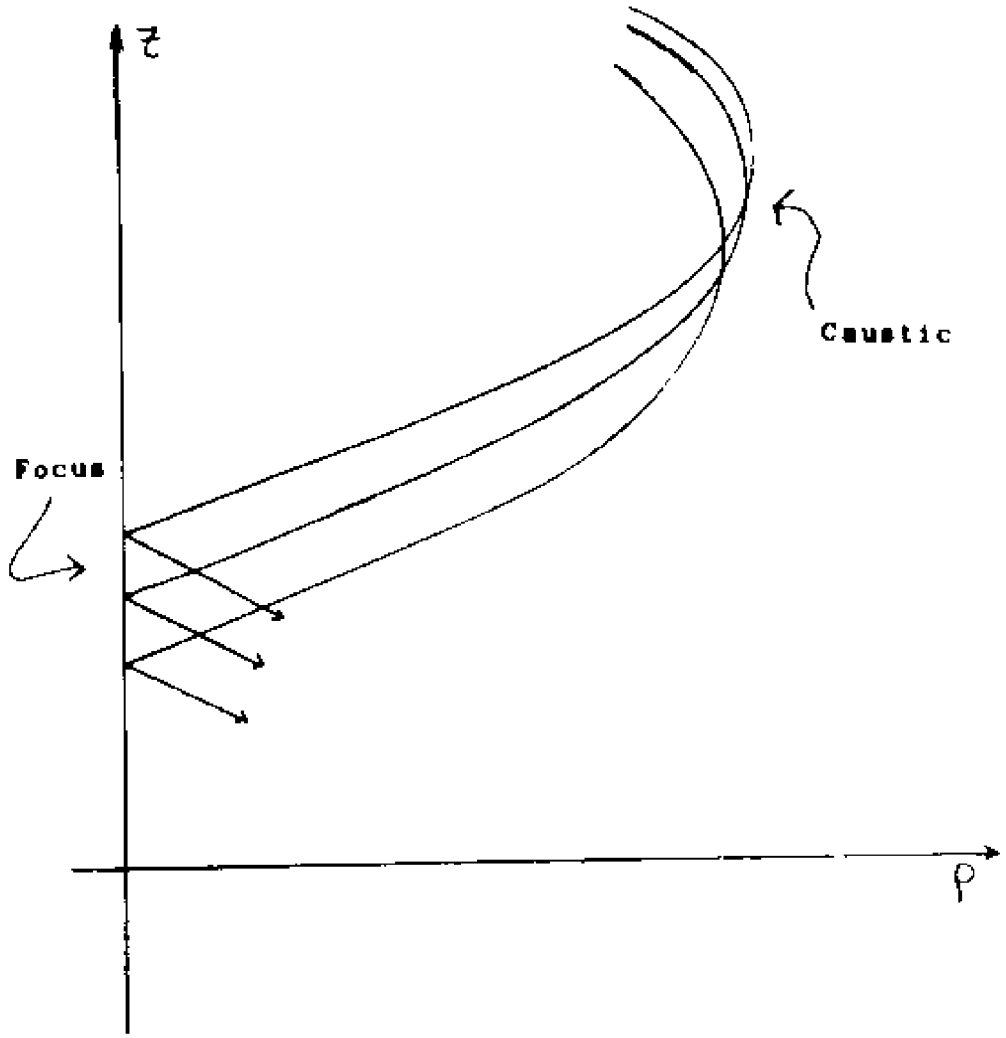

Fig. 5.2 A schematic family of trajectories showing the caustic and focus.

known as a "fold". It has been proved that when a trajectory passes through such a caustic, then the Maslov index increases by 1, and the wave undergoes a phase loss of $\pi/2$.

Near $\rho = 0$ there is another type of singular region. For m=0, trajectories can converge onto the z axis from all directions, forming a kind of focus. In Cartesian coordinates, x(t) and y(t) pass linearly through zero; in cylindrical coordinates, $\rho(t)$ goes to zero and $d\rho/dt$ changes sign discontinuously. It is possible to prove that this type of focus also produces a phase loss of $\pi/2$ (Appendix F).

If m is not zero, the focus becomes an ordinary "fold" caustic, with the forbidden region at small ρ . The same phase loss of $\pi/2$ is produced.

Therefore, in the present case, to calculate the Maslov index, we only have to count the number of caustics and foci through which the trajectory passes.

E. Summary

For a cylindrically symmetric system, suppose the wave function is given on a sphere as $u_0(\theta_0)e^{jm\phi_0}$. Then to propagate this wave outwards, use the following procedure.

(1) At each θ_0 , assign an initial momentum

$$p_\phi^0 = L_z^0 = m\hbar$$

$$p_r^0 = \left[2\left(E - V(r_0) - \frac{p_\phi^2}{2\rho^2}\right)\right]^{1/2}$$

$$p_\theta^0 = 0 \qquad (5\text{-}26)$$

(2) Compute trajectories using Hamilton's equations, and on each trajectory compute a reduced action

$$S_r = \int p_r\, dr + p_\theta\, d\theta \qquad (5\ 27)$$

(3) Compute Jacobian

$$J = r^2 \sin\theta \begin{vmatrix} \frac{\partial r}{\partial t} & \frac{\partial \theta}{\partial t} \\ \frac{\partial r}{\partial \theta_0} & \frac{\partial \theta}{\partial \theta_0} \end{vmatrix} \qquad (5\ 28)$$

and an amplitude factor

$$A = \left|\frac{J(t=0)}{J(t)}\right|^{1/2} \qquad (5\ 29)$$

In computing the derivatives in eq. (5-28), r and θ are regarded as functions of t and θ_0. In eq. (5 29) A is most easily expressed as a function of t and θ_0, but it should be regarded as a function of r and θ.

(4) Calculate the Maslov index μ by counting the number of caustics and foci through which the trajectory passes.

(5) Then the semiclassical wave function is given by

$$\psi(r,\theta,\phi) = e^{im\phi}\, u(\theta_0)\, A(r,\theta) \exp\left[i\left(S_r(r,\theta)/\hbar - \mu\frac{\pi}{2}\right)\right]$$

(5 30)

CHAPTER VI

THE FORMULAS FOR ABSORPTION SPECTRA

Since the initial introduction of our physical ideas about the ionization processes of atoms in a strong magnetic field, many pages have been spent just to prepare the mathematical tools so that we can describe the processes in a more precise way. By deriving formulas related to the processes, we should be able to make comparisons between theoretical results and experimental measurements. This constitutes the major part of the theory.

When I derive the formula for the spectra in a moment I shall assume that the summaries are well understood. Almost everything that is needed for this chapter is contained in the summaries of Chapter III, IV and V.

In the following, I will first recall our physical picture of the ionization processes, and then construct the Green's function from the closed orbits of the system. From the Green's function, I shall derive the oscillatory formula for the spectra which we have been seeking. General discussions of this formula are given afterwards. The formula will be illustrated with computations in the next chapter.

A. The Physical Picture of the Ionization Processes

Let us recall the physical picture of the ionization processes for atoms in a strong magnetic field, which I have given earlier and which has guided us through all the mathematics.

When a laser is applied to an atom in a magnetic field, the atom may absorb a photon. When the atom absorbs a photon, the electron goes into a near-zero energy Coulomb outgoing wave(we are considering ionization near threshold). This wave then propagates away from the nucleus to large distances. At large distances(not too close to the nucleus) the wave propagates according to semiclassical mechanics, and they are correlated with classical trajectories. The wave fronts are perpendicular to the trajectories and the waves propagate along the trajectories. Eventually the trajectories and the wave fronts are turned back by the magnetic field; some of the orbits return to the vicinity of the nucleus, and the associated waves(now incoming) interfere with the outgoing waves to produce the observed oscillations in the absorption spectrum.

B. The Green's Function in the Presence of a Magnetic Field

Let us begin by recalling formula (3·23), which

relates the oscillator strength density $Df(E_f)$ to the Green' function

$$Df(E_f) = -\frac{2me(E_f - E_i)}{\pi\hbar^2} \, Im \langle \psi_i D | G^+ | D\psi_i \rangle$$

Here the Green's function $G^+(\vec{r}, \vec{r}')$ is multiplied by the initial state ψ_i times the dipole operator D and integrated. Since the initial state is localized around the nucleus, it follows that we need $G^+(\vec{r}, \vec{r}')$ only for $\vec{r}$ and $\vec{r}'$ both small.

The outgoing Green's function near the ionization threshold for a Coulomb potential G_C^+ was found in eq.(4-15). The full Green's function in the combined fields can be constructed with the help of G_C^+ .

Let us write the full Green's function as the outgoing Coulomb Green's function plus an additional function G_{CB}^+ .

$$G^+ = G_C^+ + G_{CB}^+ \qquad (6\text{-}1)$$

The physical meaning of G_{CB}^+ comes from the following considerations.

In the semiclassical approximation, the Green's function is correlated with trajectories(such that each trajectory of energy E going from $\vec{r}'$ to $\vec{r}$ gives a contribution like $A(\vec{r}, \vec{r}') \exp[iS(\vec{r}, \vec{r}')/\hbar]$ to $G^+(\vec{r}, \vec{r}')$), $G_C^+(\vec{r}, \vec{r}')$ represents the amplitude for finding the electron at $\vec{r}$, assuming that it started from $\vec{r}'$ and propagated on the most direct path to $\vec{r}$. Since $\vec{r}$ and

$\vec{r}'$ are both small, in this case the electron goes from $\vec{r}'$ to $\vec{r}$ without ever going far from the nucleus. The propagation time from $\vec{r}'$ to $\vec{r}$ can therefore be no more than a few atomic units of time. In contrast, $G^+_{cB}(\vec{r},\vec{r}')$ represents contributions to G^+ in which the electron travels far from the nucleus, and then is returned back. The propagation time on such a path is about 10^5 atomic time units when the magnetic field is a few Tesla. The clear separation of time scales for these two processes provides a clear distinction between G^+_c and G^+_{cB} .

We shall now construct $G^+_{cB}(\vec{r},\vec{r}',E)$ for E close to zero.

1. Green's Function and Closed Orbits

For convenience we write G^+_c in eq. (4-15) here,

$$G^+_c(\vec{r},\vec{r}') = \sum_{lm} Y^*_{lm}(\theta',\phi')\, g_l(r,r')\, Y_{lm}(\theta,\phi) \qquad (6\text{-}2a)$$

$$g_l(r,r') = -2\pi i \frac{J_{l+\frac{1}{2}}(\sqrt{B}r_<)\, H^{(1)}_{l+\frac{1}{2}}(\sqrt{B}r_>)}{\sqrt{r r'}} \qquad (6\text{-}2b)$$

A careful examination of G^+_c shows that it represents an outgoing wave. To see this, consider the prime variables as representing the position of the source of waves(close to the nucleus). Then for large distances r, we use the asymptotic form of $H^{(1)}_{l+\frac{1}{2}}(\sqrt{B}r)$.

$$H^{(1)}_{2\mu+\frac{1}{2}}(\sqrt{\beta r}) \underset{r\to\infty}{\sim} \frac{1}{\sqrt{\pi}} \frac{1}{(2r)^{\frac{1}{4}}} \exp\left[i\left(\sqrt{\beta r} - \tfrac{1}{2}(2\mu+\tfrac{1}{2})\pi - \tfrac{\pi}{4}\right)\right] \tag{6-3}$$

We then obtain the asymptotic form for G_c^+

$$G_c^+(\vec{r},\vec{r}') \sim -i\sqrt{\pi}\, 2^{\frac{3}{4}} \frac{e^{i\sqrt{\beta r}}}{r^{\frac{1}{4}}} \cdot \left[\sum_{lm} Y^*_{lm}(\theta',\phi') Y_{lm}(\theta,\phi) \frac{J_{2\mu}(\sqrt{\beta r'})}{\sqrt{r'}} e^{-i(l+\frac{1}{2})\pi}\right] \tag{6-4}$$

Eq. (6-4) tells us that G_c^+ is outgoing. The above outgoing wave can also be regarded as a superposition of cylindrical outgoing waves,

$$G_c^+(\vec{r},\vec{r}') \sim \sum_m U_m(\theta, r; \theta', \phi', r') e^{im\phi} \tag{6-5a}$$

$$U_m(\theta, r; \theta', \phi', r') = -i\sqrt{\pi}\, 2^{\frac{1}{4}} \sum_l Y^*_{lm}(\theta',\phi') \frac{J_{2\mu}(\sqrt{\beta r'})}{\sqrt{r'}} Y_{lm}(\theta, \phi=0) \cdot \cdot e^{-i(l+\frac{3}{4})\pi} \frac{e^{i\sqrt{\beta r}}}{r^{\frac{3}{4}}} \tag{6-5b}$$

This Green's function G_c^+ does not include the effects of the magnetic field. We now wish to continue this wave into the region where B cannot be neglected.

To do this, the space is divided into two regions: the inner region $r<r_b$, and the outer region, $r>r_b$, where r_b is a radius large enough that the semiclassical approximation is valid but small enough

that the diamagnetic term can be neglected. As was shown in Chapter IV, for B$\sim$a few Teslа, any distance between 30 and 100a_0 is accepted (we took r_b=50). For $\vec{r}$ on this sphere, with $\vec{r}'$ within the domain of the initial state($r'<4a_0$), $G_c^+(\vec{r},\vec{r}')$ is given by eq.(6-5). We may now regard each cylindrical component $u_m(\theta,r_b;r',\theta',\phi')e^{im\phi}$ (with $r'\theta'\phi'$ fixed) as an "initial wave" on the surface $r=r_b$; the semiclassical method described in Chapter V is a procedure for propagating this wave outward.

The wave will go outward initially, and later the magnetic field will turn the wave back. Since the oscillator strength density involves the overlap of this wave with the initial state ψ_i localized around the nucleus, non-zero contribution to the spectrum will come only if the waves return to the vicinity of the nucleus. As we said, the waves travel along classical trajectories. To have waves return to the nucleus, there must be trajectories come back to the nucleus. We further argue that if a family of trajectories returns to the vicinity of the nucleus, then (for m=0) there will be a trajectory in the center of the family that comes exactly back to the nucleus. Similarly if there is a closed orbit coming back exactly to the nucleus, then there is a family of nearby orbits that come close the nucleus. Thus we see the close connection between closed orbits going from the nucleus to the nucleus and the spectrum.

(For m $\neq$ 0, no classical orbit passes through the

nucleus; however for every family of orbits that begins and ends in the vicinity of the nucleus, we can select a particular orbit which comes closest to the nucleus. Those orbits play the same role for $m \neq 0$ as do the closed orbits when $m=0$. For convenience, we shall also refer these central orbits as closed orbits.)

Next I shall describe this connection quantitatively.

2. Contribution from Each Closed Orbit to the Green's Function

Let me reiterate the above ideas as follows. For a given magnetic quantum number m, suppose a closed orbit going out with initial polar angle θ_i^m and returning with final angle θ_f^m is known(see Fig. 6.1). Now if the initial polar angle θ_f^m is known(see Fig. 6.1). trajectories are computed, a family of trajectories, for which the closed one is in the center, will be found. If the cylindrical wave in (6-5a) is considered as the initial wave on the surface $r=r_b$, then the wave associated with this family of trajectories can be found by using the semiclassical method of propagation along the trajectories. As the wave propagates following the trajectories, it will later come back close to the nucleus.

To compute the oscillator strength density, the resulting wave, in the vicinity of the nucleus, must be

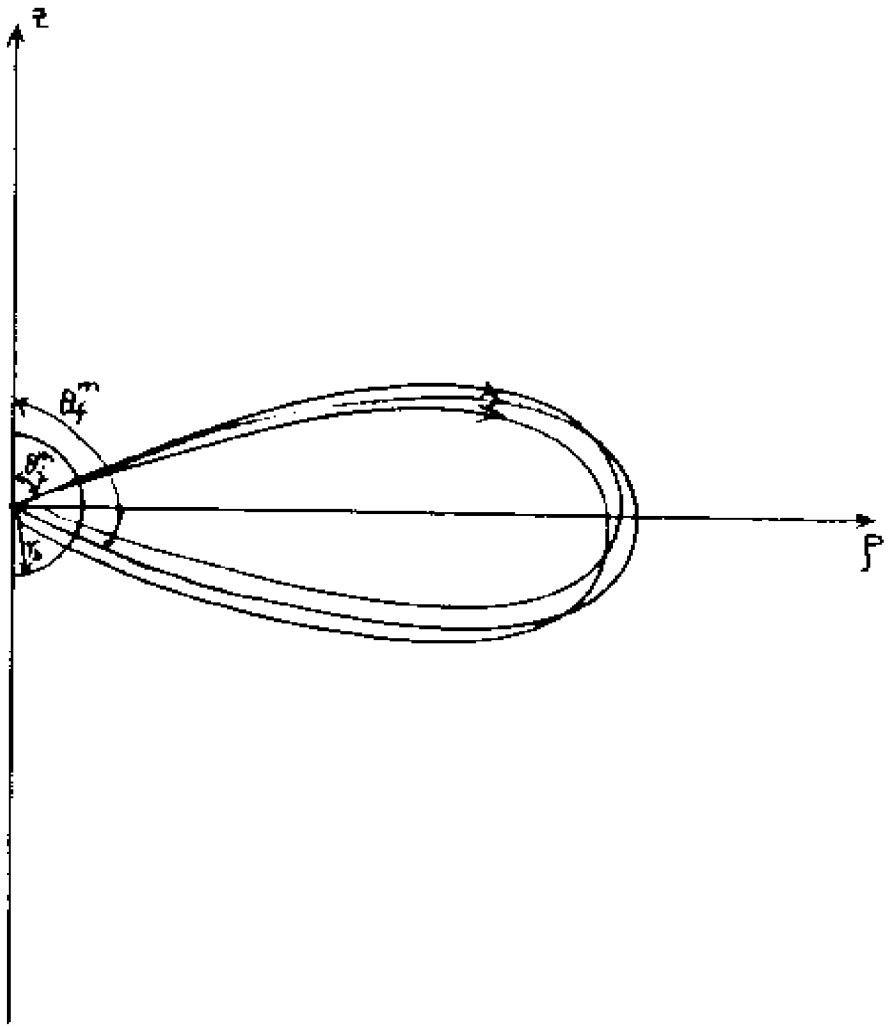

Fig. 6.1 If a closed orbit comes back to the circle r_b, then the neighboring trajectories and the associated waves come back to the vicinity of the nucleus.

calculated, for the overlap of this wave with the initial localized state ψ_i gives the oscillator strength density. But on the other hand, we know that the semiclassical method will break down if the wave is propagated too close to the nucleus. Therefore we shall instead find a partial-wave expansion formula for the returning wave close to the nucleus from the incoming semiclassical wave at moderate distance.

Let $A(\theta_f^m, r_b^f; \theta_i^m, r_b^i)$ and $S_r(\theta_f^m, r_b^f; \theta_i^m, r_b^i)$ be the amplitude factor and action in the semiclassical propagation formulism for the closed orbit from initial angle θ_i^m on a sphere with radius r_b^i to a final angle θ_f^m on a sphere r_b^f, and let $\mu(\theta_f^m, r_b^f; \theta_i^m, r_b^i)$ be the Maslov index on the same orbit. Then the returning wave in the direction θ_f^m on the sphere r_b^f is

$$\psi_m^{ret} = A(\theta_f^m, r_b^f; \theta_i^m, r_b^i)\, e^{i\left[S_r(\theta_f^m, r_b^f, \theta_i^m, r_b^i)/\hbar - \frac{\pi}{2}\mu(\theta_f^m, r_b^f, \theta_i^m, r_b^i)\right]}$$

$$\cdot U_m(\theta_i^m, r_b^i, \theta', \phi', r')\, e^{im\phi}$$

(6-6)

We now make our last approximation. We assume that the returning wave in (6-6) is approximately a cylindrical Coulomb wave of the type described in section IV.C.3, and given quantitatively by eq. (4-40). In this approximation, eq.(6-6) is equal to a constant times eq.(4-40). This constant can be found by evaluating both formulas at the chosen radius r_b^f. The same

constant multiplies the partial-wave expansion (4-39), giving the partial wave expansion of the returning wave close to the nucleus,

$$\psi_m^{ret} = \sum_l a_{lm} Y_{lm}(\theta,\phi) \frac{J_{l+\frac{1}{2}}(Jkr)}{\sqrt{r}} \qquad (6\text{-}7a)$$

and $a_{lm} = \pi^2 2^{\frac{1}{2}} (r_b^f)^{\frac{1}{2}} \cdot \sin\theta_f^m (-1)^l e^{-i\frac{\pi}{2}} e^{i\sqrt{8r_b^f}} Y_{lm}^*(\theta_f^m, 0)$

$$A(\theta_f^m, r_b^f, \theta_i^m, r_b^i) e^{i[S(\theta_f^m, r_b^f; \theta_i^m, r_b^i)/\hbar - \frac{\pi}{2}\mu(\theta_f^m, r_b^f, \theta_i^m, r_b^i)]}$$

$$u_m(\theta_i^m, r_b^i, \theta', \phi; r')$$
$$u_m(\theta_i^m, r_b^i, \theta', \phi; r')$$

(6-7b)

It is hard to see how accurate the approximation is when (6 7) is derived in this way. We can only judge that the procedure is reasonable on physical ground. Of course, we would like to have a better estimate of error for such approximation. In Appendix G, I shall show that this approximation is accurate to about three percent.

In the above derivation, the semiclassical wave in the outer region is joined to a Coulomb wave in the inner region; the joining radii are r_b^i for the outgoing wave, and r_b^f for the returning wave. A question naturally arises: will the result be the same when r_b^i and r_b^f are changed? This question is studied in detail in Appendix H. It is shown there that within the approximations made, as long as these two radii are

small enough that the magnetic field is neglible and large enough that the semiclassical approximation and the asymptotic form of J_{2DH} and $H^{(1)}_{2DH}$ can be used, the result will be independent of the values of r_b^1 and r_b^f. Hence the theory is internally consistent. The result in Appendix G show that the approximation of the returning wave by a Coulomb wave is accurate to about 3%, and numerical tests show that the coefficients very by a few percent when the joining radius is varied between 30 and 100a_0. Because of this, from now on, we can let $r_b^1 = r_b^f = r_b$ ($=50a_0$), so the formulas can be simplified somewhat.

3. The Green's Function--Contributions from All Closed Orbits

Let (n_1, k_m) label the k_m^{th} closed orbit in the subspace of a fixed magnetic quantum number m, and let $A(\theta_f^{n_1 k_m}, \theta_i^{n_1 k_m}, r_b)$, $S(\theta_f^{n_1 k_m}, \theta_i^{n_1 k_m}, r_b)$ and $\mu(\theta_f^{n_1 k_m}, \theta_i^{n_1 k_m}, r_b)$ be the amplitude factor, action and Maslov index for the closed orbit from the initial sphere r_b with initial angle $\theta_i^{n_1 k_m}$ to the final sphere r_b with final angle $\theta_f^{n_1 k_m}$. Each returning orbit produces a contribution to the Green's function given by (6-7), and the Green's function is the sum of contributions from each such orbit. Using the expression for the initial wave in (6-5b) and summing ψ_m^{ret} in (6 6) over all m's and over

all closed orbits K_m for each m, we then obtain the returning part of the Green's function in the inner region

$$G_{CB}^{+} = \sum_{m} \sum_{K_m} \sum_{l_1 l_2 = |m|} d_{l_1 l_2}^{m K_m} Y_{l_2 m}^{*}(\theta', \phi') \frac{J_{2l_2+1}(\sqrt{8r'})}{\sqrt{r'}}$$

$$G_{CB}^{+} = \sum_{m} \sum_{K_m} \sum_{l_1 l_2 = |m|} d_{l_1 l_2}^{m K_m} Y_{l_2 m}^{*}(\theta', \phi') \frac{J_{2l_2+1}(\sqrt{8r'})}{\sqrt{r'}} \qquad (6\text{-}8a)$$

where

$$d_{l_1 l_2}^{m K_m} = (-1)^{l_1+l_2+1} \cdot 2^{15/4} \pi^{5/2} r_b^{-1/4} \cdot \sin\theta_f^{m K_m} \cdot Y_{l_1 m}^{*}(\theta_f^{m K_m}, 0)\, Y_{l_2 m}(\theta_i^{m K_m}, 0) \cdot A(\theta_f^{m K_m}, \theta_i^{m K_m}, r_b)$$

$$e^{-i\frac{3}{4}\pi} e^{i2\sqrt{8 r_b}}\, e^{i[S(\theta_f^{m K_m}, \theta_i^{m K_m}, r_b)/\hbar - \frac{\pi}{2}\mu(\theta_f^{m K_m}, \theta_i^{m K_m}, r_b)]} \qquad (6\text{-}8b)$$

Clearly we have expressed the magnetic field dependent part of the Green's function in terms of the properties of all the closed orbits going from the nucleus and returning back to the nucleus. From (6-8) it is also clear that different m's are not connected, they are merely summed up. The contribution from one m does not affect in any way the contribution from different m. This fact is consistent with the fact that the magnetic quantum number m is conserved in this system.

The Green's function calculated above, $G^{+} = G_C^{+} + G_{CB}^{+}$ represents the Green's function for $\vec{r}$ and $\vec{r}'$ in the

inner region only. Constructing a Green's function for arbitrary values of $\vec{r}$ and $\vec{r}'$ would involve much more work. However, our Green's function will be multiplied by and integrated with the initial state, so only its value in the inner region is needed.

A complete Green's function is symmetric in the two arguments $\vec{r}$ and $\vec{r}'$. $G_c^+(\vec{r},\vec{r}')$ is certainly symmetric in $\vec{r}$ and $\vec{r}'$. In deriving $G_{CB}^+(\vec{r},\vec{r}')$, we have regarded $\vec{r}'$ as the source point and $\vec{r}$ the field point. Is the result obtained in this way symmetric? The answer is yes. Only a little thought is necessary to prove that G_{CB}^+ is symmetric. In fact when $\vec{r}$ and $\vec{r}'$ are exchanged in (6-8), we find only that $\mathcal{D}_2^{m\ell_m}$ and $\mathcal{D}_1^{m\ell_m}$ need to be exchanged to make G_{CB}^+ symmetric. This is certainly not a problem. Just remember that since all the closed orbits are included in (6-8), and in classical mechanics for each orbit there will be a time reversed orbit, which is equavlent to exchanging $\mathcal{D}_2^{m\ell_m}$ and $\mathcal{D}_1^{m\ell_m}$. From the relationship between a closed orbit and its time reversed orbit, we conclude G_{CB}^+ is symmetric.

C. An Oscillatory Oscillator Strength Density Formula

Using the Green's function in (6-1), we can easily compute the oscillator strength density fron the formula (3 23).

We now show that the oscillator strength density

is given by a smooth "background" term $Df_0(E)$ plus a sum of oscillatory terms, each of which is associated with a closed orbit K_m in the m subspace:

$$Df(E) = Df_0(E) + \sum_{mK_m} A_{mK_m}(E) \cdot \sin[\alpha_{mK_m}(E)] \tag{6-9}$$

The meaning of all of these quantities will be discussed after the derivation.

Assume the initial state is a Hydrogenic eigenfunction,

$$\psi_i = R_{nl}(r)\, Y_{lm}(\theta,\phi) \tag{6-10}$$

A general dipole operator can be written in the form

$$\begin{aligned} D &= a^+(x+iy) + a^-(x-iy) + a^0 z \\ &= r\left(a^+ \sin\theta e^{i\phi} + a^- \sin\theta e^{-i\phi} + a^0 \cos\theta\right) \end{aligned} \tag{6-11}$$

where a^+, a^- and a^0 are constants related to the polarization of the radiation field.

Using the relation on spherical harmonics(see Appendix B), we can write

$$\begin{aligned} D\psi_i = r R_{nl}(r) \cdot & \left\{ a^+ \left[\sqrt{\frac{(l+m+1)(l+m+2)}{(2l+1)(2l+3)}}\, Y_{l+1,m+1} - \sqrt{\frac{(l-m)(l-m+1)}{(2l+1)(2l-1)}}\, Y_{l-1,m+1} \right] \right. \\ & \left. + a^- \left[-\sqrt{\frac{(l-m+1)(l-m+2)}{(2l+1)(2l+3)}}\, Y_{l+1,m-1} + \sqrt{\frac{(l+m)(l+m-1)}{(2l+1)(2l-1)}}\, Y_{l-1,m-1} \right] \right. \end{aligned}$$

$$+ a^{\circ}\left[\sqrt{\frac{(l+m+1)(l-m+1)}{(2l+1)(2l+3)}}\,Y_{l+1,m} + \sqrt{\frac{(l+m)(l-m)}{(2l+1)(2l-1)}}\,Y_{l-1,m}\right]\Bigg\}$$

(6-12)

For convenience, let $b^{i}_{\ell m}$ denote the coefficients in this expression, and write $\mathcal{D}\psi_i$ as

$$\mathcal{D}\psi_i = \left[\sum_{\ell m} b^{i}_{\ell m}\, Y_{\ell m}\right] r R_{n\ell}(r) \qquad (6\text{-}13)$$

Now we calculate $\langle \mathcal{D}\psi_i \,|\, G_c^{+} + G_{cB}^{+} \,|\, \mathcal{D}\psi_i \rangle$, putting eq. (6-13) together with the formula (4-15) for G_c^{+} and (6-8) for G_{cB}^{+} .

$\mathcal{D}f_0(E)$ is the contribution from the direct part of the Green's function G_c^{+}. That is

$$\mathcal{D}f_0(E) = -\frac{2m_e(E-E_i)}{\pi\hbar^2}\, Im \langle \mathcal{D}\psi_i \,|\, G_c^{+} \,|\, \mathcal{D}\psi_i \rangle \qquad (6\text{-}14)$$

At zero energy

$$\mathcal{D}f_0(E=0) = -\frac{4 m_e E_i}{\hbar^2} \sum_{\ell' m} \left| b^{i}_{\ell' m}\; GI(n,\ell;\ell') \right|^2$$

(6-15)

where

$$GI(n,\ell;\ell') = \int_0^{\infty} R_{n\ell}(r)\, \frac{J_{2\ell'+1}(\sqrt{8}r)}{\sqrt{r}}\, r^3 dr \qquad (6\text{-}16)$$

As in eq.(6-10) the labels n l identify the initial state, and l' is that set of l's that are connected to the initial state by the dipole operator, as in (6-13).

Similarly, the indirect contribution, from G_{cB}^{+} , is

$$D\delta_1(E) = -\frac{2m_e(E-E_i)}{\pi\hbar^2}\, Im \langle D\psi_i | G_{C0}^{+} | D\psi_i \rangle$$

(6-17)

From eqs. (6-13) and (6- 8), straightforward algebra gives

$$D\delta_1(E) = \sum_{mK} Im\left\{ -\frac{2m_e(E-E_i)}{\pi\hbar^2} \sum_{l_1 l_2} A_{l_1 l_2}^{mK}\, b_{l_2 m}^{1*}\, b_{l_1 m}^{1}\, G1(nl_2, l_1)\, G1(nl_1, l_2) \right\}$$

(6-18)

We define the quantity in curly brackets $\{\ \}$ to be $A_{mK}(E)\, e^{2i\alpha_{mK}(E)}$ with $A_{mK}(E)$ real and positive. Then eq. (6-9) follows immediately.

As in eq. (6 15), the sum over m, l_1 l_2 in (6 18) includes those values that are connected to the initial state ψ_i by the dipole operator. K_m labels the closed orbits in the m subspace.

Let us now discuss the meaning of this equation and some of the approximations.

When we write the Green's function $G^{+} = G_C^{+} + G_{C0}^{+}$, we derived an explicit form for G_C^{+} only at zero energy. However when the energy is close to zero, the zero energy G_C^{+} can still be used. That is to say, G_C^{+} -the direct part of the Green's function depends on the energy weakly. On the other hand, G_{C0}^{+} depends on the energy very strongly. As a consequence of these two different dependences on energy, the spectra will have two very different type of contributions.

How will $G^{+}_{\alpha\beta}$ change if the energy E is changed? To find the answer to this question, we use the formula (6-8) for $G^{+}_{\alpha\beta}$ expressed in terms of the contributions from all the closed orbits. An equivalent question would obviously be: how will $d^{mk_m}_{\ell_1\ell_2}$ change when the energy E is changed? Now $d^{mk_m}_{\ell_1\ell_2}$ is related to a closed orbit, and a closed orbit is also related to an propagation of waves along the closed orbit. Let us change the energy slowly and see how each closed orbit and the wave associated with it change. Generally the initial and final angle $\theta^{mk_m}_i$, $\theta^{mk_m}_f$ depend on the energy, so each closed orbit will change to a nearby closed orbit. This change of path will also introduce a small change in the amplitude factor $A(\theta^{mk_m}_f, \theta^{mk_m}_i, \gamma_0)$. The Maslov index is a topological property of the orbit and it will not change for a little change of energy. Compared to the above relatively weak dependence on energy, the action S_γ along a closed orbit changes very rapidly. In Appendix I, it is proved that the action along a closed orbit satisfies

$$\frac{\partial S(E)}{\partial E} = T(E) \tag{6-19}$$

where T(E) is the time to go along the closed orbit. We can therefore write the oscillator strength density around E=0 as

$$Df(E) = D_0(E) + \sum_{mk_m} A_{mk_m}(E)\, \sin\left[\int_0^E T_{mk_m}(E)\, dE/\hbar + \alpha_{mk_m}(E=0)\right] \tag{6-20}$$

Since $D\delta_0(E)$, $A_{mk}(E)$ and $T_{mk}(E)$ are nearly constant over a small range of energy, we have

$$D\delta(E) = D\delta_0(E=0) + \sum_{mk} A_{mk}(E=0) \sin\left(T_{mk}(E=0)\, E/\hbar + \alpha_{mk}(E=0)\right) \qquad (6\text{-}21)$$

Now we clearly see that the spectrum in (6-21) is a smooth background and a superposition of oscillatory terms. The background is from G_c^+, the direct contribution to the spectrum. This background $D\delta_0$ is the same as if there were no magnetic field. On the other hand, the oscillatory terms are indirect contributions to the spectrum. They are the results of the co-existence of Coulomb and magnetic fields. Each term represents the amplitude for the electron being emitted from initial state ψ_i near the nucleus, and being returned at time T_{mk} later near the nucleus by the fields.

The spectra formulas in (6-9), (6-20) and (6-21) may be a surprising result at first glance. But if we recall our physical picture, we will see that these formulas are the natural consequences of it. To make this point clear, in fig. 6.2 I show schematically how a wave associated with a closed orbit induces an oscillation in energy. A and B represent the nucleus (they should be at one position, but for clarity, they are separated). Waves riding along a closed orbit from A to B at various energies are drawn. Now the phase of the wave at A is fixed. Because the path of the orbit (which is the path followed by the wave) and the wave

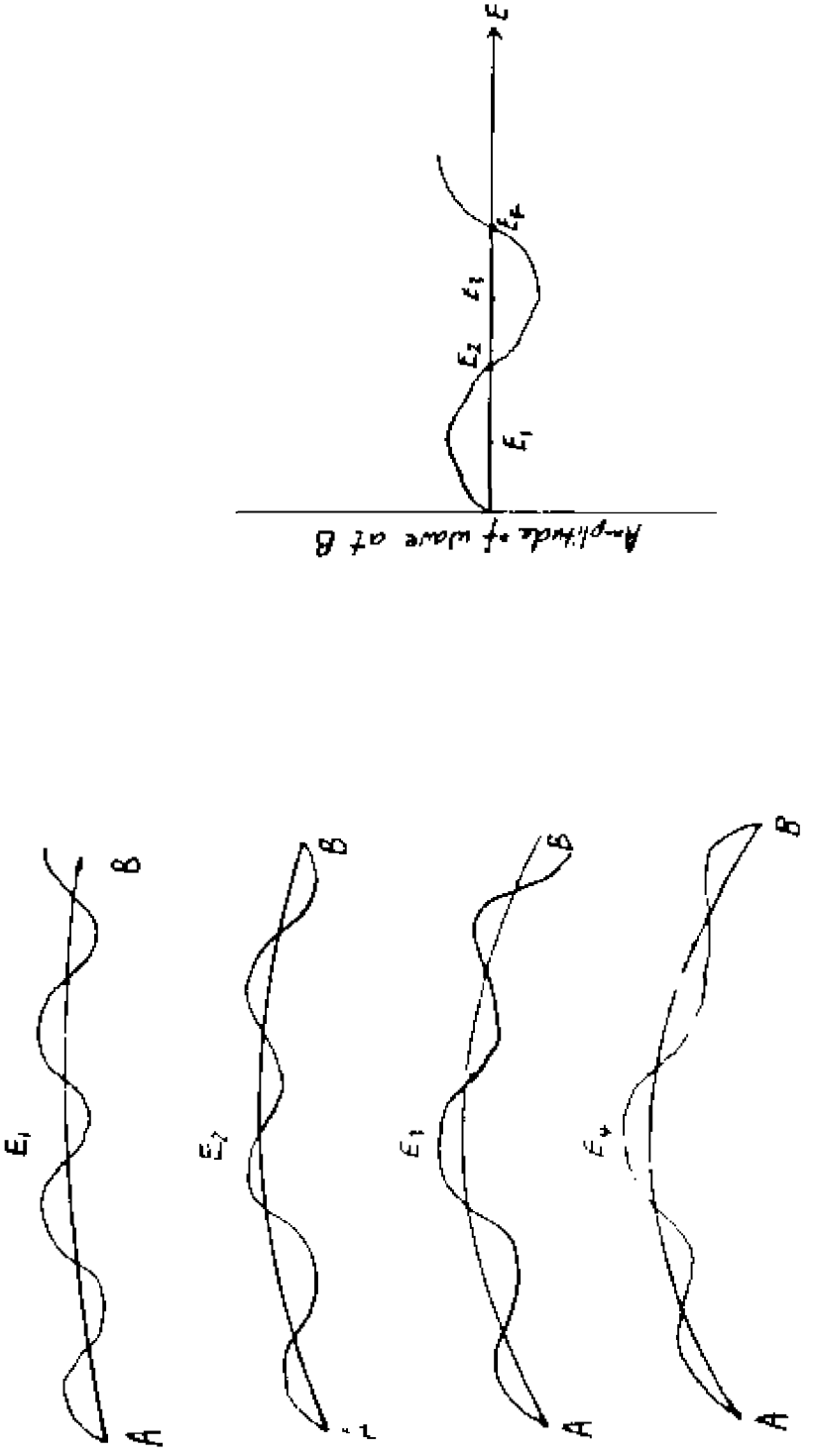

Fig. 6.2 As the energy varies the path and the wave length changes. As a result the imaginary part of the wave at B oscillates.

length change in a continuous way as the energy changes, the phase at B changes in a continuous way too. If we look at the magnitude of the wave(imaginary part of a wave like $Ae^{iS/\hbar}$) at different energy, we should get a figure like the one on the right. The magnitude at B as a function of energy oscillates. The wave length of this oscillation is determined by the theorem in (6-19). To have the phase change by 2π , the energy should change by

$$\Delta E = \frac{2\pi\hbar}{T} \qquad (6\text{-}22)$$

The above explanation shows how the oscillations in the spectrum arise in a very natural way. These results are expressed more precisely in (6-9).

From (6 9), (6·20) and (6-21) the energy spacing of each oscillation is given by (6-22). This relationship between the energy spacing and the classical period of a closed orbit in the system was first pointed out by Edmonds for one particular case[5] . Recently this relationship has been further confirmed for many new closed orbits[7] . However this relationship has been misinterpreted[5,54] and exactly how to derive it was not clear until this study. In particular, in some of the early work, the oscillations were referred to as "resonances", and it was thought that they were associated with quasibound states, which would be semiclassically associated with trajectories having

quantized values of action variables.[61] In fact, action variables do not exist for this system. The total action along the orbit is not quantized either (there is no such need in order to produce oscillations, but numerous articles on this problem have been talking about the quantized action along the orbits for many years). Actually the phenomenon is easily understood as an interference effect, with oscillations caused by the changing phase of the wave along each closed orbit.

It should be pointed out that the absolute position of each oscillation is related not only to the period of the orbit, but also to the phase $\alpha_{m\ell}(0)$ at zero energy, for example. This phase involves the partial wave expansions of $D\psi_1$ and of the zero energy Coulomb wave at small r. In this region, the semiclassical approximation is not reliable, so it appears that the absolute phase of the oscillations contains quantum effects as well as semiclassical effects(we can predict the absolute position of each oscillation in this theory. However even the misused WKB method, which quantizes the action along each closed orbit, can only give the right value of energy spacing!)

wave expansions of $D\psi_1$

Because of the relation (6-19), a longer orbit will produce a small energy spacing. As a result of this, a finite resolution measurement(all measurements have a finite resolution) can only obtain information about a finite number of closed orbits in the system.

Given the resolution ΔE_{res} in a experiment, oscillations from any orbit with period T longer than

$$T_{max} = \frac{2\pi\hbar}{\Delta E_{res}} \qquad (6\text{-}23)$$

will be averaged to zero in the spectrum. So when we do a computation, we do not have to find the entire set of closed orbits, but only those with period

$$T < T_{max} \qquad (6\text{-}24)$$

In fact we know more about the importance of each orbit than just the requirement by (6-24). In general the importance of each orbit or the oscillation in the spectrum associated with this closed orbit are determined by several factors: first, the energy spacing given by (6-22), so a short period orbit is more important than a longer one; second, the sensitivity of each oscillation to the magnetic field. We know in practice the magnetic field can not be perfectly uniform and stable. Another question then arises: what happens to the oscillations when the magnetic field is changed? By using arguments similar to these used to obtain (6-21) from (6-20), we know the amplitude A_{orbit} of each oscillation will not change much. Again the phase change is most important. In Appendix J, I prove that the change of action for each closed orbit with respect to the change of magnetic field is related to the integral along the closed orbit

by

$$\frac{\partial S}{\partial B} = -\frac{1}{4}\,\frac{e^2 B}{m_e c^2}\oint \rho^2\, dt \qquad (6\text{-}25)$$

Typical values for $\frac{\partial S}{\partial B}$ near the ionization threshould at a few Tesla are about 10^{-4}. This requires that the magnetic field has to be accurate to within less than one percent if the oscillations in the spectrum is to be visible. From (6-25) longer period orbits will have a more sensitive dependence on the magnetic field. Again only short period orbits have to be included in (6-20) and (6-21). Given the accuracy of the magnetic field ΔB, we can find an upper limit for $\frac{\partial S}{\partial B}$, and any orbit with an value of $\frac{\partial S}{\partial B}$ larger than this will averaged to zero in the observed spectrum.

Third, perhaps the most important quantity which determines the importance of each oscillation in (6-20) and (6-21) is the amplitude A_{mk} of each oscillation. Of cause, larger amplitude oscillations are more important and easier to measure in experiments then small amplitude oscillations. Without actually doing any calculation we can only draw some general conclusions about the size of amplitudes. Clearly the amplitude of oscillations in (6-20) and (6-21) are related to $d_{\ell\ell_i}^{mk}$ in (6-8b). If we examine $d_{\ell\ell_i}^{mk}$ more carefully, we see the value $d_{\ell\ell_i}^{mk}$ depends upon two very different kind of factors. The first type, which reflects the angular distribution of the initial wave

ψ_2 , are those spherical harmonics and sine functions evaluated at outing or returning angle. The second type, which is a measure of the divergence of the family of trajectories along each closed orbit, is the amplitude factor $A(\theta_f^{m_2}, \theta_i^{m_1}, r_0)$. This is a classical effect. We know the system is classically chaotic, so neighbouring trajectories always separate. In the wave picture, the wave spreads to a larger and larger area and the intensity of the wave becomes weaker and weaker. Therefore the amplitude factor will generally be smaller for longer orbits.

For orbits having similar periods, and similar classical amplitude factors, then quantum effects has a decisive role. If, for example, the classical orbit goes out or returns right at the node of a spherical harmonic in (6-8b), then the amplitude of the corresponding oscillation in the spectrum will be nearly zero. This phenomeon is clearly seen in experiments.

In conclusion, the three factors-- the energy spacing, the sensitivity of the phase to the magnetic field and the amplitude of oscilation consistently tell us that shorter period orbit are more important than longer ones.

D. Summary

1. The Green's function for computing the ionization spectrum of atoms in a strong magnetic field is found to be equal to a sum of the Green's function without magnetic field G_c^+ and a magnetic field dependent part G_D^+

$$G^+ = G_c^+ + G_D^+ \qquad (6\text{-}1)$$

G_c^+ was found in Chapter IV explicitly. G_D^+ is expressed in terms of the properties of all the closed orbits in the system in (6-8).

2. The major result of this study, which is proved by using the above Green's function, is that the ionization spectrum can be written as a smooth background plus a superposition of oscillations. Each oscillation is closely connected with a closed orbit in the system and from the properties of the closed orbit the spectrum can be completely determined.

3. If the initial state and laser polarization are specified, then the absorption spectrum near the ionization threshould can be calculated by the following procedure:

(i) Evaluate the expansion coefficients $b_{\ell m}^{i}$'s for $D\psi_i$ --the product of dipole operator D and the initial state ψ_i according to (6-10), (6-11), (6-12)and (6 13).

(ii) Calculate the radial overlap integral $GI(n,l;l')$ for $l=l'\pm1$ only as in (6-16). Some of these integrals are listed in Table 4.1.

(iii) Calculate the smooth background of the spectrum with eq. (6-15).

(iv) Find all the closed orbits with period T less than a desired value T_{max} in each subspace of m that appears in the expansion of $D\psi_i$ in (6-13). For any m, an orbit is said to be closed if it begins radially outward on the sphere $r=r_0$, and ends radially inward on the same sphere. For each such closed orbit, compute the amplitude factor A, action S_n Maslov index μ and period T.

(v) Calculate $d_{ll_i}^{m,k_n}$ from (6-8).

(vi) From (6-18), evaluate the oscillation amplitude A_{mk_n} and phase α_{mk_n}.

(vii) The spectrum near the ionization threshould is then given by (6-21).

Obvious modifications of this procedure can be made to obtain a spectrum around an energy E_i other than the threshould.

CHAPTER VII

SPECTRUM FOR TRANSITION $2P_z \rightarrow m_f = 0$

In the previous chapters, in particular in chapter VI, our original physical ideas (picture) of the ionization processes of an atom in a strong magnetic field have been turned into quantitative mathematical formulas. It is hoped that with these formulas, for example, the spectrum formula in (6-9), we can explain the already existing experimental data. And we would also like to predict what would happen if future new experiments are done. I have particularly in mind the most recent measurements of Hydrogen atom in 5.96 Tesla magnetic field for transition from $2P_z$ to final $m_f=0$ states near the ionization threshold[7] . These measurements were discussed in chapter II.

It is also my hope that in this chapter I can illustrate the theory described so far by employing it step by step in a real computation. By the end of this chapter, I wish to convince the reader that the theory is easy to implement, easy to understand, and it provides us a framework for understanding the complicated spectrum of an atom in a strong magnetic field.

A. Theoretical Spectrum for Transition $2P_z \rightarrow m_f = 0$

Our calculation in this section will be for the transition from the $2P_z$ initial state to final states near the ionization threshold with $m_f = 0$ in a magnetic field B=5.96 Teala.

1. The Background Spectrum

Given the initial state $2P_z$, the wave function for such a state is

$$\Psi_i = R_{21}\, Y_{10} \tag{7-1}$$

For transitions to final states with the same magnetic quantum number $m_f = m_i = 0$, the light must be polarized with electric field along the z-axis, so

$$D = \mathcal{E}_z \tag{7-2}$$

and, comparing (7 2) with (6-11), we find

$$\alpha^+ = \alpha^- = 0$$

$$\alpha^0 = 1 \tag{7 3}$$

Following (6-12), $D\Psi_i$ now can be written as

$$D\Psi_i = \gamma R_{21} \left[\sqrt{\frac{(1+1)(1+1)}{(2\times1+1)(2\times1+3)}}\, Y_{20} + \sqrt{\frac{(1+0)(1-0)}{(2\times1+1)(2\times1-1)}}\, Y_{00} \right]$$

$$= \gamma R_{21} \left[\sqrt{\frac{4}{15}}\, Y_{20} + \sqrt{\frac{1}{3}}\, Y_{00} \right] \tag{7 4}$$

Comparing (7-4) with (6-13), we find in the expansion

$$Df_L = \left[\sum_{l'm} b^i_{l'm} Y_{l'm} \right] r R_{nl}(r)$$

$$b^i_{20} = \sqrt{\frac{4}{15}} \ , \ b^i_{00} = \sqrt{\frac{1}{3}} \qquad (7\text{-}5)$$

and all other $b^i_{l'm}$ are zero.

The energy of the initial state is

$$E_i = -\frac{1}{2\,2^2} = -\frac{1}{8} \qquad (7\text{-}6)$$

From (6-15), the background spectrum is (in Atomic Unit):

$$Df_0(E=0) = \frac{1}{2}\left[\frac{4}{15} GI(2,1;2)^2 + \frac{1}{3} GI(2,1;0)^2 \right] \qquad (7\text{-}7)$$

Now we look up Table 4.1, and we find

$$GI(2,1;2) = I^+_{21} = 5.4142$$

$$GI(2,1;0) = I^-_{21} = 1.3535 \qquad (7\text{-}8)$$

Putting (7-8) into (7-7), finally we obtain the background spectrum

$$Df_0(E=0) = 4.2138 \quad \text{Hartrees}^{-1} \qquad (7\text{-}9)$$

This is the oscillator strength density at the ionization threshold in the absence of magnetic field, and this constant value also represents the smooth background spectrum near E=0 in the presence of a

magnetic field.

2. Trajectories and Closed Orbits in the Subspace of m=0

To compute the oscillations in the spectrum we have to study the classical trajectories of this system. Because only m=0 harmonics appear in the expansion of D^{1}_{0} in (7-5), it is enough to restrict ourselves to the m=0 subspace.

For the magnetic quantum number m being zero, and the magnetic field strength B=5.96 Tesla, we can write the Hamiltonian in either cylindrical coordinates (ρ, z)

$$H = \frac{1}{2}(p_\rho^2 + p_z^2) - \frac{1}{(\rho^2+z^2)^{1/2}} + \frac{1}{8}\left(\frac{5.96}{2.35\times10^5}\right)^2 \cdot \rho^2 \qquad (7\text{-}10a)$$

or in spherical coordinates (r, θ, ϕ)

$$H = \frac{1}{2}\left(p_r^2 + \frac{p_\theta^2}{r^2\sin\theta}\right) - \frac{1}{r} + \frac{1}{8}\left(\frac{5.96}{2.35\times10^5}\right)^2 r^2\sin^2\theta \qquad (7\text{-}10b)$$

Trajectories can now be obtained by choosing an initial condition and integrating Hamilton's equation for (7-10).

We need to find those trajectories which go out from the nucleus and later return to the nucleus.

Therefore we choose the following initial outgoing condition on a circle $r_b = 50a_0$

$$P_r = \sqrt{2\left(\frac{1}{r_b} - \frac{1}{8}\left(\frac{5.96}{2.35\times10^5}\right)^2 r_b^2 \sin^2\theta_0\right)}$$

$$P_\theta = 0$$

$$r = r_b$$

$$\theta = \theta_0$$

(7-11)

θ_0 is the polar angle from the z axis. In principle all the θ_0 from 0° to 180° should be chosen. But because the Hamiltonian in (7-10) has a symmetry in z, (namely it is unchanged when $z \to -z$), therefore the trajectory going out at angle θ_0 can be obtained by a reflection about the $\rho = 0$ axis from the trajectory going out at angle $\pi - \theta_0$. Therefore we only need to launch trajectories with initial condition as given in (7-11) for $0° \le \theta_0 \le 90°$.

The time unit in this problem is conveniently taken to be the cyclotron period

$$T_c = \frac{2\pi m_e c}{eB}$$

$$= 6.0\times10^{-12}\ \text{sec}$$

(7-12)

The available experimental spectrum corresponds to trajectories which return to the nucleus within a time $T < 10T_c$. We shall find those closed orbits.

To see the general nature of classical orbits in

this system, in Fig. 7.1 I have plotted 91 orbits starting with θ_0 at each degree from 0° to 90°. One can see from Fig. 7.1 that the trajectories starting with initial angle less than 25° can not come back close to the nucleus within $T<10T_c$. So there is no closed orbit in this range of angles.

One also sees the chaotic nature of the trajectories. Neighboring trajectories starting out with initial angles differing by only 1 degree remain close to each other only for a very short period of time (of the order of T_c). When they separate, their subsequent behaviours have no similarity.

In principle, if orbits begin sufficiently close together, then for any finite time T they remain close together. Hence if we set a fixed upper limit to the time T_{max}, then in principle we could choose $\Delta\theta_0$ sufficiently small that neighboring trajectories will be close together for all $T<T_{max}$. Thus we could learn the behavior of all of the orbits for this time $T<T_{max}$. However, one of the characteristics of chaotic classical systems is that trajectories diverge from their neighbors exponentially in time. Therefore as T_{max} gets large, the initial conditions must be taken extremely close together. (for $T_{max} \sim 10T_c$, we estimate that the continuous relationship between final and initial conditions would be visible if we computed 10^7 orbits with initial spacing $\sim 10^{-5}$ degree.)

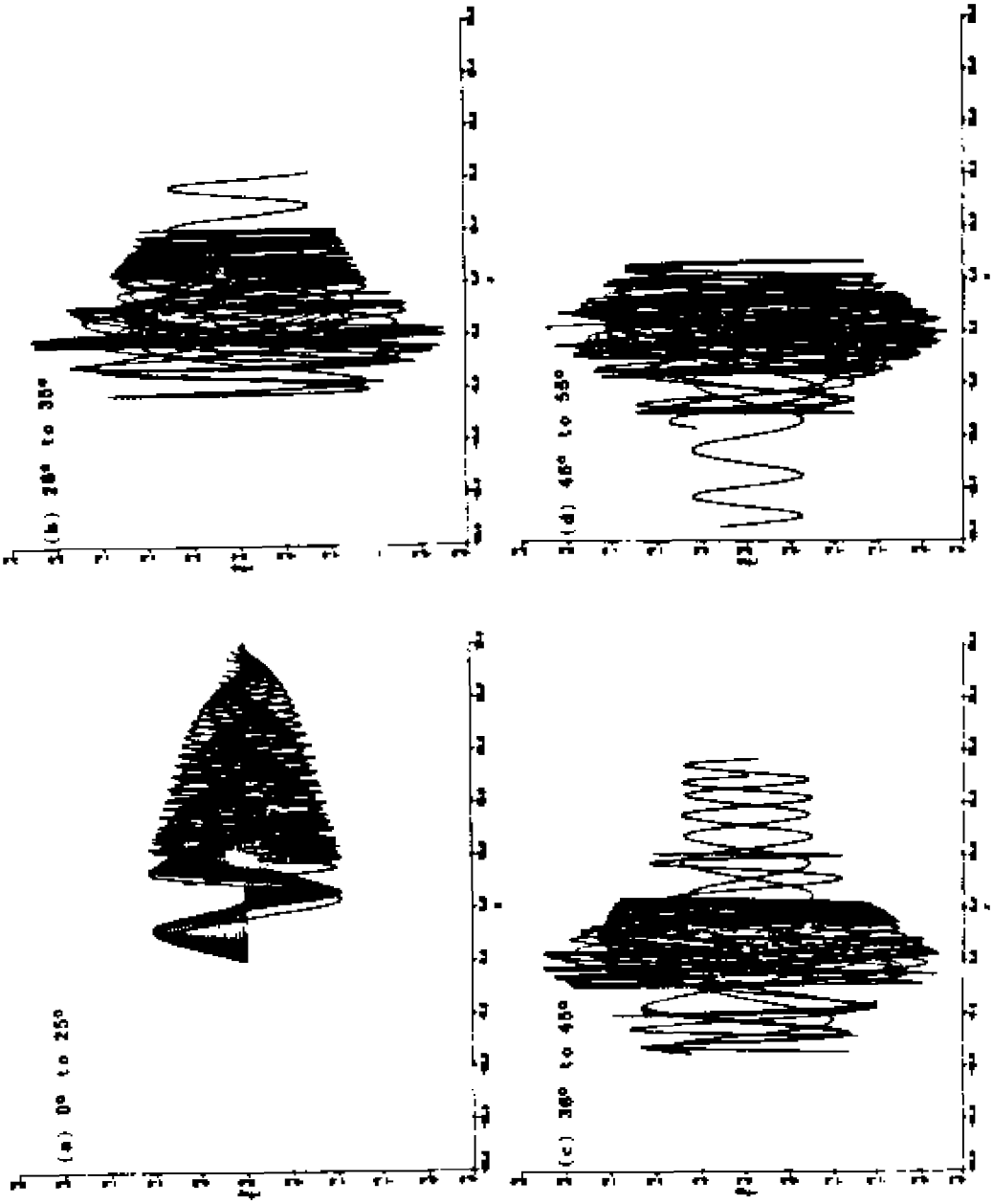

FIG. 7.1 Trajectories launched at each degree of polar angle between 0° to 90° are run for a period of time T=10^4, for Hydrogen atom in a 0 subspace and 5.96 Tesla magnetic field at zero energy. ρ (rho) and z are in 10^3 bohrs.

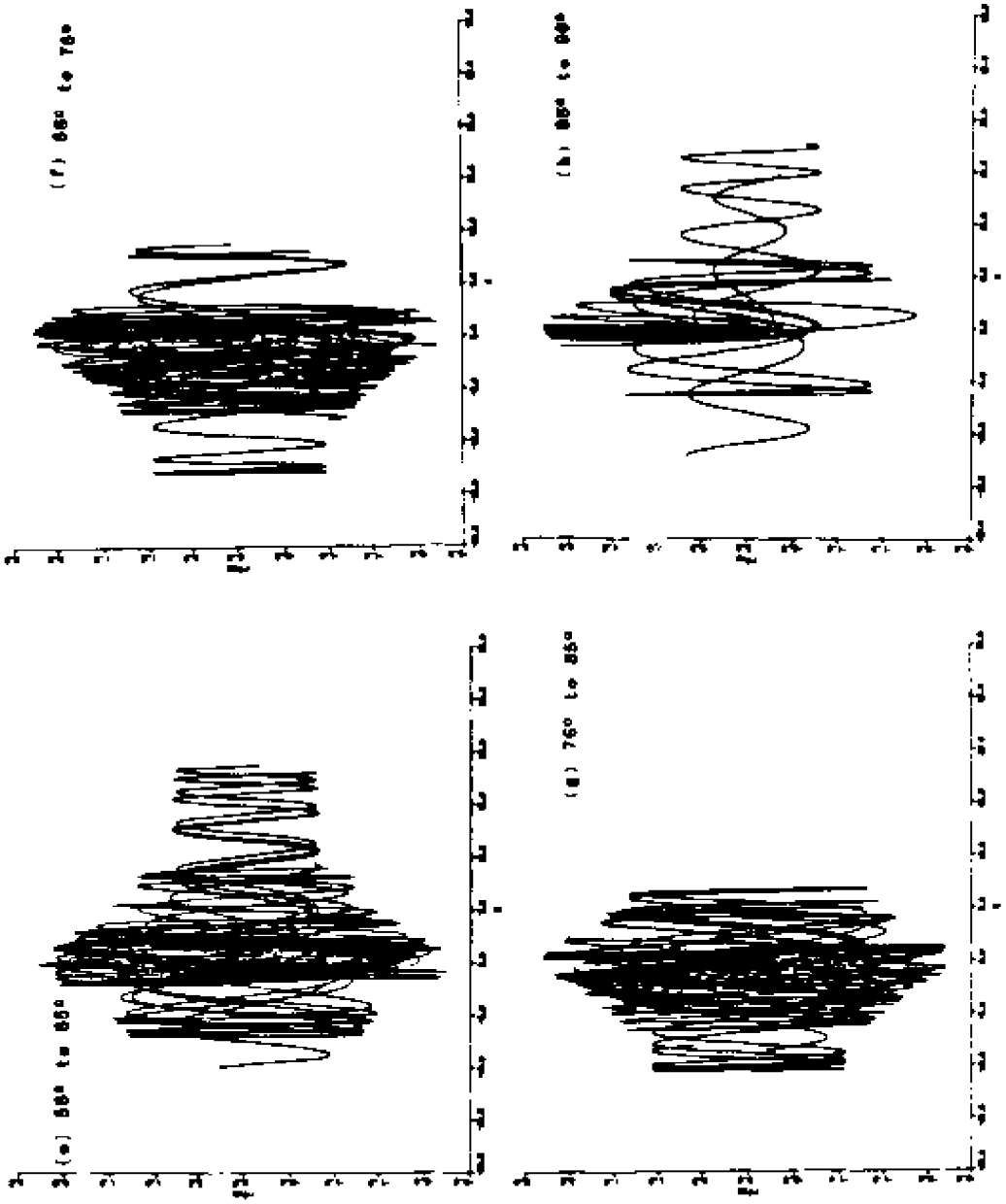

FIG. 7.1 (continued)

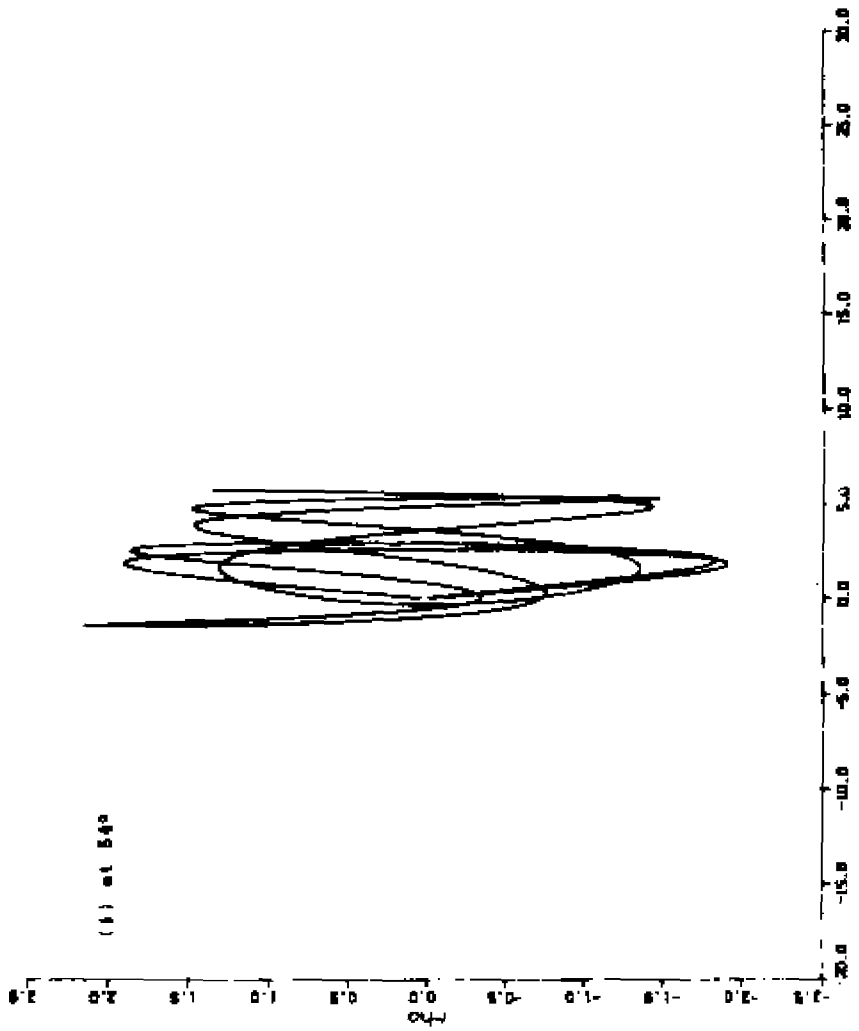

FIG. 7.1 (continued)

Nevertheless we can find the important closed orbits of the system with fewer trajectories. Each closed orbit(which returns exactly to the nucleus) is surrounded by neighbors which return to the vicinity of the nucleus. The important closed orbits are those with large amplitude factors in eq. (5-29), and the amplitudes are inversely related to the rate of divergence of neighbors from the central closed orbit. In other words, the important closed orbits are the ones from which the neighbors diverge relatively slowly. We find these as follows. Trajectories are launched from the initial circle $r=r_b$ in all directions between 0° and 90° with initial angle spacing $\Delta\theta_0$ for neighboring trajectories; then the trajectories are computed and the coordinates (r, θ) and momenta (p_r, p_θ) are monitored. A trajectory returning to the vicinity of the nucleus crosses the circle $r=r_b$. On this circle these conditions must be satisfied:

$$r = r_b$$
$$p_r < 0 \qquad (7\text{-}13)$$

If $\Delta\theta_0$ is small, we usually find families of neighboring trajectories that cross the circle. The number of such trajectories in a family is a measure of the divergence of this family of trajectories. The greater the number, the more stable this family. I shall call this number the importance number for this family and denote by N_i. In each family of trajectories, there will be a

central orbit which satisfies (7-13) and in addition satisfies

$$p_\theta = 0 \tag{7-14}$$

on the circle. We call this central orbit the closed orbit associated with the family of trajectories (for m=0 this orbit returns exactly to the nucleus.). This closed orbit can easily be found by an iteration procedure once two trajectories in a family crossing the circle are known. This closed orbit characterizes the family of trajectories. More importantly, all our formulas are expressed in terms properties of such closed orbit.

In Table 7.1, 65 closed orbits are listed. They were found by launching 6501 trajectories from 25° to 90° ($\Delta\theta_0 = 0.01°$). These 65 orbits all have the importance number N_i greater than or equal to 3. Other closed orbits having N_i less than 3 were also found but discarded. The mirror images of these 65 orbits about the p axis are another set of 65 orbits (except for the one goes exactly along the p axis). Therefore we have here 129 closed orbits in the m=0 subspace. The 65 closed orbits are also shown in Fig.7.2. We shall calculate the oscillations in the spectrum associated with each of these orbits in a moment.

But first, to see into the nature of the family of trajectories associated with a closed orbit, I plot in Fig. 7.3 the family of trajectories associated with closed

Table 7.1 65 closed orbits of the electron in a Hydrogen atom in 5.96 magnetic field at zero energy in m=o subspace

No.[a]	N_i[b]	θ_i[c]	θ_f[d]
1	404	90.0000	90.0000
2	244	53.8315	53.8315
3	121	42.8096	42.8096
4	75	63.6491	116.3509
5	68	37.3112	37.3112
6	54	81.6769	128.2460
7	53	51.7540	98.3231
8	49	33.8359	33.8359
9	38	31.3650	31.3650
10	38	67.4952	133.3209
11	37	46.6791	112.5048
12	32	41.5414	100.8855
13	31	29.4816	29.4816
14	28	72.3793	147.3385
15	28	76.0617	146.9510
16	28	79.1145	138.4586
17	26	39.6015	110.5060
18	26	69.4940	140.3985
19	26	27.9784	27.9784
20	24	36.3739	102.4857
21	24	60.2704	60.2704
22	24	77.5143	143.6261
23	23	70.9628	144.5354
24	23	26.7390	26.7390
25	23	73.1415	73.1415
26	23	75.2766	72.9452
27	23	35.4646	109.0372
28	23	33.0490	103.9383
29	23	32.6615	107.6207
30	20	25.6917	25.6917
31	19	75.5122	75.5122
32	19	64.1900	83.7954
33	19	83.7954	64.1900
34	17	72.9452	75.2766
35	12	81.1921	81.1921
36	11	66.1890	66.1890
37	11	76.8441	71.3130
38	11	71.5979	71.5979
39	10	71.3130	76.8441
40	10	45.2669	59.2104
41	9	84.6640	46.8879
42	9	80.0781	67.8881
43	9	77.1661	77.1661
44	9	59.2104	45.2669
45	9	40.3160	40.3160
46	9	67.8881	80.0781
47	8	70.2627	70.2627

Table 7.1 (continued)

No.[a]	N_i[b]	θ_i[c]	θ_f[d]
48	8	69.8278	78.2444
49	8	68.6640	68.6640
50	8	61.3044	118.6956
51	8	78.7631	78.7631
52	8	78.2444	69.8278
53	7	65.6207	47.9562
54	7	50.1847	64.9144
55	7	47.9562	65.6207
56	7	60.0954	96.9466
57	7	64.9144	50.1847
58	6	85.1381	39.7359
59	6	40.7256	40.1677
60	6	38.7169	58.7307
61	6	46.8879	84.6640
62	5	58.7307	38.7169
63	5	83.0534	119.9046
64	5	40.1677	40.7257
65	3	39.7359	85.1381

[a]The orbits are ordered according the value of the importance number N_i.

[b]N_i is the importance number.

[c]The initial outgoing polar angle(in degree) of the orbits.

[d]The final returning polar angle(in degree) of the orbits.

$r'_b - r'_b = 50a_0$ in the calculation.

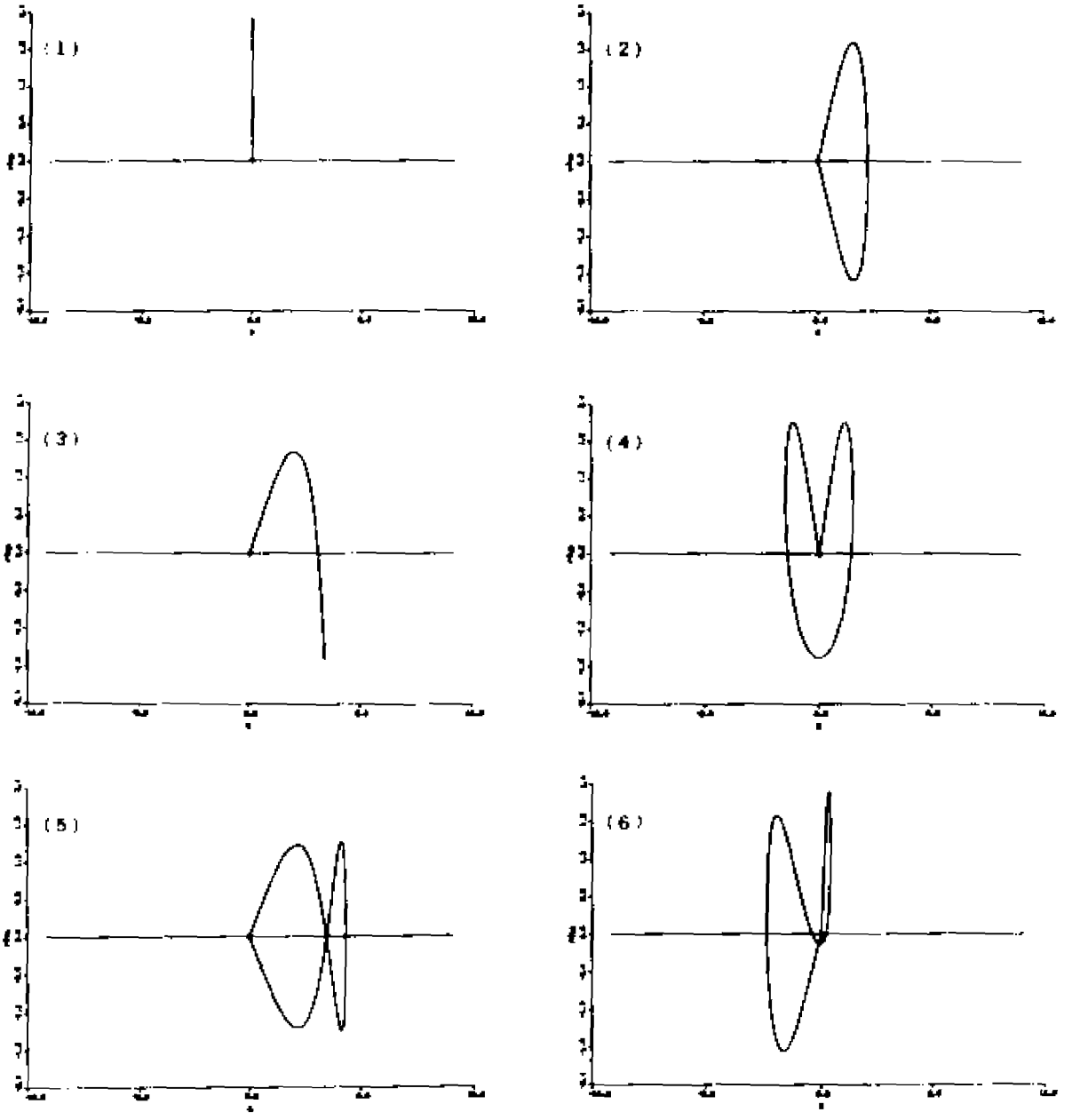

FIG. 7.2 65 closed orbits for Hydrogen atom at zero energy in 5.96 Tesla magnetic field with magnetic quantum number m being zero. These orbits all have an initial outgoing angle between 0 and 90 degrees from the z axis. Mirror images of these 65 orbits about the ρ (rho) axis give us another 65 orbits. The number in each plot corresponds to the one in the first column of Table 7.1. Both z and rho are in 10^7 Bohrs.

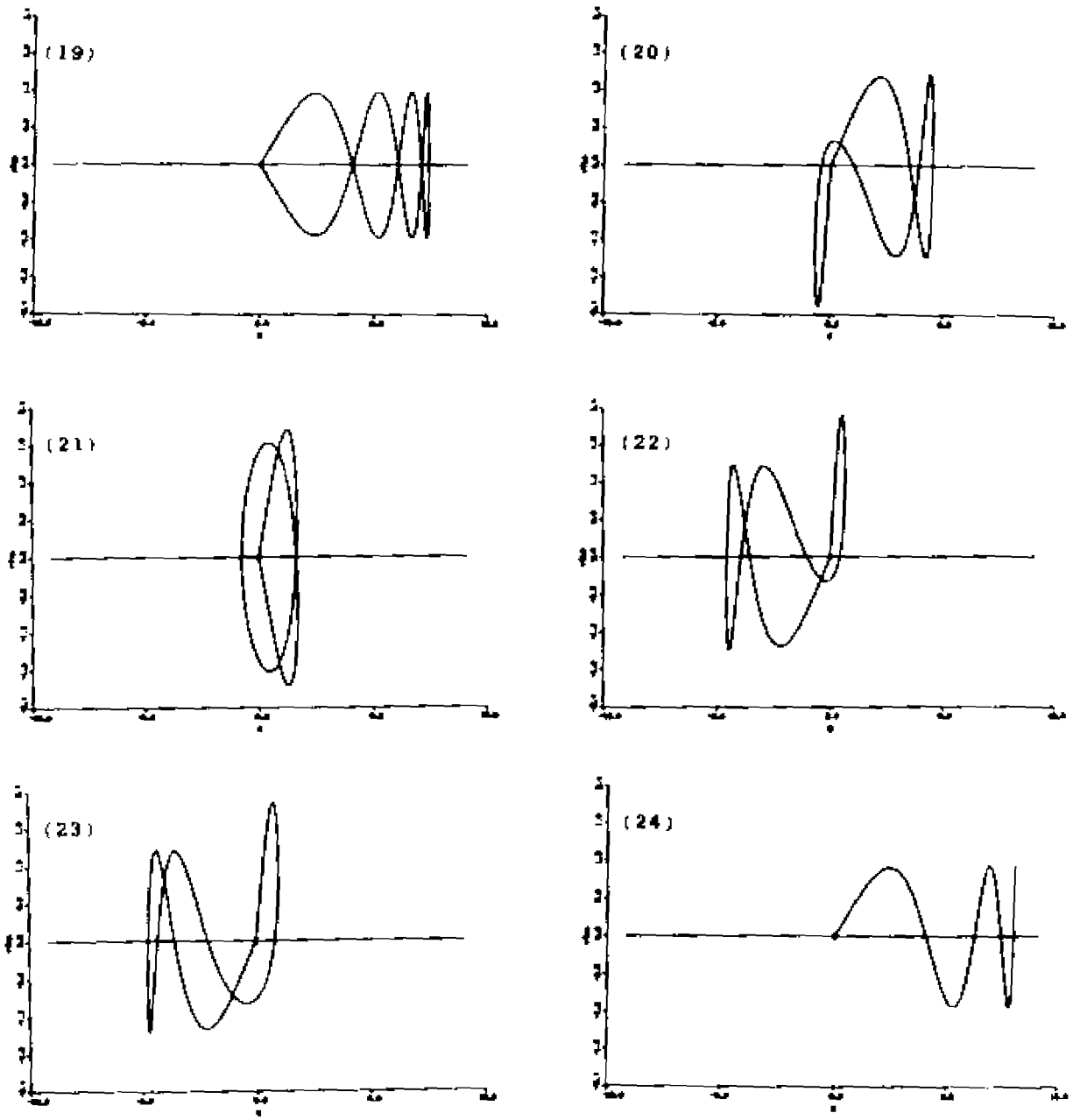

Fig. 7.2 (continued)

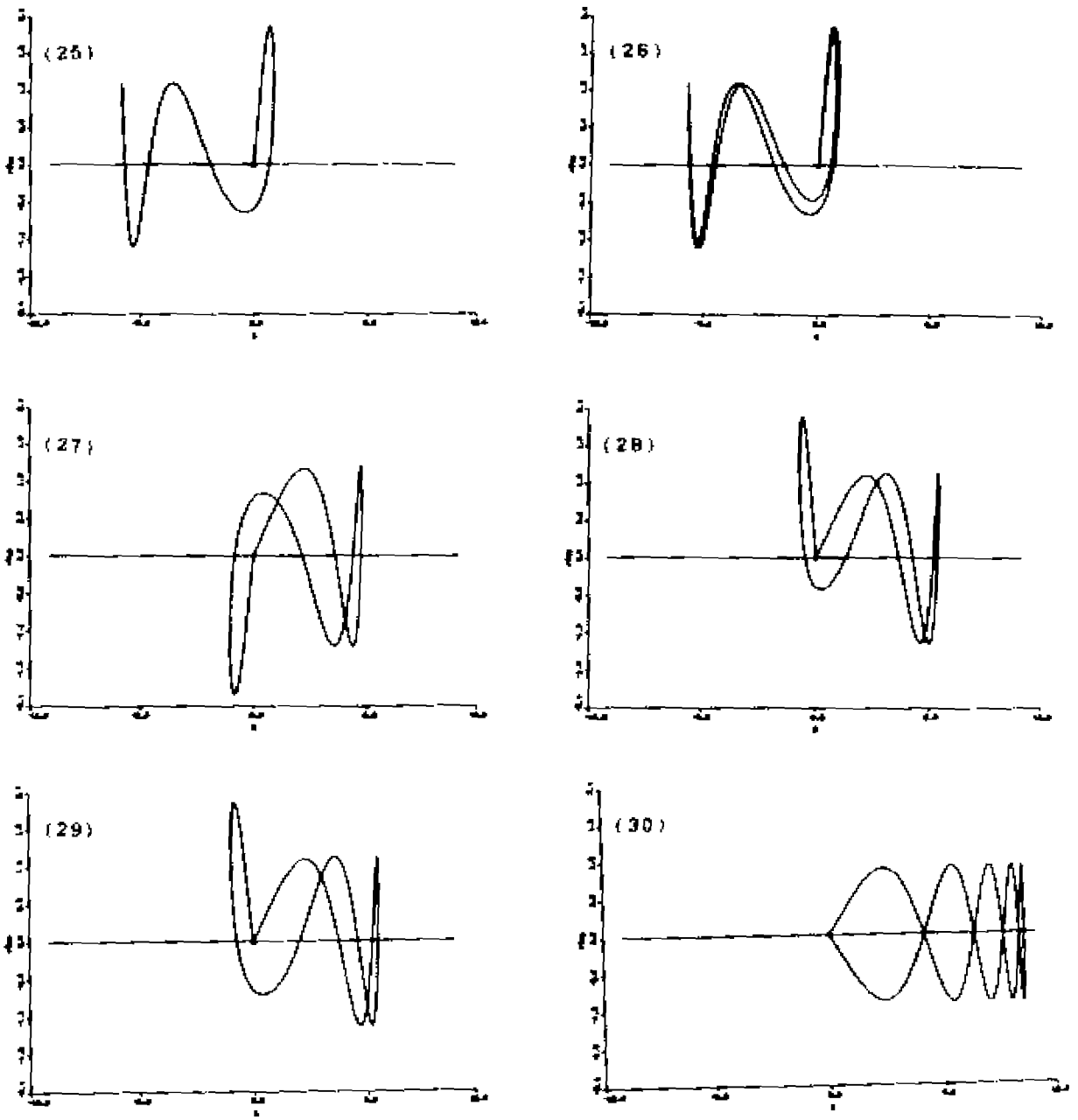

Fig. 7.2 (continued)

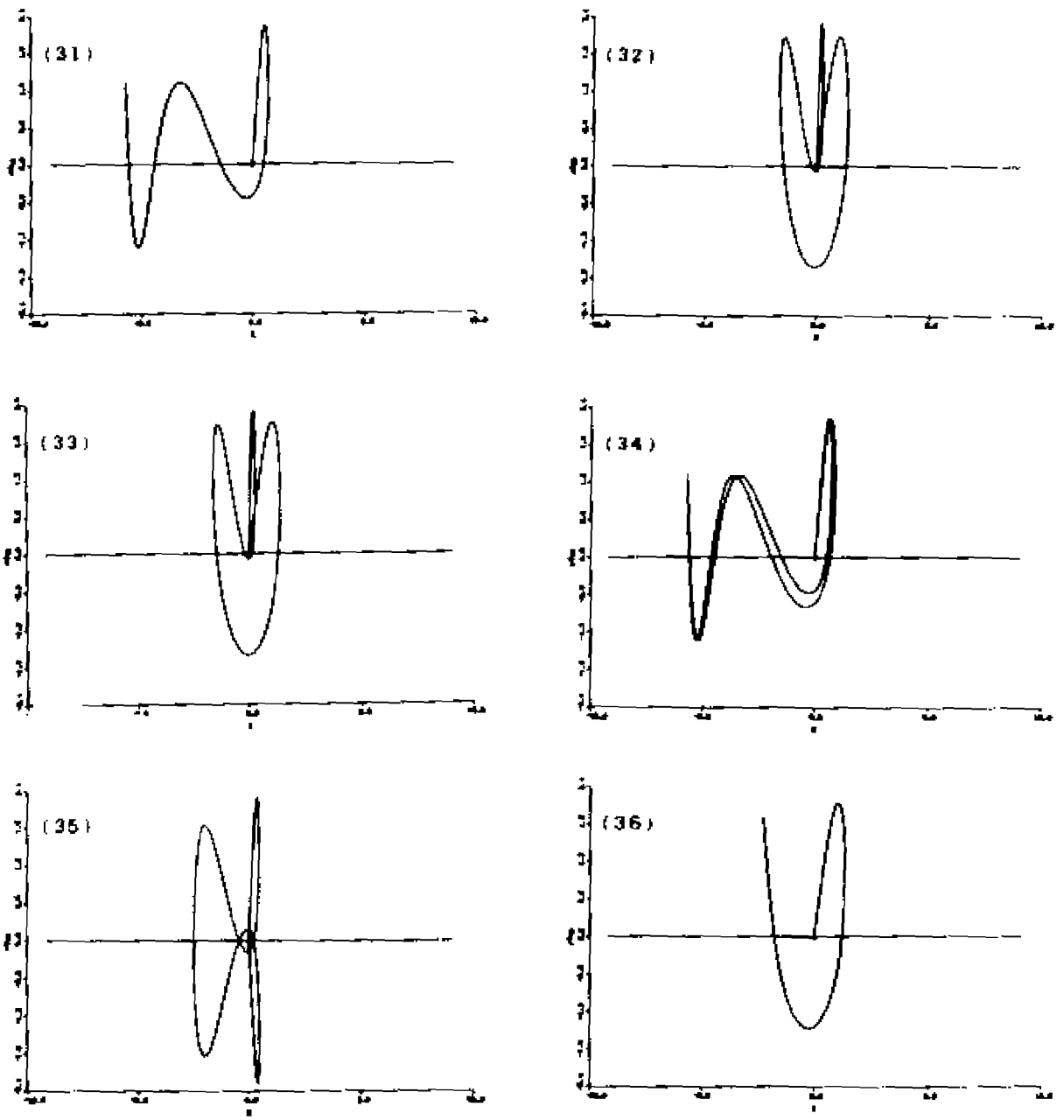

Fig. 7.2 (continued)

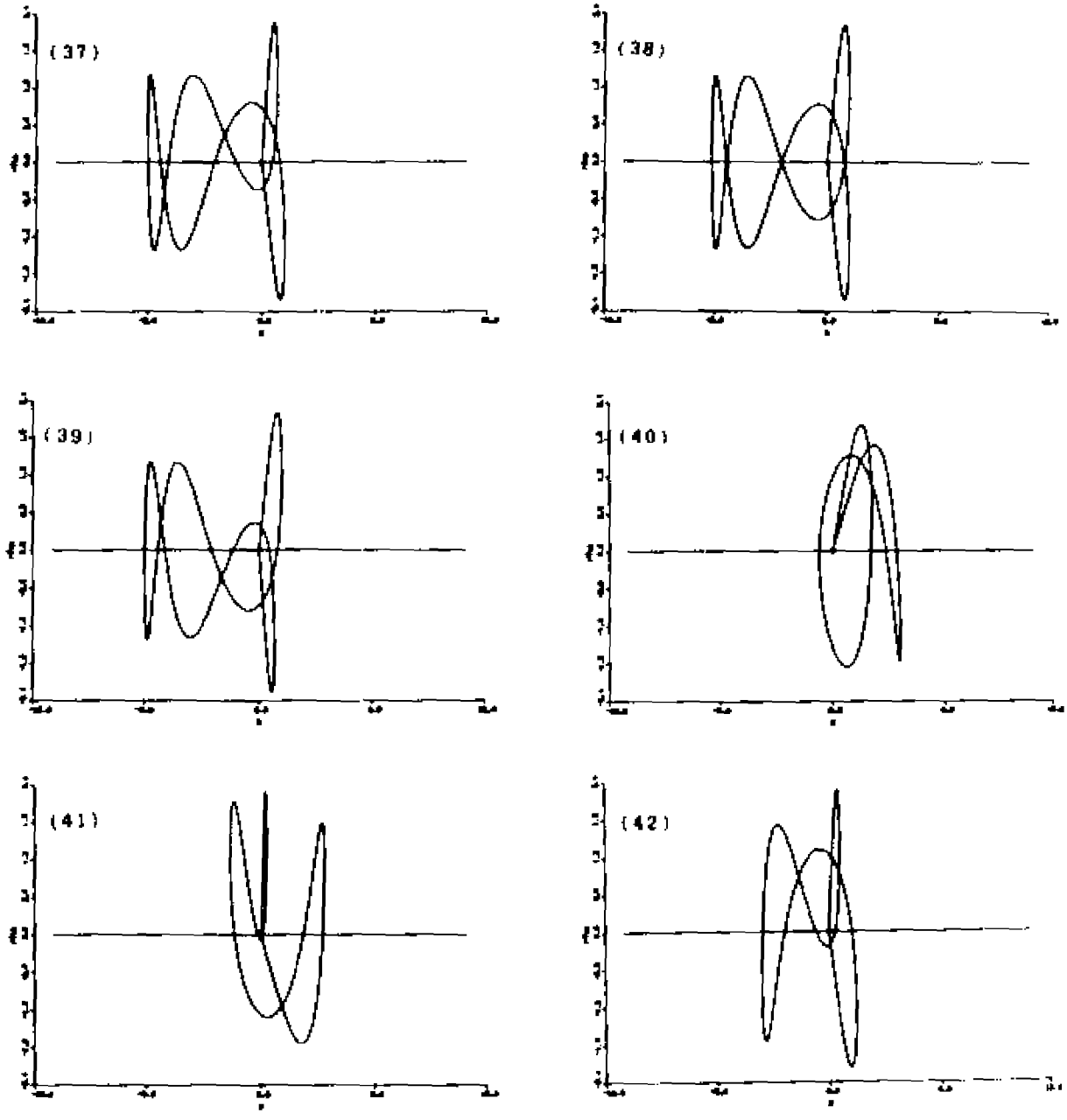

Fig. 7.2 (continued)

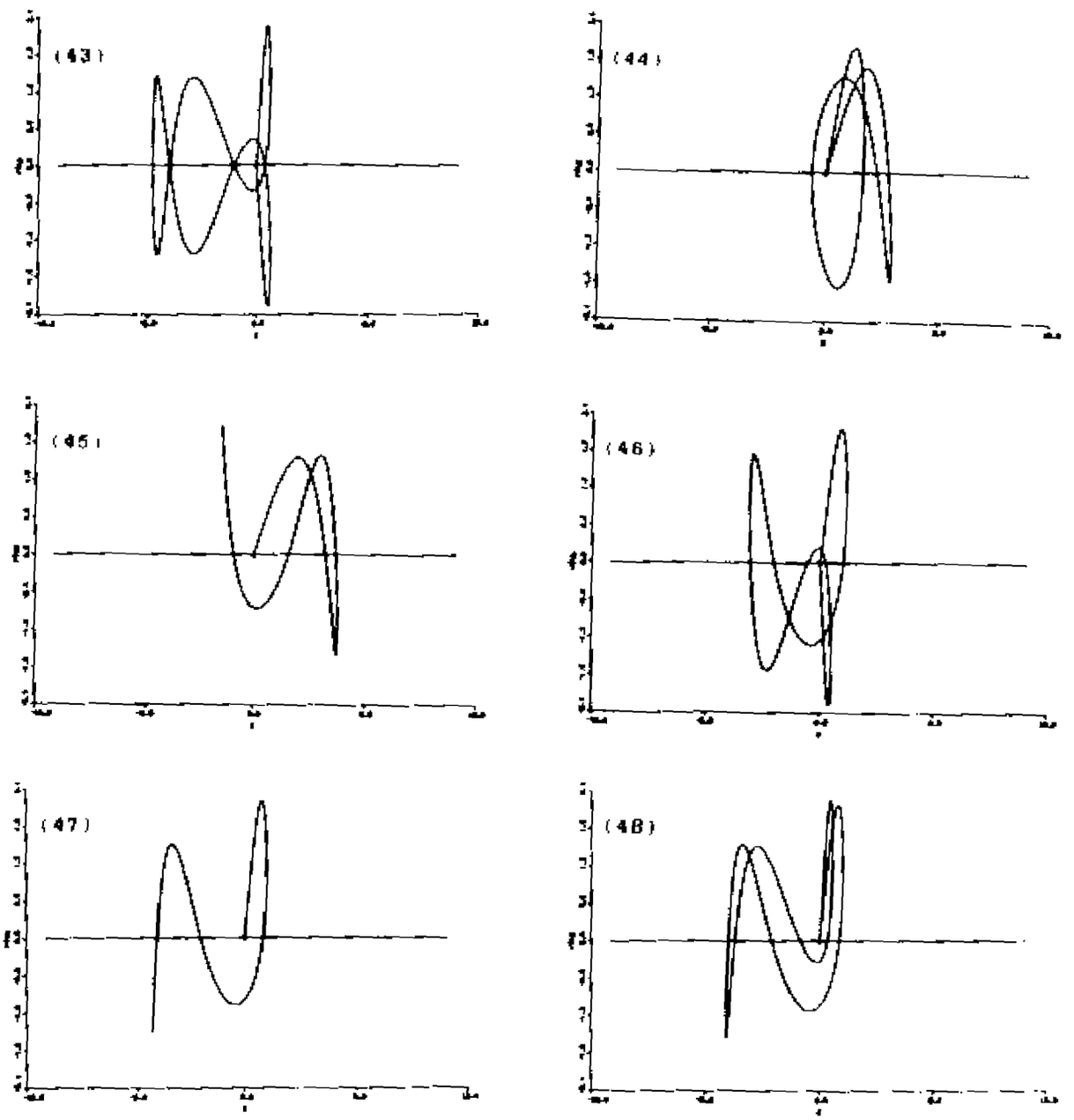

Fig. 7.2 (continued)

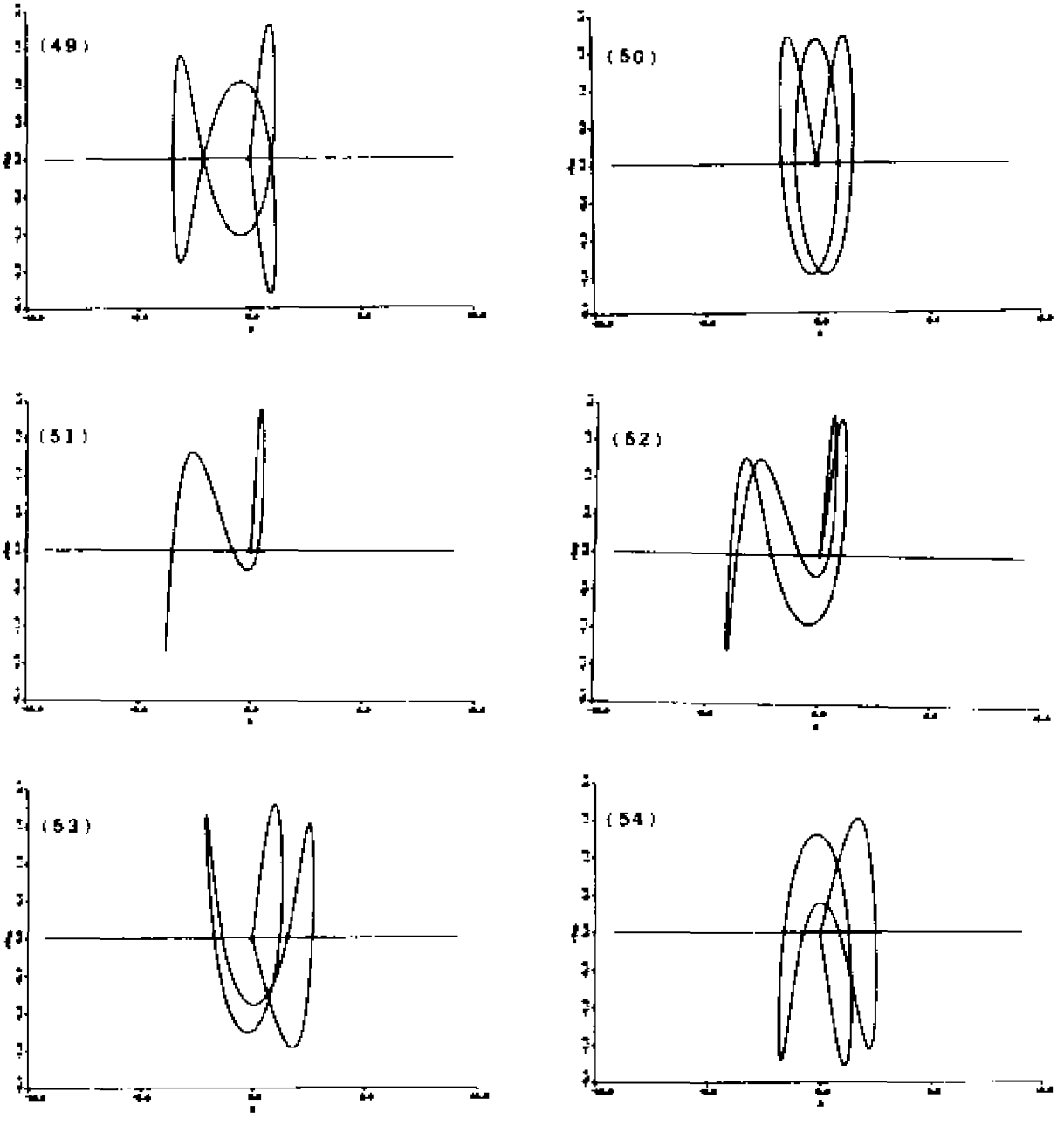

Fig. 7.2 (continued)

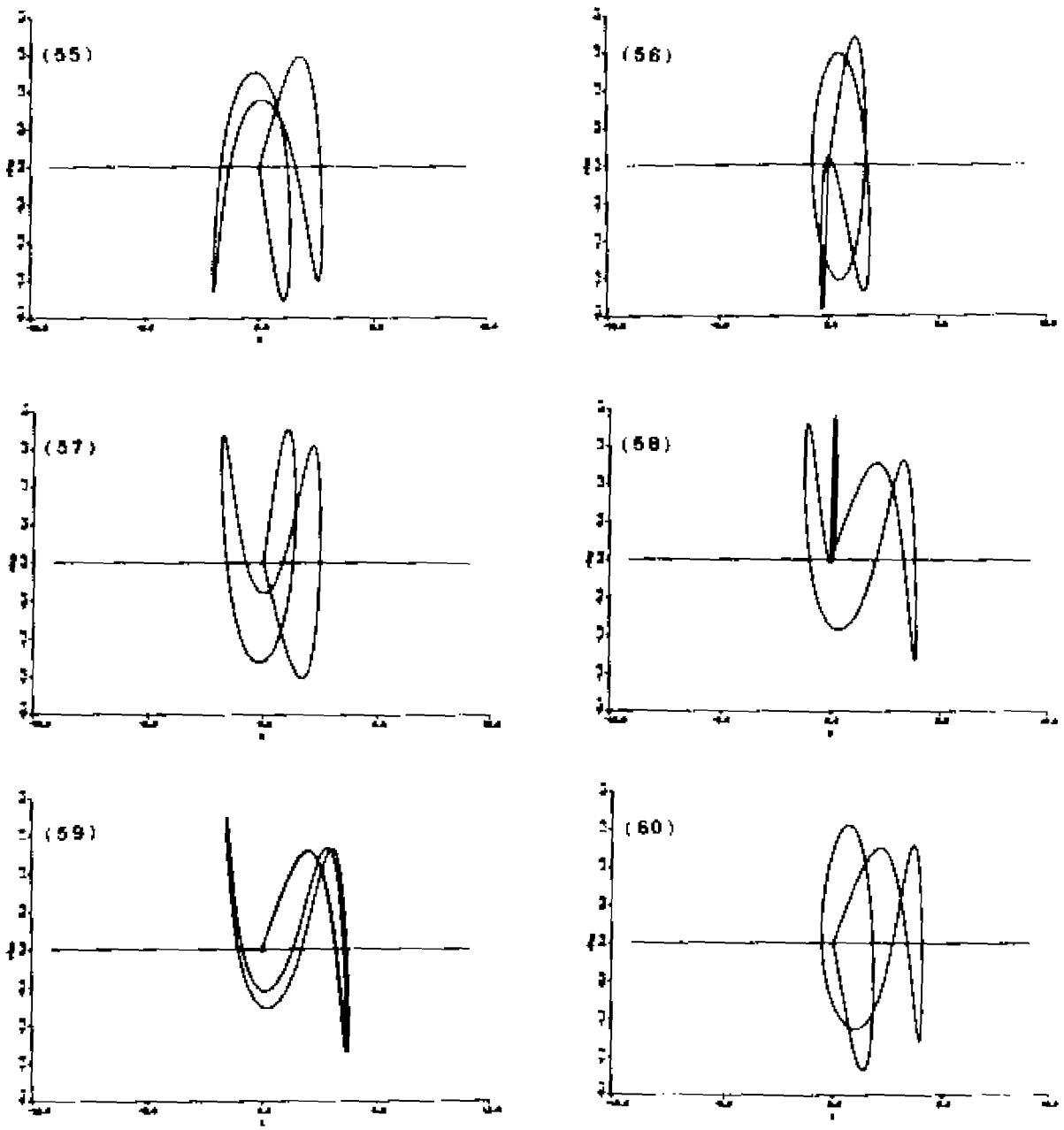

Fig. 7.2 (continued)

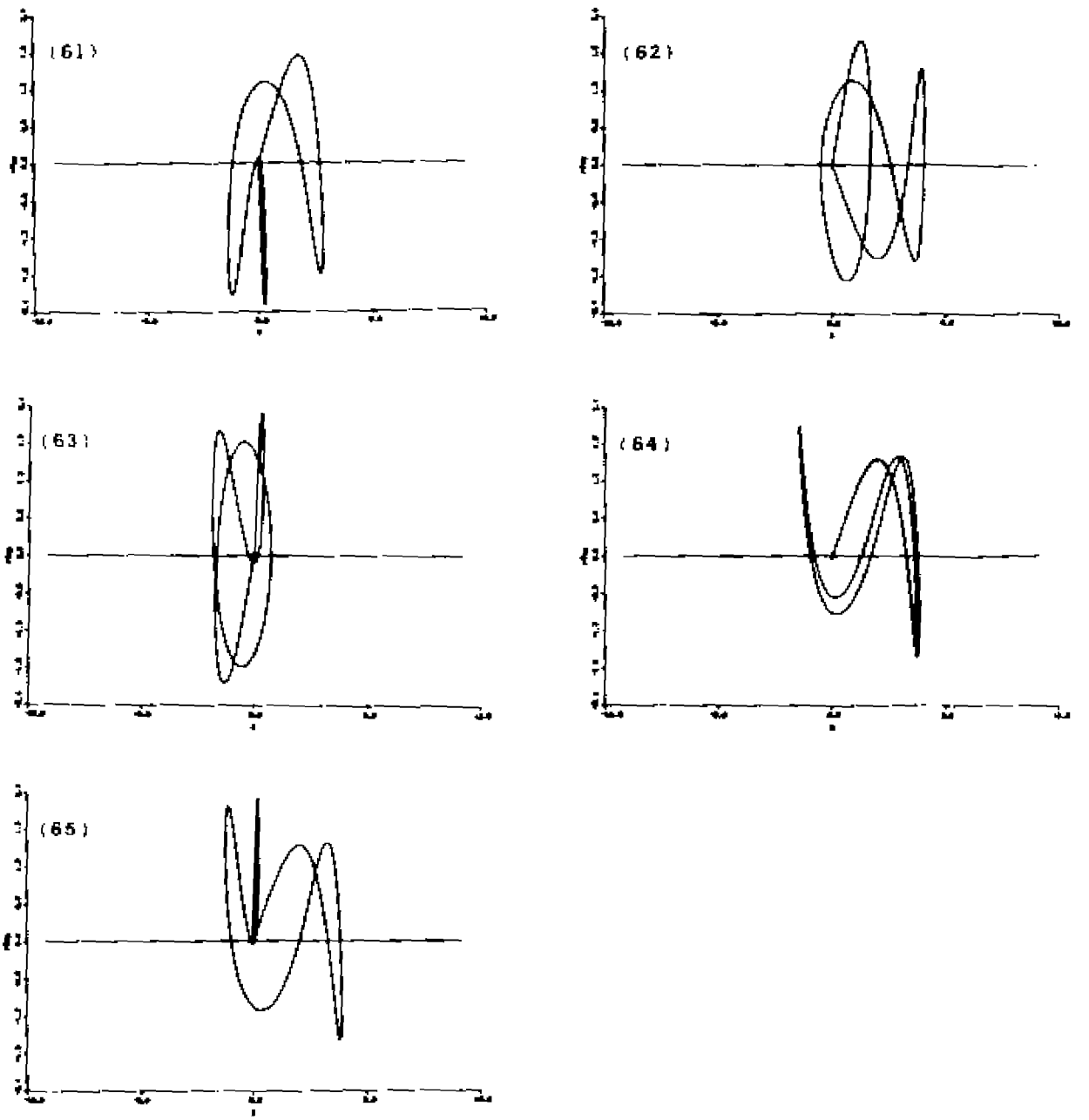

Fig. 7.2 (continued)

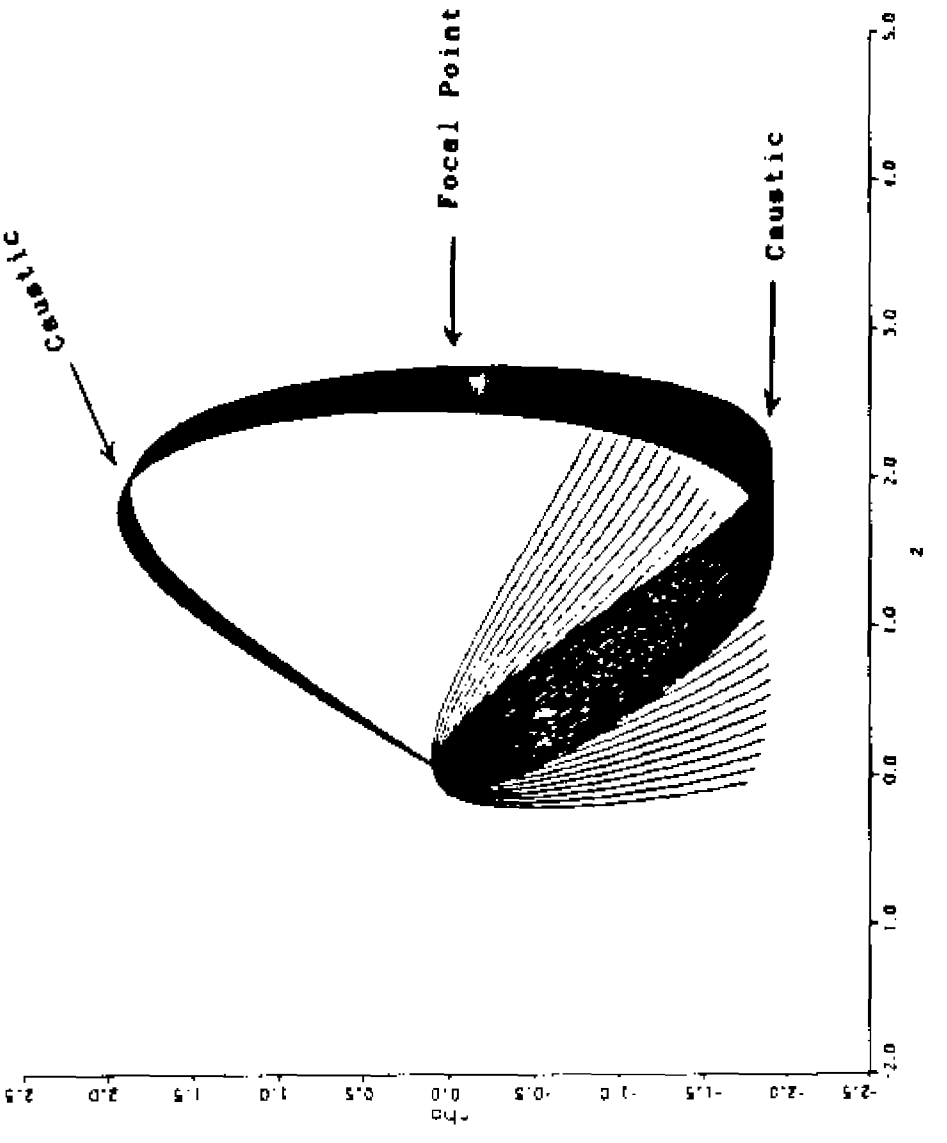

FIG. 7.3 Scattering of the family of trajectories associated with the second closed orbit. The circle in (b) and (c) is a circle with radius $50a_0$ from the nucleus. ρ (rho) and z are in $10^3 a_0$. (a) Overview.

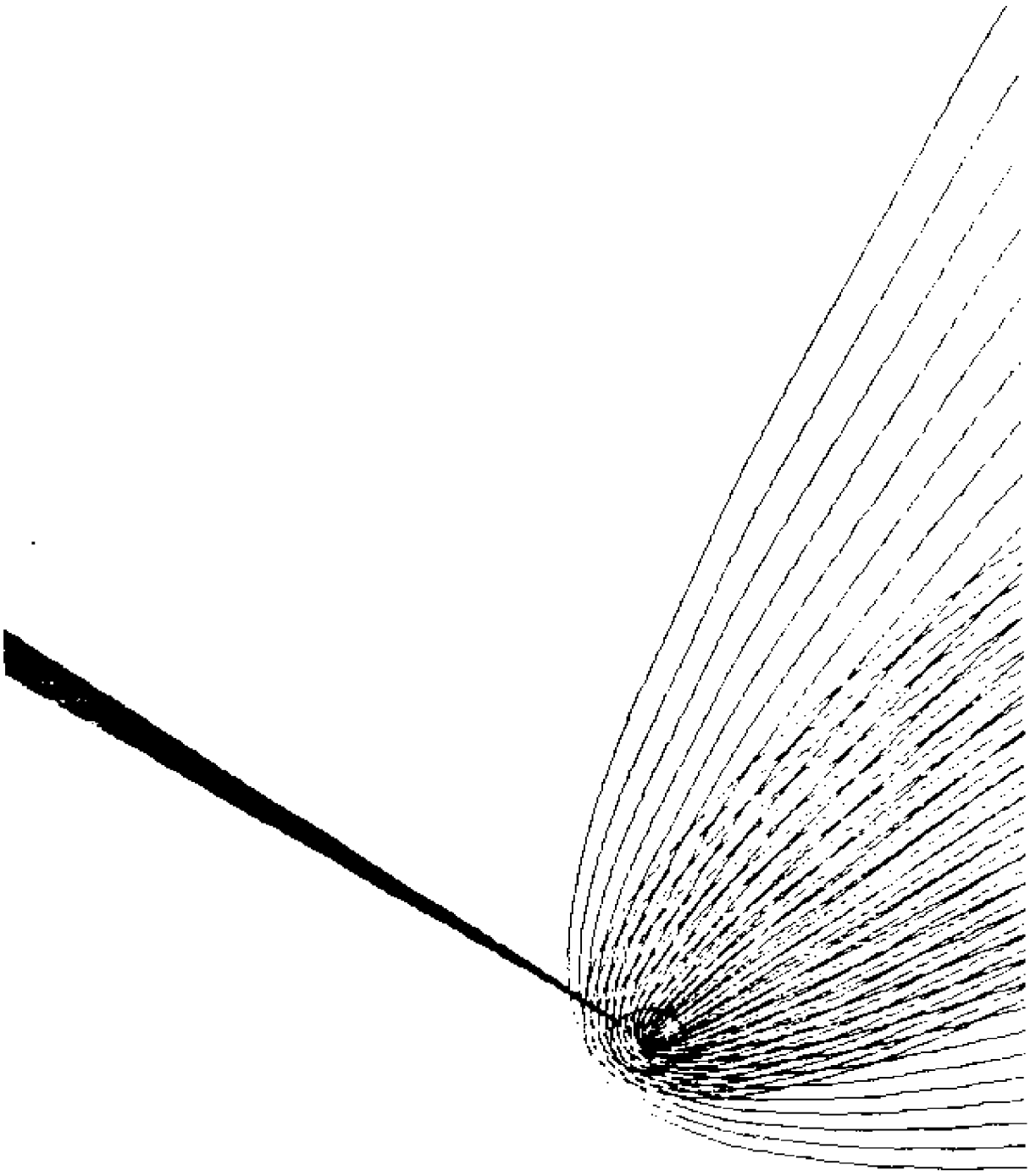

FIG. 7.3 (b) Magnified region close to the nucleus.

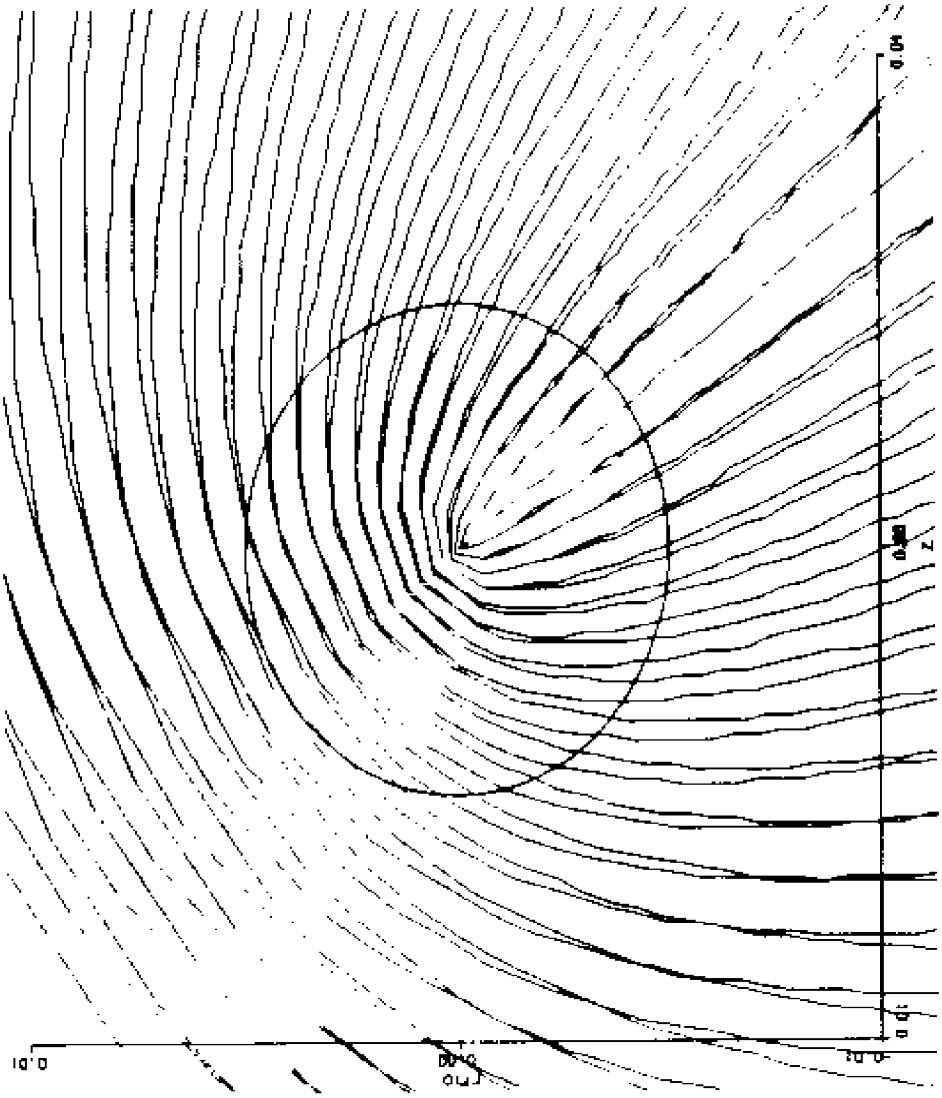

FIG. 7.3 (c) Further magnified region of the nucleus.

orbit NO. 2. The family of trajectories has two caustics, each close to a maximum of ρ, and it passes through a focus at $\rho=0$. (The focus would only be visible if the three dimensional family of trajectories were plotted.) When the trajectories return to the vicinity of the nucleus they are scattered by the Coulomb field, and each orbit is locally a parabola.

3. The Spectrum from the Closed Orbits

From the closed orbits found above, the action S_r along each closed orbit can be computed from eq. (5-25c) or (5-25d) by doing an integration. The semiclassical amplitude factor A can be calculated from eqs. (5-28) and (5-29) in principle, but in practice some manipulation of these two equations may be useful. This point is further discussed in Appendix G where practical formulas for calculating A are also given. The Maslov index for each orbit is found by summing the number of extrema in ρ direction and the number of crossings of $\rho=0$ (the z axis). Then using eq. (6-18), we can easily find the amplitude and phase of the oscillation in the absorption spectrum associated with each closed orbit. The period T of each closed orbit is also computed. These results are all listed in Table 7.2

Examining this table, we notice that the square of

the importance number is approximately proportional to the semiclassical amplitude factor A. This is no surprise, becaue both the importance number N_i and the amplitude factor A measure the divergence of the family of trajectories around each closed orbit. The importance number is more intuitive and less rigorous, while on the other hand the amplitude factor A is a well defined quantity and it enters into the formula for the spectrum.

We also note a loose connection between the period of the closed orbit and the value of the semiclassical factor A. Longer, more complicated orbits usually have a smaller value of A. We note also the shortest, most stable and most important orbit is the one that goes along the ρ axis; its effect on the spectrum is most prominent and of course was the first to be recognized.

Finally we see that there are pairs of orbits(No.32 and No. 33, for example) having identical action and period (and $A2 = A \cdot \left(\frac{\sin\theta_1}{\sin\theta_2}\right)^{1/2}$). In fact the two orbits are related by time-reversal. More generally any orbit, its time reversed orbit, its mirror image about the ρ axis and the time reversed orbit of the mirror image all contribute the same oscillation to the spectrum. We shall sum their contributions.

By summing such corresponding terms and rearranging the oscillations in deacending order of the

Table 7.2 (a) Maslov index, Semiclassical amplitude factor, action and period calculated for 65 closed orbits

No.	μ[a]	A[b]	S[c]	T[d]
1	1	21.2	207.98	0.6659
2	3	10.8	327.94	1.5690
3	5	7.30	397.95	2.5788
4	5	6.37	497.60	2.1426
5	7	5.75	450.06	3.5889
6	7	5.70	570.36	2.3613
7	7	4.47	570.35	2.3613
8	9	4.87	492.69	4.5962
9	11	4.29	529.27	5.6015
10	7	4.79	582.33	3.0418
11	7	3.75	582.33	3.0418
12	9	3.02	636.55	3.4586
13	13	3.87	561.60	6.6054
14	13	4.86	727.41	5.8533
15	13	4.89	727.10	5.6270
16	9	4.54	636.55	3.4586
17	9	2.89	641.14	3.9808
18	9	4.28	641.14	3.9808
19	15	3.55	590.75	7.6084
20	11	2.59	686.26	4.5407
21	7	3.44	652.89	2.8825
22	11	4.32	686.26	4.5407
23	11	4.24	687.88	4.9231
24	17	3.30	617.39	8.6106
25	17	4.60	961.22	7.0196
26	17	4.26	961.15	6.8979
27	11	2.58	687.88	4.9231
28	13	2.70	727.10	5.6270
29	13	2.74	727.41	5.8533
30	19	3.09	642.02	9.6123
31	17	3.77	961.05	6.7235
32	9	2.83	742.55	2.8693
33	9	3.15	742.55	2.8693
34	17	4.13	961.15	6.8979
35	11	2.38	812.12	3.1820
36	9	2.33	761.84	3.5826
37	15	2.24	923.17	5.8920
38	15	2.29	924.04	6.1913
39	15	2.16	923.18	5.8920
40	9	1.96	732.37	3.8605
41	11	2.39	828.09	3.7428
42	11	2.16	822.41	3.8724
43	15	2.12	922.00	5.5282
44	9	2.38	732.37	3.8605
45	17	2.11	1060.1	7.0086
46	11	2.02	822.41	3.8724
47	13	1.96	881.19	5.3156

Table 7.2 (a) (continued)

No.	μ[a]	A[b]	S[c]	T[d]
48	13	1.90	878.40	4.8838
49	11	1.98	829.51	4.4365
50	9	1.99	812.96	3.5407
51	13	1.96	874.63	4.3674
52	13	2.00	878.40	4.8838
53	11	2.02	850.79	4.4066
54	11	1.68	849.38	4.0582
55	11	1.64	850.79	4.4066
56	11	1.48	897.04	3.6349
57	11	1.99	849.38	4.0582
58	13	2.18	887.27	4.6645
59	17	1.67	1060.0	6.9254
60	11	1.42	788.65	4.8526
61	11	1.72	828.09	3.7428
62	11	1.94	788.65	4.8526
63	11	1.72	897.04	3.6349
64	17	1.65	1060.0	6.9254
65	13	1.38	887.27	4.6645

[a] The Maslov index associated with each closed orbit. It is equal to the number of extremes in direction plus the number of crossing of p axis.

[b] The amplitude factors are computed from circle r_b to r_b. These numbers should be mutilplied by 10^{-2}.

[c] The actions are computed from circle r_b to r_b.

[d] The period T is in T_c.

Table 7.2 (b) Calculated oscillation amplitudes, phases, and derivatives of phases with respect to the magnetic field for 65 closed orbits.

No.	A_{bK_0} [a]	α_{bK_0} [b]	$-\frac{\partial \alpha_{bK_0}}{\partial B}$ [c]
1	6.54×10^{-1}	5.30	13.9
2	4.14×10^{-2}	2.72	20.6
3	2.02×10^{-1}	0.49	24.5
4	7.96×10^{-3}	5.89	30.1
5	2.51×10^{-1}	5.47	27.4
6	6.68×10^{-2}	3.25	34.1
7	6.68×10^{-2}	3.25	34.1
8	2.59×10^{-1}	0.98	29.8
9	2.53×10^{-1}	3.01	31.8
10	4.14×10^{-2}	2.65	34.8
11	4.14×10^{-2}	2.65	34.8
12	9.71×10^{-2}	3.47	37.8
13	2.42×10^{-1}	0.77	33.6
14	9.39×10^{-2}	0.08	42.9
15	1.15×10^{-1}	6.05	42.9
16	9.71×10^{-2}	3.47	37.8
17	5.89×10^{-2}	1.77	38.1
18	5.89×10^{-2}	1.77	38.1
19	2.31×10^{-1}	1.65	35.3
20	1.00×10^{-1}	6.06	40.6
21	2.31×10^{-5}	0.96	38.8
22	1.00×10^{-1}	6.06	40.6
23	7.16×10^{-2}	1.39	40.7
24	2.20×10^{-1}	0.02	36.8
25	5.89×10^{-2}	4.55	56.0
26	6.05×10^{-2}	4.49	56.0
27	7.16×10^{-2}	1.39	40.7
28	1.11×10^{-1}	6.05	42.9
29	9.39×10^{-2}	0.08	42.9
30	2.08×10^{-1}	2.65	38.1
31	6.37×10^{-2}	4.38	56.0
32	2.07×10^{-2}	5.80	43.8
33	2.07×10^{-2}	5.80	43.8
34	6.05×10^{-2}	4.49	56.0
35	5.89×10^{-2}	3.10	47.7
36	7.96×10^{-3}	6.24	44.8
37	3.02×10^{-2}	1.07	53.9
38	2.39×10^{-2}	1.92	53.9
39	3.02×10^{-2}	1.07	53.9
40	3.18×10^{-3}	1.90	43.2
41	4.46×10^{-2}	3.37	48.6
42	2.39×10^{-2}	0.84	48.2
43	4.14×10^{-2}	6.17	53.8
44	3.18×10^{-3}	1.90	43.2
45	7.32×10^{-2}	2.90	61.5
46	2.39×10^{-2}	0.84	48.2
47	1.75×10^{-2}	6.20	51.5

Table 7.2 (b) (continued)

No.	A_{0K_0} [a]	χ_{0K_0} [b]	$-\frac{d\chi_{0K_0}}{dB}$ [c]
48	2.55×10^{-2}	3.42	51.4
49	1.27×10^{-2}	1.65	48.6
50	3.34×10^{-4}	0.81	47.7
51	4.30×10^{-2}	5.93	51.2
52	2.55×10^{-2}	3.42	51.4
53	1.11×10^{-2}	0.94	49.8
54	7.96×10^{-3}	5.81	49.7
55	1.11×10^{-2}	0.94	49.8
56	2.45×10^{-4}	0.07	52.4
57	7.96×10^{-3}	5.81	49.7
58	5.73×10^{-2}	2.87	51.9
59	5.73×10^{-2}	2.85	61.5
60	4.77×10^{-3}	4.77	46.3
61	4.46×10^{-2}	3.37	48.6
62	4.77×10^{-3}	4.77	46.3
63	1.75×10^{-4}	3.21	52.4
64	5.73×10^{-2}	2.85	61.5
65	5.73×10^{-2}	2.87	51.9

[a] Amplitudes of the closed orbits.
[b] Phases of the closed orbits.
[c] Derivatives of the phases with respect to the magnetic field in $Tesla^{-1}$.

period T, Table 7.3 is obtained. These are the theoretical spectrum (oscillations in (6-21)). We next compare them to the experimental results.

4. Comparisons Between Theoretical and Experimental Spectrum

If the spectrum $\overline{Df(E)}$ is plotted according to (6-21), taking the oscillations from Table 7.3 and the background in (7-9), we get the spectrum in Fig. 7.4. For comparison I also show the experimental spectrum. Both theoretical and experimental spectra are so wildly oscillatory that it seems to be impossible to compare them directly. The comparison between theory and experiment has to be made in a different way.

One method to compare them is to choose a "window" function with proper width, and average the experimental spectrum locally. In doing so the small-scale oscillations in the spectrum will be averaged to zero. What is left over is the large-scale oscillations. In Fig. 7.4 (e) is an experimental spectrum(measured at somewhat lower resolution than that in Fig. 7.4 (f) and the result obtained by smoothing that spectrum---light line: spectrum; heavy line: smoothed spectrum). This smoothed absorption spectrum is directly comparable to our theoretical spectrum including only the lowest T oscillation

Table 7.3 The oscillatory spectrum for transition $2P_z$ to $m_r=0$ near threshold of a Hydrogen atom in 5.96 Tesla magnetic field.

T_{oK_o}	A_{oK_o}	α_{oK_o}	
0.6659	6.54×10^{-1}	5.30	①
1.5690	8.28×10^{-2}	2.72	②
2.1426	1.59×10^{-2}	5.89	
2.3613	2.67×10^{-1}	3.25	
2.5788	4.04×10^{-1}	0.49	③
2.8693	8.28×10^{-2}	5.80	
2.8825	4.62×10^{-5}	0.96	
3.0418	1.66×10^{-1}	2.65	
3.1820	1.18×10^{-1}	3.10	
3.4586	3.88×10^{-1}	3.47	
3.5407	6.68×10^{-4}	0.81	
3.5826	1.59×10^{-2}	6.24	
3.5889	5.03×10^{-1}	5.47	④
3.6349	9.80×10^{-4}	0.07	
3.7428	1.78×10^{-1}	3.37	
3.8605	1.27×10^{-2}	1.90	
3.8724	9.55×10^{-2}	0.84	
3.9808	2.36×10^{-1}	1.77	
4.0582	1.59×10^{-2}	5.81	
4.3674	8.59×10^{-2}	5.93	
4.4066	4.46×10^{-2}	0.94	
4.4365	2.55×10^{-2}	1.65	
4.5407	4.01×10^{-1}	6.06	
4.5962	5.19×10^{-1}	0.98	⑤
4.6645	2.29×10^{-1}	2.87	
4.8526	1.91×10^{-2}	4.47	
4.8838	1.02×10^{-1}	3.42	
4.9231	2.86×10^{-1}	1.39	
5.3156	3.50×10^{-2}	6.20	
5.5282	8.28×10^{-2}	6.17	
5.6015	5.06×10^{-1}	3.01	⑥
5.6270	4.58×10^{-1}	6.05	
5.8533	3.76×10^{-1}	0.08	
5.8920	1.21×10^{-1}	1.07	
6.1913	4.77×10^{-2}	1.92	
6.6054	4.84×10^{-1}	0.77	⑦
6.7235	1.27×10^{-1}	4.38	
6.8979	2.42×10^{-1}	4.49	
6.9254	2.29×10^{-1}	2.85	
7.0086	1.46×10^{-1}	2.90	
7.0196	1.18×10^{-1}	4.55	
7.6084	4.62×10^{-1}	1.65	⑧
8.6106	4.39×10^{-1}	0.02	⑨
9.6123	4.17×10^{-1}	2.65	⑩

This table is obtained by summing up the same oscillations in Table 7.2 and the same oscillations from the mirror images of 65 orbits.

Table 7.3*The oscillatory spectrum as in Table 7.3 from the first and second harmonics of No. 1 orbit.

T_{0K_0}	A_{0K_0}	α_{0K_0}	μ	
1.3318	3.25×10^{-1}	3.51	4	*
1.9977	1.68×10^{-1}	1.74	7	**

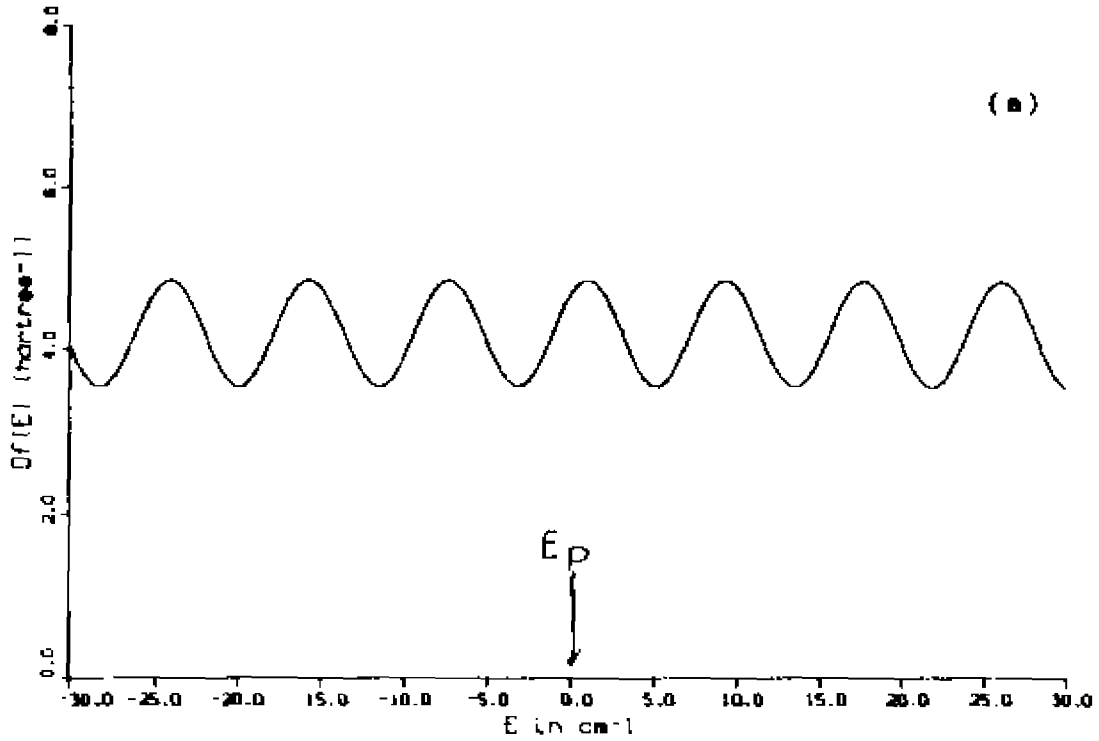
(a)
Df(E) (hartree⁻¹)
E_P
E (in cm⁻¹)

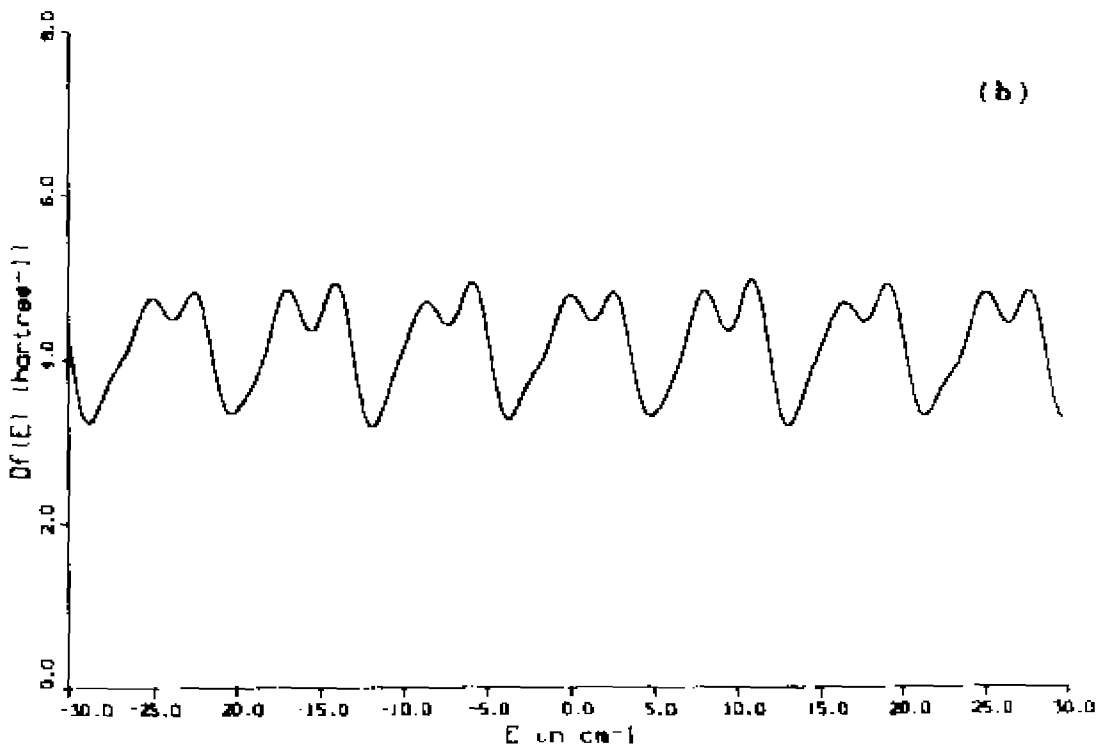
(b)
Df(E) (hartree⁻¹)
E (in cm⁻¹)

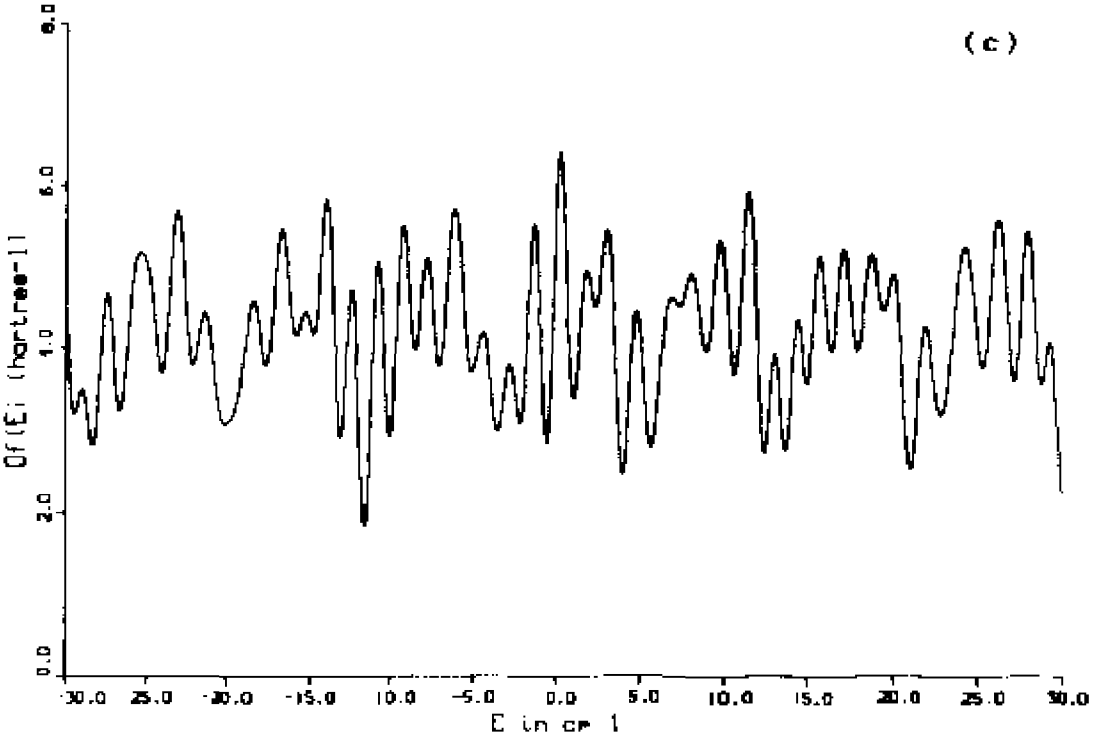
(c)
Of(E) (hartree-1)
E in cm-1

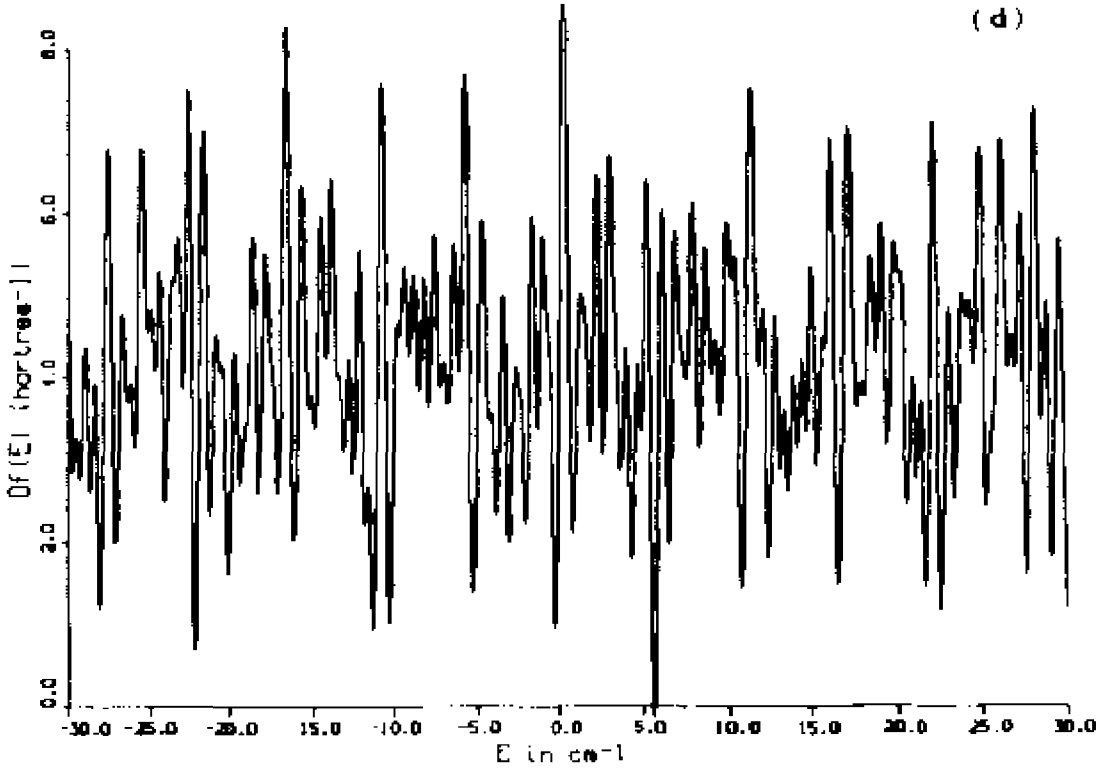
(d)
Of(E) (hartree-1)
E in cm-1

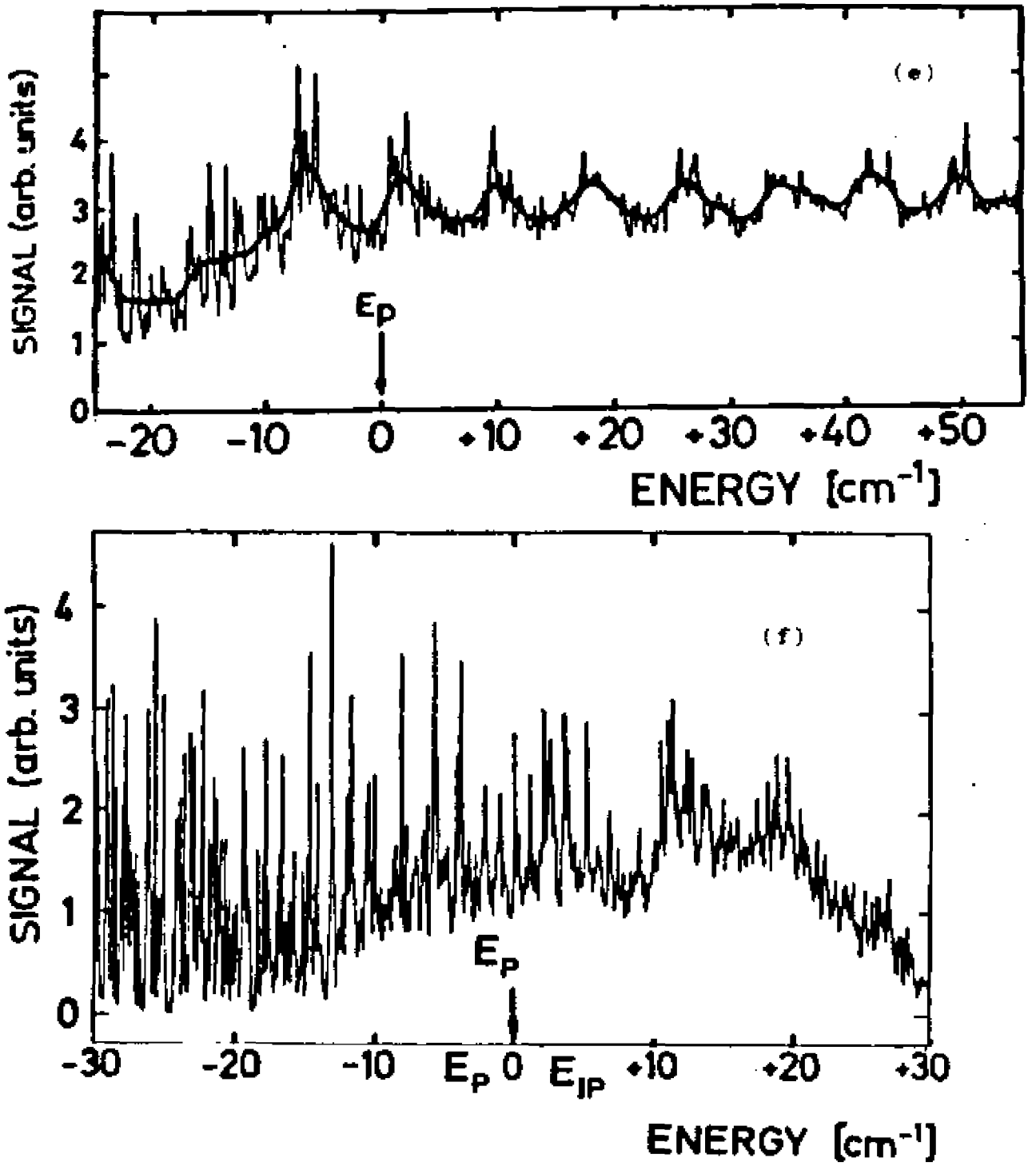

FIG. 7.4 Theoretical spectrum (a), (b), (c) and (d) are from eq. (6-21) with background from (7-9) and oscillations taken from Table 7.3 and 7.3* with only $T<1.0T_c$, $T<2.0T_c$, $T<4.0T_c$ and $T<10.0T_c$ terms respectively. Lower and higher resolution experimental spectrum (e) and (f) are from Ref. and respectively.

(Fig. 7.4 (a)). I call the reader's attention to a few facts from Fig. 7.4 (a) and Fig. 7.4 (e). The theory predicts: first, the magnitude of the lowest oscillation compared to the background; second, the energy-spacing of the oscillation; third, the absolute phase of the oscillation(I mark zero energy with an arrow and denote by E_p). These predictions all seem to agree with experiment very well.

A better method of comparing theory with experiment, which enables us to make quantitative comparison for many oscillations, is the Fourier transformation. Suppose $\overline{D_f(E)}$ represents the spectrum in $[E_1<E<E_2]$. We make a Fourier transformation to change energy variable E to time variable T,

$$F\overline{D_f(T)} = \int_{E_1}^{E_2} \overline{D_f(E)}\, e^{-iTE}\, dE \qquad (7\text{-}15)$$

now we use (6-21) to substitute for $\overline{D_f(E)}$ in (7-15) and do the integral. The result is

$$F\overline{D_f}(T) = D_f(0)\, e^{-i\frac{T}{2}(E_1+E_2)}\, \frac{\sin\frac{T}{2}(E_2-E_1)}{\frac{T}{2}}$$
$$+\sum_{mK_m} \frac{A_{mK_m} e^{i\alpha_{mK_m}}}{2i}\, e^{-i\frac{(T-T_{mK_m})}{2}(E_2+E_1)}\, \frac{\sin(T-T_{mK_m})(E_2-E_1)/2}{(T-T_{mK_m})/2}$$
$$-\sum_{mK_m} \frac{A_{mK_m} e^{-i\alpha_{mK_m}}}{2i}\, e^{-i\frac{(T+T_{mK_m})(E_2+E_1)}{2}}\, \frac{\sin(T+T_{mK_m})(E_2-E_1)/2}{(T+T_{mK_m})/2} \qquad (7\text{-}16)$$

We shall restrict ourselves to positive T. Then the second sum can be neglected and we obtain

$$F\overline{D_f}(T) = D_f(0)\, e^{-i\frac{T}{2}(E_1+E_2)}\, \frac{\sin\frac{T}{2}(E_2-E_1)}{T/2}$$

$$+\sum_{n,k} \frac{A_{nk}\, e^{i\alpha_{nk}}}{2i}\, e^{-i\frac{(T-T_{nk})(E_2+E_1)}{2}}\, \frac{\sin(T-T_{nk})(E_2-E_1)/2}{(T-T_{nk})/2}$$

(7-17)

Now if $|F\overline{D_f}(T)|^2$ against T is plotted and if T_{nk} are well separated, we should see peaks at each T_{nk}. Further more the height of each peak is proportional to the square of the proper oscillation amplitude A_{nk}.

In Fig. 7.5 I plot the square of the Fourier transformation of spectrum in Fig. 7.4 (f) in dashed line and the square of the oscillation amplitudes from theory in solid line(this picture discriminates against the smaller oscillations in the spectrum). Because the experimental spectrum is in arbitrary unit, the experimental spectrum is normalized so that the highest peak(at $T=0.66T_c$) matches the corresponding theoretical one.

Let me explain this Fig. 7.5 a little more. These orbits associated with the peaks marked by ① through ⑥ and 6^* are also marked in Table 7.3 and Table 7.3*. From Table 7.3, 7.3*, 7.2 and 7.1 we can find the properties of these orbits (initial angle, final angle, period, etc.). The orbit associated with the peak ① is an orbit that goes along the φ axis. This orbit has

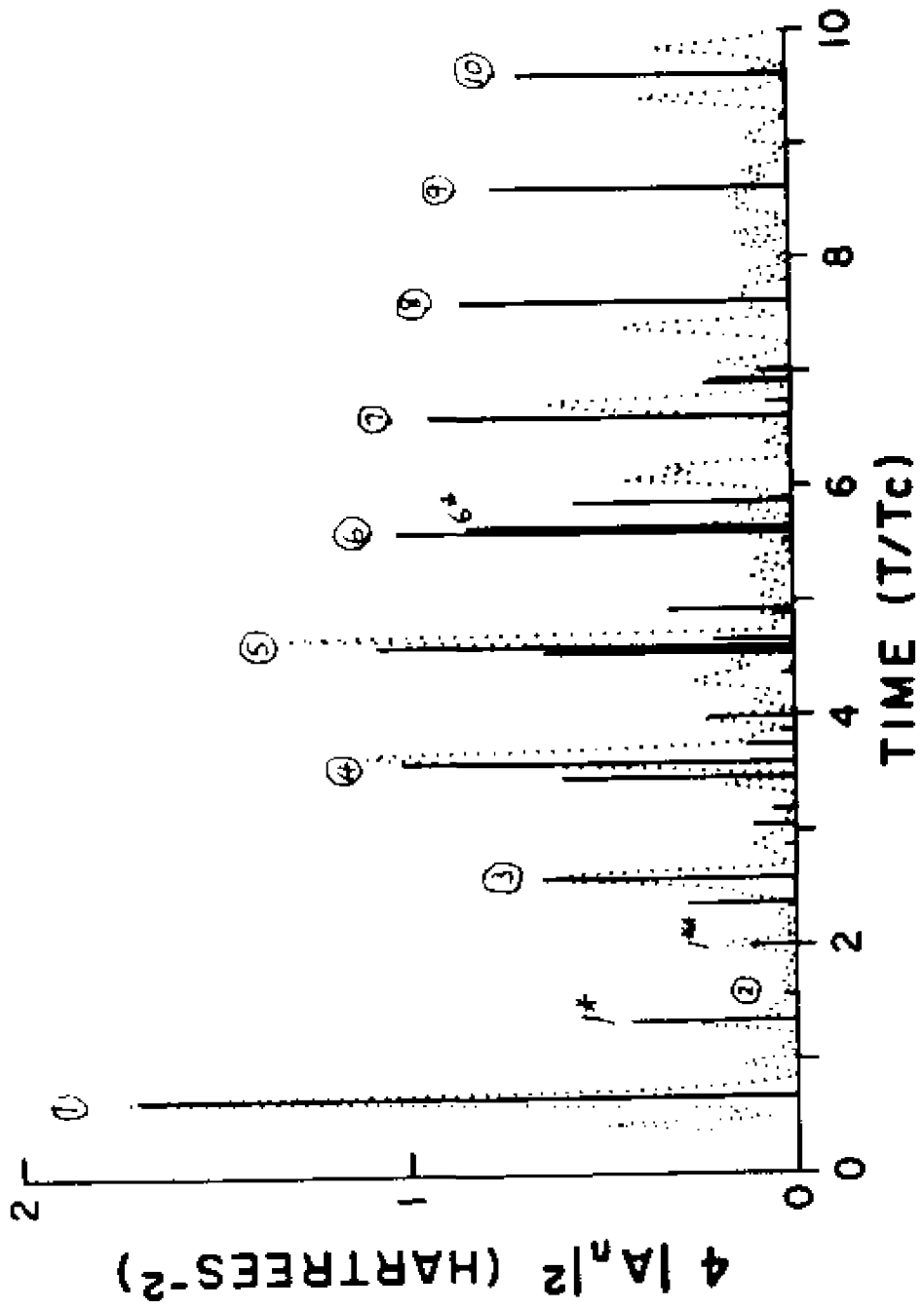

Fig. 7.5 Fourier-transformed spectrum. Vertical lines show calculated amplitudes $|A_{kL}|^2$ vs orbit periods T_{orb}. Light dotted line is experimental result from Ref. 76. The experimental result was normalized to match the height of the largest peak (T/T_c -0.67).

been known to be correlated with the largest oscillation in the observed spectrum since 1970[5] . The orbits associated with the peaks ② through ⑦ were found more recently[7] . All other closed orbits presented here are new ones.

There are some interesting features in Figure 7.5 which should be pointed out. The orbits lablled ① and ② are the most stable and the next most stable orbits of the system (stability is measured by the value of the amplitude factor A. A more stable orbit has a larger value of A--look in Table 7.2). Their values of amplitude factors differ by only a factor of 2; however, their oscillation amplitudes A_{osc} differ by almost an order of magnitude. Why is ① the highest peak and ② so small?

To understand this, we must usefind $\int G_c^+(\vec{r},\vec{r}')\,D\psi_i(\vec{r}')\,d\vec{r}'$. outgoing Green's function $G_c^+(\vec{r},\vec{r}')$ to find $\int G_c^+(\vec{r},\vec{r}')\,D\psi_i(\vec{r}')\,d\vec{r}'$. The above integral represents the outgoing wave caused by the absorption of a photon in state $2P_z$. If we do the integral, we would find that it is an outgoing wave having an angular amplitude distribution. This distribution is a linear combination of an S wave and a D wave. The D wave dominates the S wave(D wave amplitude is about 4 times of the s wave amplitude). By examining the initial outgoing angle of orbit ① and ② we find that the initial angle of ② is close to the node of the D wave and ① is on the peak of the D wave. Therefore the waves propagated outward in these two

different directions have very different intensity. their contributions to the spectrum are thus very different. Similarly returning angle also makes a great difference for the contribution of any closed orbit to the spectrum. The effects of initial and final angles may amplify each other and thus produce a drasatic contrast in the spectrum like ① and ② .

As I have just mentioned, ① is the orbit going along the ρ axis and returning to the nucleus. What would be the contribution to the spectrum if the orbit repeats itself a few times? The orbits marked by 1* and 1** are the contributions of repeated orbits of ① . 1* goes out from the nucleus along the ρ axis, returning to the nucleus, going out again and returning back to the nucleus. 1** just repeats one more time than 1*. The contributions of ① , 1* and 1** in a decreasing order may be easily understood. We know that the propagating waves always spread in this system and as they do so, their amplitude becomes smaller. So when the waves travel one more time over the path, the resulting contribution to the spectrum will be smaller. This consideration also suggests a relationship among the heights of ① , 1* and 1**---the ratio of height of ① against 1* is approximately equal to the ratio of height of 1* to 1**. The numbers shown in Table 7.3 and 7.3* confirm this.

The peaks marked by ⑥ and 6* might be more

interesting. We see the experimental peak there is rather small. Now from theory we found two much higher peaks contributed by two very different orbits. In fact ⑥ is from a periodic orbit, but 6* is from a closed one. How can we explain this apparent paradox? Well, it turns out that the phases of the oscillations from these two orbits differ almost by π. The theory actually agrees with experiment there.

Overall the agreement between theory and experiment up to $6T_c$ is impressive. Above $6T_c$ the theory has predicted some very distinct peakes. The experimental data does not match these peakes. We have no reason to believe that the theory is less accurate for the longer-period orbits, so we tentatively ascribe this discrepancy to problems of experimental resolution: longer period orbits produce very small-scale fluctuations in the spectrum, which would be difficult to measure accurately.

I have so far made comparisons with only available experimental data. The theory predicts results of experiments that have not yet been done. From (7-17) we can obtain the phase of each oscillation :

$$\alpha_{mk} = Arg\ F\bar{D}f(T_{mk}) + \frac{\pi}{2} \qquad (7\text{-}18)$$

So if we do the Fourier transformation of the spectrum, and find the argument of the resulting complex number at the peaks , we would get the phases of the

oscillations. This information can be calculated directly from the experimental data, but such calculations have not been reported. The reason is largely due to the lack of a complete theory in the past. No theory in the past has been able to predict the amplitude and phase of the oscillations in the spectrum. Those scattered, very incomplete theories have found the correct relationship between the spacing of each oscillation and the period of some kind of orbit. Exactly what kind orbit and the relationship between peak spacing and period of orbit can only now be understood correctly!

B. Remarks on Closed Orbits

In the above comparisons between the Fourier transformed experimental spectrum and the computed amplitude of oscillations, I have used the theoretical values at zero energy only. This is a reasonable simplification, because we know if the range of energy for the experimental specrum is not too large, the amplitude and period of each oscillation can be regarded as constants. More precise calculations could be made if we repeat the computations at different energies to obtain the amplitudes, phases and periods of orbits as functions of energy (see eq. (6-9)). Another interesting phenomenon then arises. In general any particular closed orbit existed only in a certain

range of energy. So when we change energy, we find most of the time orbits just change their shapes, but some orbits may vanish suddenly. If this happens, the contributions from these vanished orbits to the spectrum also vanish. Conversely new orbits may be born at certain energies. In this case, we would add their contribution to the spectrum. Fig. 7.6 illustrates this point very clearly.

From this, we obtain a unified picture for the atom in a strong magnetic field. Suppose we start from any energy, such as E=0. There we have a set of closed orbits which represent a superposition of oscillations in the spectrum. Now we lower the energy. Most closed orbits evolve continuously with energy. Some will disappear and some others may appear. This process can be repeated for any desired range of energy, and we would obtain a spectrum for the whole range of energy. At various energies we will have different set of closed orbits contributing to the spectrum, but we retain the view that the closed orbits produce oscillations in the spectrum.

C. What Has Been Learned

In this study I have extended the ideas of Gutzwiller, Berry and Tabor, who showed that periodic orbits produce fluctuations in the density of states.

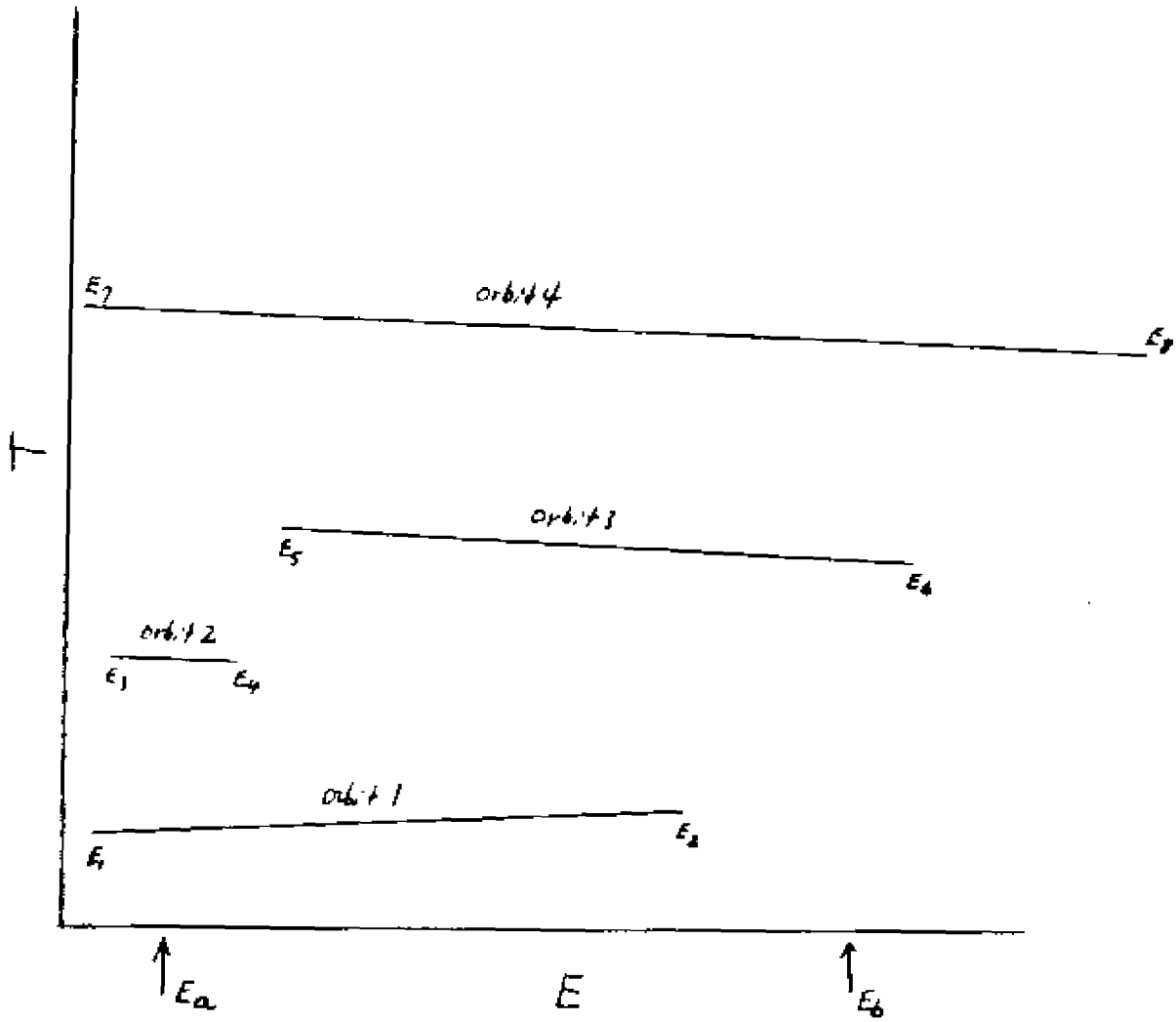

FIG. 7.6 A schematic picture of orbits over a range of energy. T and E are the period and energy of closed orbits respectively. Orbit 1 exists only between E_1 and E_2. Similarly other orbits exist in different ranges. At energy E_a we have orbits 1, 2 and 4. When we increase the energy we will see orbit 2 vanishes at E_4, orbit 3 appears at E_3 and orbit 1 disappears at E_2, while orbit 4 only changes its shape. When the energy reaches E_b orbits 3 and 4 have replaced the orbits 1, 2 and 4 at E_a.

I have shown that closed orbits produce oscillations in the absorption spectrum.

Quantitative formulas were established for a particular class of problems---atoms in external magnetic fields.

Computations were done for the transition $2P_1 \rightarrow m_f$. Theoretical results agree well with the available experimental data. New predictions have been made, and it is hoped that improved experiment will confirm these predictions in the future.

This study started with the desire to understand the quantum spectrum of a classical chaotic system. Now it can be concluded that through the connection between oscillations in the spectrum and the closed orbits in the system the quantum spectrum of a chaotic system possesses order. But it is another kind of order. The eyes would have a hard time to find such oredr by looking at the high resolution spectrum--- it becomes more chaotic when the resolution is increased. This is contrary to the behaviour of regular systems.

D. What More Can Be Done

The ideas here can be used for many other systems. In particular for atoms in strong magnetic field, different initial states ψ_i, polarizations D and field strengths can be chosen; computations for each case can easily be done. Also atoms in electric fields or in

parallel electric and magnetic fields can be studied with no modification of the formulas.

Then if the Green's function G_c^t is modified a little, one could study the above systems over a wide range of energy.

These and others will be the subjects of future research.

APPENDIX A

ENERGY AVERAGE

An energy-averaged Green's function is related to the finite time propagator. To see this, let us define

$$K^+(\xi,t;\xi',0)=\begin{cases} K(\xi,t;\xi',0) & t\geq 0 \\ 0 & t<0 \end{cases} \qquad (A-1)$$

Thus eq.(3-10) is written as

$$G^+(\xi,\xi';E)=\frac{1}{i\hbar}\int_0^\infty dt\, K^+(\xi,t;\xi',0)\exp\left(\frac{iEt}{\hbar}\right)$$
$$=(i\hbar)^{-1}\int_{-\infty}^{+\infty} dt\, K^+(\xi,t;\xi',0)\exp\left(\frac{iEt}{\hbar}\right) \qquad (A-2)$$

Let us also define in general

$$\bar{G}_g^+(\xi,\xi';E)\equiv(i\hbar)^{-1}\int_0^\infty K^+(\xi,t;\xi',0)\,\tilde{g}(t)\exp\left(\frac{iEt}{\hbar}\right)dt \qquad (A-3)$$

where $\tilde{g}(t)$ is a general cut-off function. We define $\tilde{g}(t)$ to be symmetric in time, so $\tilde{g}(-t)=\tilde{g}(t)$.

We shall now prove that $\bar{G}_g^+$ is an energy-averaged Green's function, specifically,

$$\bar{G}_g^+(\xi,\xi';E)=\int G^+(\xi,\xi';E')\,g(E-E')\,dE' \qquad (A-4)$$

where

$$g(E)=\frac{1}{2\pi\hbar}\int_{-\infty}^{+\infty}\tilde{g}(t)\,e^{iEt/\hbar}\,dt$$
$$=\frac{1}{\pi\hbar}\int_{0}^{\infty}\tilde{g}(t)\cos(Et/\hbar)\,dt$$

(A-5)

Proof:

From (A-2), the inverse Fourier transform gives

$$K^{+}(q,t;q',0)=\frac{i}{2\pi}\int_{-\infty}^{+\infty}G^{+}(q,q';E)\,e^{-iEt/\hbar}\,dE$$

(A-6)

substituting this formula for K^{+} into eq. (A-3), we obtain

$$\bar{G}_{g}^{+}(q,q';E)=\frac{1}{i\hbar}\int_{-\infty}^{+\infty}K^{+}(q,t;q',0)\cdot\hat{g}(t)\exp(iEt/\hbar)\,dt$$
$$=\frac{1}{i\hbar}\int_{-\infty}^{+\infty}\left[\frac{i}{2\pi}\int_{-\infty}^{+\infty}G^{+}(q,q';E)\,e^{-iE't/\hbar}dE'\right]\hat{g}(t)$$
$$\cdot\exp(iEt/\hbar)\,dt$$
$$=\frac{1}{2\pi\hbar}\int_{-\infty}^{+\infty}dE'\,G^{+}(q,q';E')\int_{-\infty}^{+\infty}dt\,\hat{g}(t)\,e^{i(E-E')t/\hbar}$$
$$=\int_{-\infty}^{+\infty}dE'\,G^{+}(q,q';E')\cdot g(E-E')$$

in the above the order of integration was changed.

The specific form of the convolution function depends on the form chosen for $\hat{g}(t)$. For example, if $\tilde{g}(t)$ gives a sudden cutoff,

$$\hat{g}(t)=1 \qquad |t|\le T$$
$$=0 \qquad |t|>T$$

(A 7a)

then

$$g(E-E') = \frac{1}{\pi}\,\frac{\sin[(E-E')\,T/\hbar]}{(E-E')}$$

(A-7b)

If $\hat{g}(t)$ is exponential or Gaussian, then Lorentzian or Gaussian convolution functions are obtained,

$$\hat{g}(t) = \exp[-|t|/T] \Longleftrightarrow g(E-E') = \frac{1}{\pi}\,\frac{\hbar/T}{(\hbar/T)^2 + (E-E')^2}$$

(A-7c)

$$\hat{g}(t) = \exp(-t^2/2T^2) \Longleftrightarrow g(E-E') = \frac{T}{\sqrt{2\pi}\,\hbar}\exp[-(E-E')^2 T^2/2\hbar^2]$$

(A-7d)

Always the relationship between the time and energy window is retained, $T\Delta E \sim 2\pi\hbar$.

An energy-averged oscillator-strength density is related to the finete time propagator and to the energy-averaged Green's function. If the propagator $\hat{K}(t,0)$ is calculated for only a finite time interval $0 \le t \le T$, then an averaged oscillator-strength density is determined, and the spectrum can be calculated to a corresponding resolution. The same "low-resolution" spectrum can be calculated from the energy-averaged Green's function.

Let us define

$$\overline{Df}_g(E) = (E-E_i)\int (E'-E_i)^{-1}\, Df(E')\cdot g(E-E')\,dE'$$

(A-8a)

When the width of $g(E-E')$ is much smaller than $|E-E_i|$, then

$$\overline{Df}_g(E) = \int Df(E')\; g(E'-E)\,dE'$$

(A-8b)

that is, $\overline{Df_g}(E)$ is just an average of $Df(E)$.

It is easy to prove that

$$\overline{Df_g}(E) = -\frac{2m_e(E-E_i)}{\hbar^2} \, Im \langle D\psi_f | \bar{G}_g^+(E) | D\psi_i \rangle \tag{A-9}$$

and that

$$\overline{Df_g}(E) = \frac{2m_e(E-E_i)}{\pi\hbar^3} \, Re \int_0^\infty \langle D\psi_f | \hat{K}(t,0) | D\psi_i \rangle \hat{g}(t) \, e^{iEt/\hbar} \, dt \tag{A-10}$$

Proof:

Eq.(A-9) follows trivially from (A-8), (3-23) and (A-4). Then eq. (A-10) follows from (A-9) and (A-1).

Ideally we should take $g(E'-E)$ in (A-8) in the same form as that for the laser profile. However, while the resulting theoretical averaged-oscillator-strength density should depend upon the width ΔE of the convolution function, it should not be sensitive to the detailed form of this function. Therefore we consider the special case that $\hat{g}(t)$ corresponds to a sharp cutoff, as in eq. (A-7a). In this case we use only a finite-time propagator, $\hat{K}(t,0)$ for $0 \le t \le T$, and the resulting oscillator-strength-density is averaged over energy with the convolution function (A-7b). In this way, we obtain a theoretically averaged oscillator-strength-density, $\overline{Df_{theor}}(E)$. This quantity will be compared to the experimentally averaged measurements $\overline{Df_{exp}}(E)$.

We take the width (in energy) of the theoretical convolution functon $g_{theor}(E_f-E)$ comparable to the

energy width of the laser beam, which is contained in $g_{Exp.}(E_f - \mathcal{E})$. Equivalently, we evaluate the propagator up to a maximum time T which is comparable to $2\pi\hbar/$ (experimental energy resoluton).

APPENDIX B

HYDROGEN WAVE FUNCTIONS

The eigenfunction of Hydrogen atom is the product of a radial function R_{nl} and a spherical harmonic. Some lower order such functions are listed here. Phase conventions are those of ref. 56. Although all observable quantities are independent of the choice of phase convention, it is important to use one internally consistent convention throughout the calculation. The functions and relations listed here are the ones used in the calculations in this thesis.

Table B-1 Lower Order Radial Functions

$$R_{10} = 2e^{-r}$$

$$R_{20} = \frac{1}{\sqrt{2}} e^{-\frac{r}{2}} \left(1 - \frac{1}{2} r\right)$$

$$R_{21} = \frac{1}{2\sqrt{6}} e^{-r/2} \cdot r$$

$$R_{30} = \frac{2}{3\sqrt{3}} e^{-r/3} \left(1 - \frac{2}{3} r + \frac{2}{27} r^2\right)$$

$$R_{31} = \frac{4}{81\sqrt{30}} e^{-r/3} r^2$$

$$R_{32} = \frac{4}{81\sqrt{30}} \cdot e^{-r/3} r^3$$

$$R_{40} = \frac{1}{4} e^{-r/4} \left(1 - \frac{3r}{4} + \frac{r^2}{8} - \frac{r^3}{192}\right)$$

$$R_{41} = \frac{1}{16}\sqrt{\frac{5}{3}} \cdot e^{-r/4} r \cdot \left(1 - \frac{r}{4} + \frac{r^2}{80}\right)$$

$$R_{42} = \frac{1}{64\sqrt{5}} e^{-r/4} r^2 \left(1 - \frac{r}{12}\right)$$

$$R_{43} = \frac{1}{768\sqrt{35}} e^{-r/4} r^3$$

Table B-2 Lower Order Spherical Harmonics

$$Y_{00} = \frac{1}{\sqrt{4\pi}}$$

$$Y_{10} = \sqrt{\frac{3}{4\pi}}\cos\theta$$

$$Y_{11} = \sqrt{\frac{3}{8\pi}}\sin\theta\, e^{i\varphi}$$

$$Y_{20} = \sqrt{\frac{5}{4\pi}}\left(\frac{3}{2}\cos^2\theta - \frac{1}{2}\right)$$

$$Y_{21} = \sqrt{\frac{15}{8\pi}}\sin\theta\cos\theta\, e^{i\varphi}$$

$$Y_{22} = \frac{1}{4}\sqrt{\frac{15}{2\pi}}\sin^2\theta\, e^{2i\varphi}$$

$$Y_{30} = \sqrt{\frac{7}{4\pi}}\left(\frac{5}{2}\cos^3\theta - \frac{3}{2}\cos\theta\right)$$

$$Y_{31} = \frac{1}{4}\sqrt{\frac{21}{4\pi}}\sin\theta\,(5\cos^2\theta - 1)\, e^{i\varphi}$$

$$Y_{32} = \frac{1}{4}\sqrt{\frac{105}{2\pi}}\sin^2\theta\cos\theta\, e^{2i\varphi}$$

$$Y_{33} = \frac{1}{4}\sqrt{\frac{35}{4\pi}}\sin^3\theta\, e^{3i\varphi}$$

$$Y_{40} = \sqrt{\frac{9}{4\pi}}\left(\frac{35}{8}\cos^4\theta - \frac{15}{4}\cos^2\theta + \frac{3}{8}\right)$$

$$Y_{41} = \frac{3}{4}\sqrt{\frac{5}{4\pi}}\left(7\cos^3\theta - 3\cos\theta\right)\sin\theta\, e^{i\varphi}$$

$$Y_{42} = \frac{3}{4}\sqrt{\frac{5}{8\pi}}\sin^2\theta\,(7\cos^2\theta - 1)\, e^{2i\varphi}$$

$$Y_{43} = \frac{3}{4}\sqrt{\frac{35}{4\pi}}\sin^3\theta\cos\theta\, e^{3i\varphi}$$

$$Y_{44} = \frac{3}{8}\sqrt{\frac{35}{8\pi}}\sin^4\theta\, e^{4i\varphi}$$

To obtain the other half of spherical harmonic functions (m negative), relation

$$Y^*_{\ell m} = (-1)^m Y_{\ell -m}$$

is used.

For evaluating dipole matrix elements, the following relations are helpful:

$$\cos\theta\, Y_{lm} = \sqrt{\frac{(l+m+1)(l-m+1)}{(2l+1)(2l+3)}}\, Y_{l+1,m} + \sqrt{\frac{(l+m)(l-m)}{(2l+1)(2l-1)}}\, Y_{l-1,m}$$

$$\sin\theta\, e^{i\varphi} Y_{lm} = \sqrt{\frac{(l+m+1)(l+m+2)}{(2l+1)(2l+3)}}\, Y_{l+1,m+1} - \sqrt{\frac{(l-m)(l-m-1)}{(2l+1)(2l-1)}}\, Y_{l-1,m+1}$$

$$\sin\theta\, e^{-i\varphi} Y_{lm} = -\sqrt{\frac{(l-m+1)(l-m+2)}{(2l+1)(2l+3)}}\, Y_{l+1,m-1} + \sqrt{\frac{(l+m)(l+m-1)}{(2l+1)(2l-1)}}\, Y_{l-1,m-1}$$

APPENDIX C

THE FORMULA FOR INTEGRAL $I^{\pm}_{n\ell}$

Here we shall derive a general formula for integral

$$G(n,\ell,\ell') = \int_0^\infty R_{n\ell}(r)\, r^3 \cdot \frac{J_{2\ell'+1}(\sqrt{8r})}{\sqrt{r}}\, dr \qquad (C-1)$$

Then $I^{\pm}_{n\ell}$ is the special case of $G(n,\ell,\ell')$ when $\ell' = \ell \pm 1$.

Since the radial function $R_{n\ell}(r)$ is a product of $e^{-\frac{r}{n}}$ and a polynomial of order (n-1),

$$R_{n\ell}(r) = e^{-\frac{r}{n}} \sum_{k=0}^{n-1} a_k\, r^k \qquad (C-2)$$

integral G(n,l,l') is a linear combination of integral

$$F(n,k,\ell') = \int_0^\infty e^{-\frac{r}{n}} \cdot r^k \cdot \frac{J_{2\ell'+1}(\sqrt{8r})}{\sqrt{r}}\, dr \qquad (C\ 3)$$

for k going grom 3 to (n+2),

$$G(n,\ell,\ell') = \sum_{k=3}^{n+2} a_{k-3} \cdot F(n,k,\ell') \qquad (C-4)$$

To evaluate F(n,k,l'), we first make e change of variable $x=\sqrt{8r}$ in the integral, then

$$F(n,k,\ell') = \frac{1}{4\,8^{k-\frac{1}{2}}} \int_0^\infty e^{-\frac{x^2}{8n}}\, x^{2k} \cdot J_{2\ell'+1}(x)\, dx \qquad (C\ 5)$$

Now we use formula 11.4.28 of Ref. 57,

$$\int_0^\infty e^{-a^2t^2}\, t^{\mu+1}\, J_\nu(bt)\, dt$$
$$= \frac{\Gamma(\frac{1}{2}\nu+\frac{1}{2}\mu)\,(\frac{1}{2}\frac{b}{a})^\nu}{2a^\mu\,\Gamma(\nu+1)}\, M(\tfrac{1}{2}\nu+\tfrac{1}{2}\mu,\ \nu+1,\ -\tfrac{b^2}{4a^2})$$

$$(\mathrm{Re}(\mu+\nu)>0\ ,\ \mathrm{Re}\,a^2>0)$$

where the notation M(a,b,z) stands for the confluent hypergeometric function, which has a Taylor expansion

$$M(a,b,z) = 1 + \frac{az}{b} + \frac{(a)_2 z^2}{(b)_2\, 2!} + \cdots + \frac{(a)_n z^n}{(b)_n\, n!} + \cdots$$

where

$$(a)_n = a(a+1)(a+2)\cdots(a+n-1)\ ,\quad (a)_0 = 1$$

The result for F(n,k,l') is

$$F(n,k,l') = 2^{l'+\frac{1}{2}}\cdot n^{k+l'+1}\,\frac{\Gamma(k+l'+1)}{\Gamma(2l'+2)}\, M(k+l'+1,\ 2l'+2,\ -2n)$$

APPENDIX D

STATIONARY PHASE APPROXIMATION

For real functions $g(x)$, $\phi(x)$, under stationary phase approximation

$$\frac{1}{(2\pi)^{\frac{1}{2}}} \int dx\ g(x)\ \exp i\phi(x)$$
$$\doteq \sum_i \frac{g(x_i)}{|\phi''(x_i)|^{\frac{1}{2}}} \cdot \exp\left[i\phi(x_i) + \frac{i\pi}{4} \operatorname{sgn}(\phi''(x_i)) \right] \qquad (D\text{-}1)$$

where i labels the stationary points of $\phi(x)$ ---the points where $\phi'(x_i)=0$.

APPENDIX E

PROOF OF SEMICLASSICAL WAVE APPROXIMATION

Here for completeness I shall give a short proof that the semiclassical approximation used in this thesis for the wave function is asymptotically accurate to order $\hbar$.

We write the wave function in the form

$$\psi(q) = A(q)\exp\left[\frac{i}{\hbar}S(q)\right] \tag{E-1}$$

and further we assume that A(q) can be expanded in power of $\hbar$,

$$A(q) = A^{[0]}(q) + \hbar A^{[1]} + \hbar^2 A^{[2]} + \cdots, \tag{E-2}$$

This expansion (E-1) and (E-2) are substituted into the Schroedinger equation,

$$\left[\frac{(-i\hbar\nabla_q)^2}{2m} + V(q) - E\right]\psi(q) = 0 \tag{E-3}$$

and we demand that the quantities of different order of $\hbar$ to be zero,

$$\hbar^0: \quad H(\nabla S, q) = \frac{|\nabla_q S|^2}{2m} + V(q) - E = 0 \tag{E-4a}$$

$$\left(\frac{-i\hbar^1}{2m}\right): \quad 2\nabla A^{[0]}\nabla S + (\nabla^2 S)A^{[0]} = 0 \tag{E-4b}$$

$$\left(\frac{-i\hbar^2}{2m}\right):\quad 2\nabla A^{[1]}\nabla S + (\nabla^2 S)A^{[1]} - i\nabla^2 A^{[0]} = 0$$

(E-4c)

Thus we obtain the Hamilton-Jacobi equation (E 4a), a "transport equation" (E-4b) and a set of differential equations defining $A^{[j]}$ in terms of $A^{[j-1]}$ for $j \geq 1$.

From the above equations we also note

$$\left|(H-E)A^{[0]}(\theta)\, e^{iS(\theta)/\hbar}\right| = \left|\frac{\hbar^2}{2m}\nabla^2 A^{[0]}\right|$$

(E-5)

therefore if $A^{[0]}$ and its derivatives are bounded by a constant, K, then the right hand side of (E-5) is less than $\frac{\hbar^2}{2m}K$. When $\hbar$ goes to zero this upper bound also goes to zero as $\hbar^2$. We say that $A^{[0]}e^{iS/\hbar}$ is a "formal asymptotic approximation" for the solution of the Schroedinger equation.

Now write $\nabla S(\theta)/m = \vec{v}(\theta)$ in (E-4b) and think of v(q) as a velocity field, then

$$2\vec{v}\,\nabla A^{[0]} + (\nabla \vec{v})A^{[0]} = 0$$

(E 6a)

multiply (E 6a) by $A^{[0]}$ and set $\rho = A^{[0]2}$, it becomes

$$(\vec{v}\cdot\vec{\nabla})\rho + (\vec{\nabla}\cdot\vec{v})\rho = 0$$

(E-6b)

or

$$\vec{\nabla}\cdot(\rho\vec{v}) = 0$$

(E-6c)

This is the time-independent form of the equation of continuity,

$$\frac{\partial \rho}{\partial t} + \vec{\nabla}\cdot(\rho\vec{v}) = 0 \qquad \text{(E-6d)}$$

or

$$\frac{d\rho}{dt} + \rho\,\vec{\nabla}_q\cdot\vec{v}(q) = 0 \qquad \text{(E-6e)}$$

The solutions of (E-4a) and (E-4b) are constructed in a procedure described in more detail in Chapter V. Briefly we begin by specifying an initial surface of (n-1)-dimension in the n dimensional configuration space. Let points on this initial surface be specified by coordidinates q^0 . For each initial point q^0 , we require that the momentum satisfies the energy equation,

$$H(P^0(q^0), q^0) - E = 0 \qquad \text{(E-7)}$$

and the equation

$$dS^0 = P^0(q^0)\,dq^0 = \sum_i P_i^0(q^0)\,dq_i^0 \qquad \text{(E 8)}$$

then starting from each point q^0 on the initial surface and using $P^0(q^0)$ as the initial momentum, trajectories are computed by integrating Hamilton's equation. Let w_i $(i=1,\ldots,n-1)$ be the coordinates of the initial surface, we have functions

$$\vec{q} = \vec{q}(t, w) \qquad \text{(E-9a)}$$

$$\vec{P} = \vec{P}(t, w) \qquad \text{(E-9b)}$$

then the solutions of (E-4a) and (E-4b) are

$$S(q) = S(q^0(q)) + \int P(t) \cdot \frac{dq(t)}{dt}\, dt$$

(E-10)

and

$$\rho(q) = \rho^0(w)\ \frac{J(0,w)}{J(t,w)}$$

(E 11a)

where

$$J(t,w) = \frac{\partial q(t,w)}{\partial(t,w)}$$

(E 11b)

and $\rho^0(w)$ is an arbitrary "initial" density function.

We now show that if a solution to (E-4a) exists and it is equal to $S^0(q^0)$ on the initial surface, then that solution is given by (E-10). Let S(q) be a solution to (E-4a) in a given domain, including the initial surface, on which $S(q) = S^0(q^0)$, and define the function $P_i(q)$ as

$$P_i = \frac{\partial S(q)}{\partial q_i}$$

(E-12)

Differentiating (E 4a) with respect to q_i, we have

$$\sum_j \frac{\partial H}{\partial P_j}\ \frac{\partial^2 S}{\partial q_i \partial q_j} + \frac{\partial H}{\partial q_i} = 0$$

(E 13)

Now starting from a particular point q^0 on the initial surface, define a path q(t) such that

$$\frac{dq_i}{dt} = \frac{\partial H(P,q)}{\partial P_i}\Big|_{P=P_q S} \qquad i=1,\ldots,n$$

(E-14)

Here we differentiate H(q,p) with respect to p_i, then substitute $p=\nabla_q S(q)$, so that the right-hand side is a function of only q, and (E-14) is a closed set of n equations determining the path q(t) from the initial point q^0. Now consider the function

$$P_i(t) \equiv P_i(q(t)) = \frac{\partial S(q)}{\partial q_i} \Big/ q = q(t) \qquad \text{(E-15)}$$

This satisfies

$$\frac{dP_i}{dt} = \sum_j \frac{\partial P_i}{\partial q_j} \frac{dq_j}{dt} = \sum_j \frac{\partial^2 S}{\partial q_j \partial q_i} \frac{\partial H}{\partial p_j}$$

$$= -\frac{\partial H}{\partial q_i} \qquad \text{(E 16)}$$

where we have used (E-12) and (E-13). Eqs.(E-15) and (E-16) are Hamilton's equations, which therefore provide an alternative way of specifying the path defined by (E-14). On this path, let us define $S(t)=S(q(t))$; it follows that

$$\frac{dS}{dt} = \sum_i \frac{\partial S}{\partial q_i} \frac{dq_i}{dt} = \sum_i P_i(q(t)) \frac{dq_i}{dt} = P(q(t)) \frac{dq}{dt} \qquad \text{(E 17)}$$

This is a differential form for which the integral is (E-10).

To prove that $P(q)$ defined in (E-11) is a solution of the transport equation (E-6e), which is equivalent to (E-4b), we need first to show that for any non-singular NxN matrix, with elements J_{ij}, then

$$\frac{d}{dt}\ln(\det J) = Tr\left[\left(\frac{dJ}{dt}\right) J^{-1}\right]$$

(E-18)

To prove this, consider the matrix of cofactors C_{ij}, each of which is equal to $(-1)^{i+j}$ times the determinant of the matrix obtained by striking out the ith row and jth column of J. From well-known theorems in linear algebra,

$$\det J = \sum_i J_{ij} C_{ij}$$

so

$$\frac{\partial \det J}{\partial J_{ij}} = C_{ij}$$

furthermore

$$(J^{-1})_{ij} = C_{ji} / \det J$$

therefore

$$\frac{d}{dt}(\det J) = \sum_{ij} \frac{\partial \det J}{\partial J_{ij}} \frac{dJ_{ij}}{dt} = \sum_{ij} C_{ij} \dot{J}_{ij}$$

$$= \sum_{ij} (\det J)(J^{-1})_{ji} \dot{J}_{ij} = (\det J) Tr(J^{-1}\dot{J})$$

Now let the paths q(t) be generated according to (E-14), which we write in the form

$$\frac{dq_i}{dt} = f_i(q)$$

(E-19)

we will need the matrix

$$F_{ij} = \frac{\partial f_i}{\partial q_j}$$

(E-20)

Let the solutions q(t) be regarded as a function

of the n variables $\zeta_j = (t, w)$, with w being the n-1 variables that specify a point on the initial surface. Consider the matrix J having elements

$$J_{ij} = \frac{\partial \beta_i}{\partial \zeta_j} \qquad \text{(E 21)}$$

its time derivative is given by

$$\frac{d}{dt} J_{ij} = \frac{d}{dt} \frac{\partial \beta_i}{\partial \zeta_j} = \frac{\partial}{\partial \zeta_j} \frac{d\beta_i}{dt} = \frac{\partial}{\partial \zeta_j} f_i(\beta)$$

$$= \sum_k \frac{\partial f_i}{\partial \beta_k} \frac{\partial \beta_k}{\partial \zeta_j} = (FJ)_{ij} \qquad \text{(E-22)}$$

furthermore, according to eq. (E-11b),

$$J(t,w) = \det J \qquad \text{(E-23)}$$

from (E 11a) we find

$$\frac{dP(\beta)}{dt} = - \frac{\rho^0(w)\, J(0,w)}{J(t,w)^2} \frac{dJ(t,w)}{dt}$$

using (E-23), (E-18) and (E 22), we obtain

$$\frac{dP(\beta)}{dt} = - \frac{\rho^0(\beta^0)\, J(0,w)}{J(t,w)} \operatorname{Tr} F \,,$$

and from (E-20), (E-19) and the Hamiltonian ($H = p^2/2m + v(q)$),

$$\frac{dP(\beta)}{dt} = - P(\beta) \frac{\nabla_\beta P(\beta)}{m} \qquad \text{(E-24)}$$

so the function $P(\beta)$ defined in (E-11) satisfies the continuity equation (E-6).

APPENDIX F

PHASE LOSS THROUGH A FOCUS

For $m \neq 0$ the $\rho = 0$ line is a potential barrier (m^2/ρ^2 in the effective potential). The family of trajectories is turned back when moving toward the barrier. As a result the structure in the phase space for this family of trajectories forms an ordinary fold, and a phase loss of $\frac{\pi}{2}$ is produced when the wave passes through this region.

For $m = 0$, the $\rho = 0$ line is a focus instead. WKB approximation for the wave function in this region is poorly understood. However, simple physical argument suggests that the wave function is like a Bessel function in ρ direction and a phase loss is also $\frac{\pi}{2}$.

Recall the Schroedinger equation for a Hydrogen atom in a magnetic field when $m=0$ in cylindrical coordinate can be written as

$$\left[-\frac{\hbar^2}{2m_e}\left(\frac{\partial^2}{\partial\rho^2} + \frac{1}{\rho}\frac{\partial}{\partial\rho}\right) + V(\rho,z) \right] \psi(\rho,z) = E\psi(\rho,z) \qquad (F\ 1)$$

where

$$V(\rho,z) = -\frac{1}{\sqrt{\rho^2+z^2}} + \frac{1}{8}\left(\frac{B}{c}\right)^2 \rho^2 \qquad (F\text{-}2)$$

In the region far away from the origin but close to $\rho = 0$ line, we make a WKB like approximation for the

z-dependence of the wave-function

$$\psi(\rho,z) = \exp\left[i\int p_z(\rho,z')\,dz'/\hbar \right]\cdot\phi(\rho,z)$$

Then the equation satisfied by $\phi(\rho,z)$ is approximately

$$\left[-\frac{\hbar^2}{2m_e}\left(\frac{\partial^2}{\partial\rho^2}+\frac{1}{\rho}\frac{\partial}{\partial\rho}\right)+V(\rho,z)-p_z^2(0,z)/2m_e-E\right]\phi(\rho,z)=0$$

where we have neglected derivatives of ϕ with respect to z. Defining

$$k^2(\rho,z)=\frac{2m_e}{\hbar^2}\left[E-V(\rho,z)-\frac{p_z^2(0,z)}{2m_e}\right]$$

it is easy to show that an expansion of $k^2(\rho,z)$ in powers of ρ contains no linear term. Dropping the quadratic term, we replace $k^2(\rho,z)$ by $k^2(0,z)$. Now the equation satisfied by $\phi(\rho,z)$ is

$$\left[\frac{d^2}{d\rho^2}+\frac{1}{\rho}\frac{d}{d\rho}+k^2(0,z)\right]\phi=0$$

where we have suppressed the dependence of k^2 upon ρ. This is Bessel's equation, and the solution is

$$\phi = J_0(k\rho)$$

The lowest order approximation to (F 1) in the focus region is therefore

$$\psi(\rho,z) = c\cdot e^{i\int p_z\,dz/\hbar}\cdot J_0(k\rho) \qquad \text{(F-3)}$$

By means of a long derivation (which is not presented here) it is possible to show that eq.(F-3) represents the first term in a formal asymptotic expansion for ψ in powers of $\hbar$.

Now use the asymptotic form of the Bessel

function,

$$J_0(x) \sim \sqrt{\frac{2}{\pi x}} \cdot \cos\left(x - \frac{\pi}{4}\right) \qquad \text{(F-4)}$$

clearly from (F-3) and (F-4) a phase loss of $\frac{\pi}{2}$ is produced for a wave going through the focus.

APPENDIX G

THE APPROXIMATION OF RETURNING WAVES

In oredr to show that the returning wave in (6 6) is well approximated by the formula in (4 40) we numerically compute the returning wave associated with the trajectories around the second closed orbit in Chapter VII, which is shown in Fig. 7.3.

The comparison is made both in the radial and angular directions. In Fig. G-1 the real and imaginary part of the wave on a circle $r_f = 50a_0$ but at different final angles are shown; in Fig. G-2 the real and imaginary part of the wave at the fixed incoming angle $\theta_f = 53.8315°$ but at different final radius r_f is shown. The squares and circles are the wave computed numerically using the semiclassical approximation in the outer region. The solid lines are the analytic approximation (cylindrically modified-zero energy Coulomb-scattering wave). The agreement between the two is very good.

Another way of checking the accuracy of the approximation is to compute the expansion coefficient a_{l0} in (6-7) and see if its value is independent of the redius of the final circle where the semiclassical approximation is joined to the analytic approximation. For the same case, a_{l0} is computed at different final

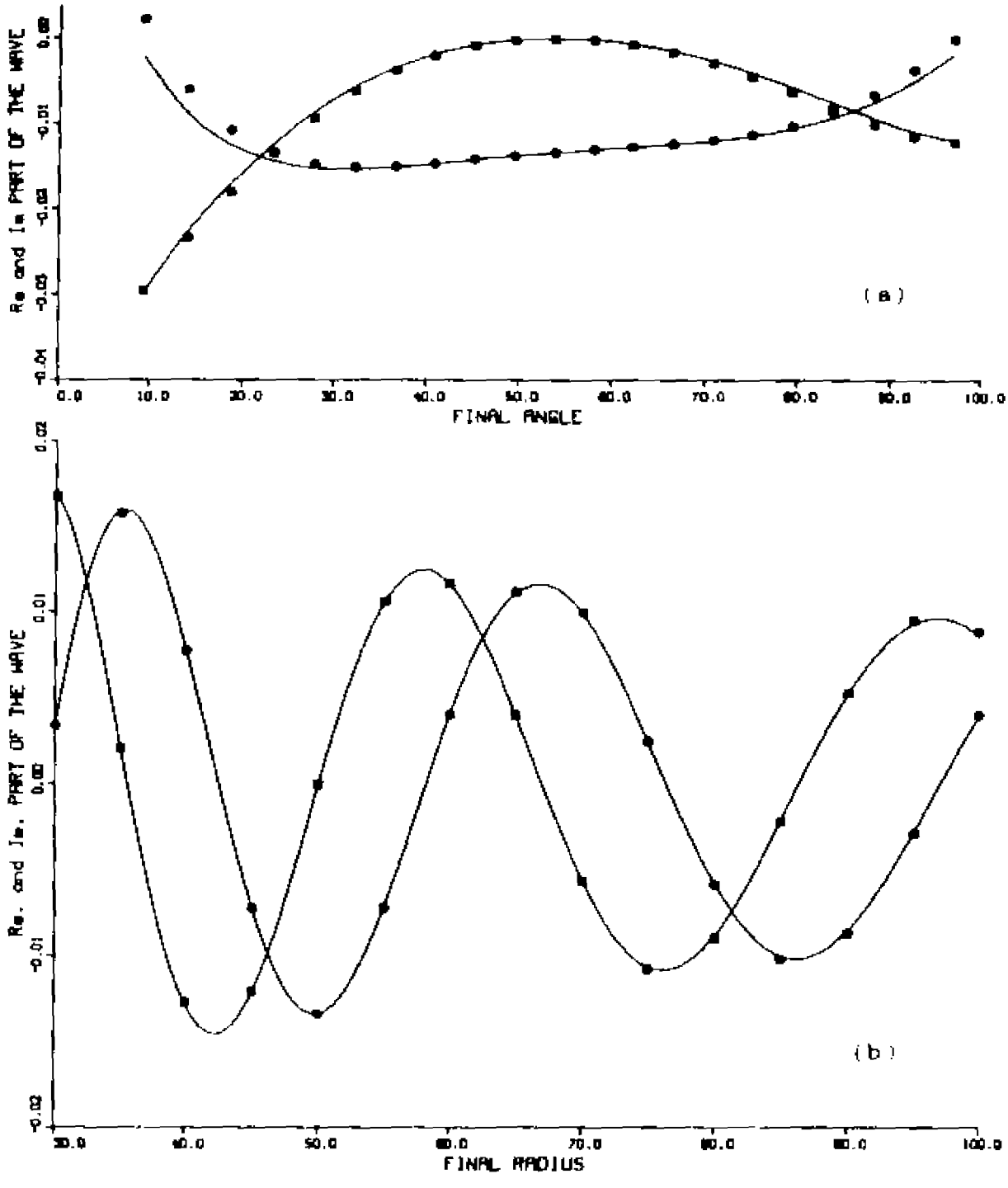

Fig. G-1 Comparisons between the numerically computed returning wave and the analytic expression. See text for explainations.

radii r_f (Table G-1). We find when r_f changes from $30a_0$ to $100a_0$, the magnitude of a_{10} varies by about 3%, and the phase changes insignificently.

Table G-1 Expansion Coefficient a_{10}

r_f	amp. of a_{10}	phase of a_{10}
$30.00a_0$	1.723	344.794
$35.00a_0$	1.729	344.795
$40.00a_0$	1.734	344.795
$45.00a_0$	1.739	344.795
$50.00a_0$	1.744	344.795
$55.00a_0$	1.748	344.796
$60.00a_0$	1.753	344.796
$65.00a_0$	1.757	344.796
$70.00a_0$	1.761	344.796
$75.00a_0$	1.765	344.795
$80.00a_0$	1.769	344.796
$85.00a_0$	1.773	344.796
$90.00a_0$	1.776	344.796
$95.00a_0$	1.780	344.796
$100.00a_0$	1.783	344.797

APPENDIX H

THE RESULTS ARE INDEPENDENT OF THE JOINING RADII

In Appendix G, I showed numerically that the value of the coefficient a_{is} defined in eq. (6-7) is independent of the final joining radius r_f. Here I shall establish that the results are independent of both the initial and final radii analytically. If either the initial or final radius r'_b or r^f_b are changed in a proper range the expansion coefficient a_{is} in (6 7) remains unchanged. Therefore the formula for the spectral oscillations (6 20) is independent of the joining radii.

The range of r is such that the Coulomb term dominates other terms (magnetic term and the term from ϕ motion) in the effective potential. So the classical motion of the electron in the region is governed by the two dimensional Hamiltonian

$$H = \frac{P^2}{2} - \frac{1}{\sqrt{P^2 + z^2}} \qquad (H-1)$$

Now let us assume

$$r_b^i \longrightarrow r_b^{i\,\prime}$$

We allow $r_b^{i\,\prime}$ to be any value in the range $30a_0$ to $100a_0$. In this region, the radially outgoing trajectories keep radially outgoing, so the outgoing angle of each trajectory does not change.

The Maslov index does not change since the region under consideration has no contribution to μ.

According to eq. (6 5b)

$$U_m \to U_m \left(\frac{r_b^2}{r_b^{2\prime}}\right)^{3/4} e^{i\left(\sqrt{8r_b^{2\prime}} - \sqrt{8r_b^2}\right)}$$

and from eq. (5-27)

$$S_r \to S_r - \left(\sqrt{8r_b^{2\prime}} - \sqrt{8r_b^2}\right)$$

Combining eqs. (5-28) and (5 29), since initially the trajectories are going outward radially, we find

$$\frac{\partial r}{\partial t} \propto \frac{1}{\sqrt{T}}$$

$$\frac{\partial \theta}{\partial \theta_0} = \text{const}$$

therefore

$$A \to A \left(\frac{r_b^{2\prime}}{r_b^2}\right)^{3/4}$$

As a result a_{rs} is unchanged: the change in the initial value of the wave function on the boundary is cancelled by the change in the semiclassical wave propagator

$$U_m A e^{iS_r/\hbar} = U_m' A' e^{iS_r'/\hbar}$$

so a_{rs} is unchanged.

Similarly when r'_b changes,

$$r_b t \to r_b t'$$

we have

$$(r_b t)^{1/2} \to (r_b t)^{1/2} \left(\frac{r_b t'}{r_b t}\right)^{1/2}$$

$$e^{i\sqrt{8r_b^f}} \to e^{i\sqrt{8r_b^f}}\left[e^{i(\sqrt{8r_b^{f'}}-\sqrt{8r_b^f})}\right]$$

$$s_r \to s_r - \left[\sqrt{8r_b^{f'}} - \sqrt{8r_b^f}\right]$$

$$\mu \to \mu$$

$$u_m \to u_m$$

under the approximation that the incoming trajectories are the same as if the electron comes in from infinity, we have the equation of motion

$$\frac{l^2}{r} = 1 + \cos\theta$$

from which we get

$$\frac{\partial\theta}{\partial\theta_0} \propto \frac{1}{\sqrt{r}}$$

and from the energy equation we also get

$$\frac{\partial r}{\partial t} \propto \frac{1}{\sqrt{r}}$$

therefore

$$A \to A \cdot \left(\frac{r_b^f}{r_b^{f'}}\right)^{1/2}$$

and again a_{lm} is invariant under such changes.

$$a_{lm} \to a_{lm}$$

APPENDIX 1

ACTION AND TIME THEOREM

We now prove a theorem which relates the action to time along a trajectory.

Consider a trajectory with energy E_1 going from $\vec{q}'$ to $\vec{q}''$. When the energy is changed from E_1 to energy E_2 which is close to E_1, the trajectory going from $\vec{q}'$ to $\vec{q}''$ will follow a different but nearby path. How are the actions along the two paths related?

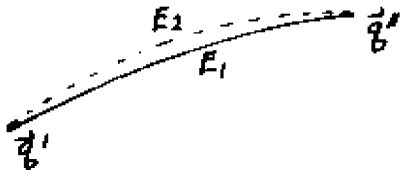

Theorem:

$$\left(\frac{\partial S}{\partial E}\right)_{\vec{q}',\vec{q}''} = T(E) \tag{I 1}$$

where T(E) is the time needed to go from $\vec{q}'$ to $\vec{q}''$.

This theorem says that the difference of action for two nearby trajectories having the same ends is equal to energy change times the transit time.

Proof:

The trajectory going from $\vec{q}'$ to $\vec{q}''$ at energy E can be written as

$$\vec{q} = \vec{q}(t, E, \vec{q}', \vec{q}'')$$
$$\vec{p} = \vec{p}(t, E, \vec{q}', \vec{q}'') \tag{I-2}$$

The action along the trajectory is defined as

$$S(\vec{q}',\vec{q}'',E)=\int_{\vec{q}'}^{\vec{q}''}\vec{p}(t,E,\vec{q}',\vec{q}'')\,d\vec{q}(t,E,\vec{q}',\vec{q}'')$$
$$-\int_{t'}^{t''}\vec{p}(t,E,\vec{q}',\vec{q}'')\frac{\partial\vec{q}(t,E,\vec{q}',\vec{q}'')}{\partial t}\,dt \qquad (I\ 3)$$

where in (I 3), t' and t'' are the times that the particle arrives at $\vec{q}'$ and $\vec{q}''$. Taking derivatives of (I-3),

$$\frac{\partial S}{\partial E}=\int_{t'}^{t''}\left[\frac{\partial\vec{p}}{\partial E}\cdot\frac{\partial\vec{q}}{\partial t}\,dt+\vec{p}\,\frac{\partial^2\vec{q}}{\partial E\partial t}\,dt\right]$$
$$+\vec{p}\,\frac{\partial\vec{q}}{\partial t}\cdot\frac{\partial t}{\partial E}\Big|_{t'}^{t''} \qquad (I\text{-}4)$$

a partial integration of the second term gives us

$$\frac{\partial S}{\partial E}=\int_{t'}^{t''}\left[\frac{\partial\vec{p}}{\partial E}\cdot\frac{\partial\vec{q}}{\partial t}-\frac{\partial\vec{q}}{\partial E}\cdot\frac{\partial\vec{p}}{\partial t}\right]dt$$
$$+\vec{p}\,\frac{\partial\vec{q}}{\partial E}\Big|_{t'}^{t''}+\vec{p}\cdot\frac{\partial\vec{q}}{\partial t}\,\frac{\partial t}{\partial E}\Big|_{t'}^{t''} \qquad (I\ 5)$$

in the expression of (I-5) the derivative is taken as if the two end points $\vec{q}'$ and $\vec{q}''$ were free. If the two end points $\vec{q}'$ and $\vec{q}''$ are fixed, we have two equations

$$\vec{q}(t',E,\vec{q}',\vec{q}'')=\vec{q}'$$
$$\vec{q}(t'',E,\vec{q}',\vec{q}'')=\vec{q}'' \qquad (I\ 6)$$

taking derivatives in (I 6) and keeping in mind that the endpoints $\vec{q}'$ and $\vec{q}''$ are fixed, we find

$$\left[\frac{\partial\vec{q}}{\partial E}+\frac{\partial\vec{q}}{\partial t}\,\frac{\partial t}{\partial E}\right]_{\vec{q}',\vec{q}'}$$

to be zero at t' and t''. Therefore we have

$$\left(\frac{\partial S}{\partial E}\right)_{\vec{q}'\vec{q}''}=\int_{t'}^{t''}\left[\frac{\partial\vec{p}}{\partial E}\cdot\frac{\partial\vec{q}}{\partial t}-\frac{\partial\vec{p}}{\partial t}\cdot\frac{\partial\vec{q}}{\partial E}\right]dt \qquad (I\text{-}7)$$

using Hamilton's equation in (I-7),

$$\left(\frac{\partial S}{\partial E}\right)_{\vec{q}'\vec{q}''} = \int_{t'}^{t''} \left[\frac{\partial \vec{p}}{\partial E} \frac{\partial H}{\partial \vec{p}} + \frac{\partial H}{\partial \vec{q}} \frac{\partial \vec{q}}{\partial E} \right] dt$$

$$= \int_{t'}^{t''} \frac{\partial H}{\partial E}\, dt$$

$$= \int_{t'}^{t''} dt$$

$$= T(E)$$

Q.E.D.

APPENDIX J

THE DEPENDENCE OF ACTION ON MAGNETIC FIELD

When a Hamiltonian contains a parameter such as the magnetic field B, we would like to know how the action depend on the parameter?

Let us assume,

$$H = H(\vec{q}, \vec{p}, \lambda) \tag{J-1}$$

and a trajectory γ going from $\vec{q}'$ at t' to $\vec{q}''$ at t'',

$$\vec{q} = \vec{q}(t, \lambda, E, \vec{q}', \vec{q}'') \tag{J-2a}$$

$$\vec{p} = \vec{p}(t, \lambda, E, \vec{q}', \vec{q}'') \tag{J-2b}$$

If λ is changed to $\lambda + \Delta\lambda$, there will be a nearby trajectory close to the original one at the same energy going from $\vec{q}'$ to $\vec{q}''$. How are the actions associated with the two trajectories related to each other?

Theorem:

$$\left(\frac{\partial S}{\partial \lambda}\right)_{E,\vec{q}',\vec{q}''} = -\int_{\gamma} \frac{\partial H}{\partial \lambda}\, dt \tag{J 3}$$

Proof:

Take the derivative of S

$$S = \int_{t'}^{t''} \vec{p}\, \frac{\partial \vec{q}}{\partial t}\, dt$$

with respect to λ, holding E, $\vec{q}'$, $\vec{q}''$ fixed,

$$\left(\frac{\partial S}{\partial \lambda}\right)_{E,\vec{q}',\vec{q}''} = \int_{t'}^{t''} \left[\frac{\partial \vec{p}}{\partial \lambda}\, \frac{\partial \vec{q}}{\partial t} + \vec{p}\, \frac{\partial^2 \vec{q}}{\partial \lambda \partial t} \right] dt + \vec{p}\, \frac{\partial \vec{q}}{\partial t}\, \frac{\partial t}{\partial \lambda} \Bigg|_{t'}^{t''}$$

$$= \int_{t'}^{t''} \left[\frac{\partial \vec{p}}{\partial \lambda} \cdot \frac{\partial \vec{q}}{\partial t} - \frac{\partial \vec{p}}{\partial t} \cdot \frac{\partial \vec{q}}{\partial \lambda} \right] dt + \left[\vec{p} \cdot \frac{\partial \vec{q}}{\partial \lambda} + \vec{p} \cdot \frac{\partial \vec{q}}{\partial t} \frac{\partial t}{\partial \lambda} \right] \Big|_{t'}^{t''}$$

(J-4)

where in the second step, a partial integration has been performed. The terms outside of the integral sign in (J 4) exactly cancel. This can be seen by taking derivatives of the two constrains,

$$\vec{q}' = \vec{q}(t', \lambda, E, \vec{q}', \vec{q}'') \qquad \text{(J-5a)}$$

$$\vec{q}'' = \vec{q}(t'', \lambda, E, \vec{q}', \vec{q}'') \qquad \text{(J-5b)}$$

therefore

$$\left(\frac{\partial S}{\partial \lambda}\right)_{E, \vec{q}', \vec{q}''} = \int_{t'}^{t''} \left[\frac{\partial \vec{p}}{\partial \lambda} \cdot \frac{\partial \vec{q}}{\partial t} - \frac{\partial \vec{p}}{\partial t} \cdot \frac{\partial \vec{q}}{\partial \lambda} \right] dt$$

(J-6)

Now use Hamilton's equation,

$$\frac{d\vec{q}}{dt} = \frac{\partial H}{\partial \vec{p}}$$

$$\frac{d\vec{p}}{dt} = -\frac{\partial H}{\partial \vec{q}}$$

we obtain

$$\left(\frac{\partial S}{\partial \lambda}\right)_{E, \vec{q}', \vec{q}''} = \int_{t'}^{t''} \left[\frac{\partial \vec{p}}{\partial \lambda} \cdot \frac{\partial H}{\partial \vec{p}} + \frac{\partial H}{\partial \vec{q}} \cdot \frac{\partial \vec{q}}{\partial \lambda} \right] dt$$

$$= \int_{t'}^{t''} \left[\frac{dH(\vec{q}, \vec{p}, \lambda)}{d\lambda} - \frac{\partial H}{\partial \lambda} \right] dt$$

since $E = H(\vec{q}, \vec{p}, \lambda)$ is held fixed, we have

$$\left(\frac{\partial S}{\partial \lambda}\right)_{E, \vec{q}', \vec{q}''} = -\int_{t'}^{t''} \left(\frac{\partial H}{\partial \lambda}\right) dt \qquad \text{(J-7)}$$

Q.E.D.

In the present case, we want to know how the action changes as the magnetic field changes. Since

$$H = \frac{1}{2}\vec{p}^2 - \frac{1}{\gamma} + \frac{1}{8m_e}\left(\frac{eB}{c}\right)^2 \rho^2$$

then

$$\frac{\partial H}{\partial B} = \frac{B}{4m_e}\left(\frac{e}{c}\right)^2 \rho^2$$

so

$$\frac{\partial S}{\partial B} = -\frac{B}{4m_e}\left(\frac{e}{c}\right)^2 \int_\gamma \rho^2 dt \qquad \text{(J-8)}$$

APPENDIX K

PRACTICAL FORMULA FOR EVALUATING SEMICLASSICAL WAVE AMPLITUDE

When computing the semiclassical wave amplitude A as in (5-28) and (5-29) the derivatives of r and θ with respect to the initial surface at a fixed time

$$\left(\frac{\partial r}{\partial \theta_0}\right)_t \quad , \quad \left(\frac{\partial \theta}{\partial \theta_0}\right)_t$$

are needed. However, because usually we do not use a uniform time step $\Delta t = Const$ in our numerical integration, we do not have the data for neighbouring trajectories at the same time.

In our case we launch a family of trajectories at t=0 from the initial circle and each of these trajectories is propagated with a varied time step size according to the location of the electron. Trajectories are stopped right on the final circle r_f constant. Apparently trajectories in this family do not arrive at the final circle at the same time.

Let us express the desired quantities in terms of other quantities which are readily obtained.

From running the trajectories, we could, in principle, obtain two functions,

$$r = r(t, \theta_0) \qquad \text{(K 1a)}$$

$$\theta = \theta(t, \theta_0) \qquad \text{(K 1b)}$$

We have from the first one,

$$dr = \left(\frac{\partial r}{\partial \theta_0}\right)_t d\theta_0 + \left(\frac{\partial r}{\partial t}\right)_{\theta_0} dt \qquad (K\text{-}2)$$

on the final circle r is a constant, we obtain

$$\left(\frac{\partial r}{\partial \theta_0}\right)_t = -\left(\frac{\partial r}{\partial t}\right)_{\theta_0}\left(\frac{\partial t}{\partial \theta_0}\right)_r \qquad (K\ 3)$$

This is one of the relation.

From (K 1b) we have

$$d\theta = \left(\frac{\partial \theta}{\partial t}\right)_{\theta_0} dt + \left(\frac{\partial \theta}{\partial \theta_0}\right)_t d\theta_0 \qquad (K\text{-}4)$$

which, on the final circle, is

$$\left(\frac{\partial \theta}{\partial \theta_0}\right)_t = \left(\frac{\partial \theta}{\partial \theta_0}\right)_r - \left(\frac{\partial \theta}{\partial t}\right)_{\theta_0}\left(\frac{\partial t}{\partial \theta_0}\right)_r \qquad (K\text{-}5)$$

This is another relation.

Eqs. (K 3) and (K 5) are the ones used in our calculation of A. To evaluate the right hand side of eqs. (K 3) and (K-5) we need the momenta of each trajectory and the time of two neighbouring trajectories arriving at the final circle. These are the informations obtained when Hamilton's equation are integrated.

REFERENCES

1. M. L. Du and J. B. Delos, Phys. Rev Lett. 58, 1731 (1987).
2. (a) G. Casati (ed.), Chaotic Behavior in Quantum Systems, (Plenum, New York, 1985). (b) Y.S.Kim and W.W.Zachary (eds.), The Physics of Phase Space, (Springer-Verlag, 1987).
3. I. C. Percival, Adv. Chem. Phys. 36, 1 (1977).
4. W. R. S. Garton and F. S. Tomkins, Astrophys. J. 158, 839 (1969).
5. A. R. Edmonds, J. Phys. (Paris) Colloque 31,71 (1970)
6. An interpretation based upon Gaussian wave packets has been given by W. P. Reinhardt, J. Phys. B 16, L635 (1983).
7. (a) A. Holle, G. Wiebusch, J. Main, B. Hager, H. Rottke, and K. H. Welge, Phys. Rev. Lett. 56, 2594 (1986); (b) J. Main, G. Wiebusch, A. Holle and K. H. Welge, ibid 57, 2789 (1986).
8. Recall that in integrable systems, eigenvalues are correlated not with periodic orbits but with quasiperiodic orbits---see Chapter 1.
9. (a) M. C. Gutzwiller, J. Math. Phys. 11,1791 (1970); (b) M. C. Gutzwiller, J. Math. Phys. 8, 1979 (1967); (c) M. C. Gutzwiller, J. Math. Phys.

10, 1004 (1969) (d) M. C. Gutzwiller, J. Math. Phys. 12, 343 (1971).

10. Here ψ_i and ψ_f are the initial and final states of the system with energies E_i and E_f, D is the dipole operator, $\rho(E_f)$ is the density of final states, and $g(E_f-E)$ is a smoothing or averaging function with width corresponding to the finite resolution of the experiment---see Chapter III.

11. The orbits are not necessarily periodic with period T; They may leave the nucleus in one direction and return from another---see later chapters.

12. A. Messiah, Quantum Mechanics, (North-Holland, Amsterdam, 1961) pp. 27-42.

13. Max Born, The Mechanics of the Atom, (Unger, New York, 1960).

14. D. Ter Haar, The Old Quantum Theory, (Pergamon Press, 1967).

15. L. I. Schiff, Quantum Mechanics, (McGraw-Hill, 1955).

16. A. J. Lichtenberg and M. A. Lieberman, Regular and Stochastic Motion, Applied Mathematical Sciences, 38, (Springer-Verlag, 1983).

17. M. V. Berry, Topics in Nonlinear Dynamics, ed., S. Jorna, AIP Conf. Proc. 46 (1978) pp.16 120.

18. M. V. Berry, in Chaotic Behavior of Deterministic Systems, edited by G. Iooss, R. H. G. Helleman, and R. Stora, (North Holland, Amsterdam, 1983).

19. H. Goldstein, Classical Mechanics, (Addison-

Wesley, 1965).

20. (a) V. I. Arnol'd, Mathematical Methods of Classical Mechanics, (Springer-Verlag, New York, 1978). (b) M. Henon, Phys. Rev. B., 9 1921 (1974).

21. V. I. Arnol'd and A. Avez, Ergotic Problem of Classical Mechanics, (Benjamin, New York, 1965).

22. Fundamental Problems in Statistical Mechanics, ed., E. G. D. Cohen, Vol. III (North-Holland, Amsterdam, 1975).

23. Ya. G. Sinai, Russ. Math. Surv. 25, 137 (1970).

24. L. A. Bunimovich, Commun. Math. Phys. 65, 295 (1979).

25. M. Henon and C. Heiles, Astron. J., 69, 73 (1964).

26. P. J. Richens and M. V. Berry, Physica 2D, 495 (1981).

27. (a) A. N. Kolmogorov, Dokl. Akad. Nauk. 98, 527 (1954). (b) V. I. Arnol'd, Russ. Math. Surve. 18, No.5 (1963) 13-39; No. 6, 61-196. (c) J. Moser, Nachr. Akad. Wiss. Gottingen 1, 1 (1962).

28. (a) V. P. Maslov and M. V. Fedoriuk, Semiclassical Approximation in Quantum Mechanics, (Reidel, Boston 1981). (b) J. B. Delos, Adv. Chem. Phys. 65, 161 (1986).

29. S. K. Knudson, J. B. Delos, and B. Bloom, J. Chem. Phys. 83, 5703 (1985); S. K. Knudson, J. B. Delos, and D. W. Noid, ibid. 84, 6886 (1986).

30. R. L. Waterland, J. B. Delos, and M. L. Du, Phys. Rev. A 35, 5064 (1987).

31. M. V. Berry, J. Phys. A. 12, 811 (1979).

32. M. Tabor, Adv. Chem. Phys. 46, 73 (1981).

33. (a) E. J. Heller, Phys. Rev. Lett. 53, 1515 (1984). (b) E. B. Bogomol'nyi, JETP Lett. 44, 561 (1986).

34. C. W. Clark and K.T. Taylor, J. Phys. B. 15, 1175 (1982).

35. C. F. Porter (ed.) Statistical Theory of Spectra: Fluctuations, (Academic Press, N. Y., 1965).

36. A. Einstein, Verh. Dtsch. Ges. 19, 82 (1917); L. Brillouin, J. de Physique (Ser. 6) 7, 353 (1926); J. B. Keller, Ann. Phys. (N.Y.) 4, 180 (1958).

37. (a) D. W. Noid and R. A. Marcus, J. Chem. Phys. 62, 2119 (1975). (b) R. T. Swimm and J. B. Delos, J. Chem. Phys. 71, 1706 (1979). (c) I. C. Percival and N. Pomphrey, Mol. Phys. 35, 649 (1978).

38. (a) M.V. Berry, Aspects of Degeneracy, G. Casati (ed.) Chaotic Behavior in Quantum Systems: Theory and Applications (Plenum, New York, 1985). (b) M. V. Berry, Proc. R. Soc. Lond. A 392, 45 (1984).

39. D. Wintgen and H. Friedrich, Phys. Rev. A, 35, 1464 (1987).

40. M. V. Berry, in The Wave-Particle Dualism, S. Diner et. al. (eds.) (D.Reidel, 1984).

41. R. Balian and C. Bloch, Ann Phys. N. Y. 60, 401 (1970); 64, 271 (1971); 69, 76 (1972); 85, 514 (1974).

42. M. V. Berry and K. E. Mount, Rep. Prog. Phys. 35, 315 (1972).

43. M. V. Berry and M. Tabor, Proc. Roy. Soc. A349, 101 (1976).

44. E. U. Condon and G. H. Shortley, The Theory of Atomic Spectra, (Cambridge University Press, Cambridge, 1979).

45. J. C. Gay in Progress in Atomic Spectroscopy, Part C, edited by H. J. Beyer and H. Kleinpoppen (Plenum, New York, 1984), pp. 177-246; P. M. Koch, in Rydberg States of Atoms and Molecules, edited by R. F. Stebbings and F. B. Dunning (Cambridge University, Cambridge, 1983), pp. 473-512.

46. (a) D. Kleppner, M. G. Littmann, and M. L. Zimmerman, in Rydberg States of Atoms and Molecules, edited by R. F. Stebbings and F. B. Dunning (Cambridge University, Cambridge, 1983), pp. 73-116; (b) C. W. Clark, K. T. Lu, and A. F. Starace, in Progress in Atomic Spectroscopy, Part C, edited by H. J. Beyer and H. Kleinpoppen (Plenum, New York, 1984), pp. 247-320; (c) R.H. Garstang, Rep. Prog. Phys. 40, 105 (1977); (d) Atomic and Molecular Close to the Ionization Threshold in High Fields, J. Phys. (Paris) Colloq. C2 43 (1982); (e) Atomic Excitation and Recombination in External Fields, M. H. Nayfeh and C. W. Clark (ed.) (Gordon and Breach, New York,1985); (f) J. E. Bayfield, Phys. Rep. 51, 317 (1979).

47. The paramagnetic term can also be eliminated by "transforming the system to a frame of reference that rotates at the Larmor frequency about the direction of

the magnetic field"---See J. B. Delos, S. K. Knudson, and D. W. Noid, Phys. Rev. A28, 7 (1983).

48. Atomic, Molecular and Optical Physics, in the series Physics Through the 1990's, (National Academy Press, Washington DC, 1986).

49. (a) J. B. Delos, S. K. Knudson, and D. W. Noid, Phys. Rev. A 30, 1208 (1984); (b) M. Robnik, J. Phys. A 14,3195 (1981); (c) D. Wintgen and H. Friedrich, Phys. Rev. A35, 1464 (1987); (d) G. Wunner, U. Woelk, I. Zech, G. Zeller, T. Ertl, F. Geyer, W. Schweitzer, and H. Ruder, Phys. Rev. Lett. 57, 3261 (1986).

50. F. S. Tomkins and H. M. Crosswhite, in Atomic Excitation and Recombination in External Fields, edited by M. H. Nayfeh and C. W. Clark (Gorden and Breach, New York, 1985).

51. (a) G. Wunner, J. Phys. B 19, 1623 (1986); (b) T. P. Grozdanov and H. S. Taylor, J. Phys. B 19, 4075 (1986).

52. D. Richards, J. Phys. B 16, 749 (1983); E. A. Solov'ev, Sov. Phys. JETP 55, 1017 (1982).

53. (a) A. Holle, G. Wiebusch, J. Main, and K. H. Welge, G. Zeller, G. Wunner, T. Ertl, and H. Ruder, Z. Phys. D 5, 279 (1987).

54. (a) A. F. Starace, J. Phys. B 6, 585 (1973); (b) A. R. P. Rau, Phys. REv. A 16, 1613 (1977); (c) J. A. C. Gallas, E. Gerck and R. F. O'Connell, Phys. Rev. Lett. 50, 324 (1983).

55. L. I. Schiff, Quantum Mechanics, 2nd ed. (McGraw-

Hill, New York,1955).

56. H. A. Bethe and E. E. Salpeter, Quantum Mechanics of One- and Two-Electron Atoms, (Plenum, New York, 1977).

57. M. Abramowitz and I. Stegun, Handbook of Mathematical Functions, N. B. S. Applied Mathematics Series, 55, (1972).

58. J. D. Jackson, Classical Electrodynamics, (Wiley, New York, 1975).

59. D. Ter. Haar, Problems in Quantum Mechanics, London: Pion, 1975 3rd ed.

60. J. B. Delos, J. Chem. Phys. 86, 425 (1986).

61. M. A. AL-Laithy', P. F. O'Mahony and K. T. Taylor J. Phys. B 19, L773 (1986).

VITA

Mengli Du

Born in Changan county, Shanxi province, China, July 3, 1962. Graduated from Fengxi high school in that county in 1978. Was one of the final 50 winners in All China High-School Mathematics Contest in 1978. Received B.Sc from Chinese University of Science and Technology with a major in physics in 1982 and subsequently became a graduate student in the Institute of Theoretical Physics, Academia Sinica, Beijing.

In August 1983, the author entered the College of William and Mary as a graduate assistant in the Department of Physics through the CUSPEA program(China and US Physics Examination and Application). Received a M.S. in physics in 1984 from the College of William and Mary. He is going to work as a Postdoctoral Fellow in Harvard-Smithsonian Center for Astrophysics after getting the Ph.D degree.